Expedition 329 summary[1]

Expedition 329 Scientists[2]

Chapter contents

Abstract

Integrated Ocean Drilling Program Expedition 329 made major strides toward fulfilling its objectives. Shipboard studies documented (1) fundamental aspects of habitability and life in this very low activity subseafloor sedimentary ecosystem and (2) first-order patterns of basement habitability. A broad range of postexpedition studies will complete the expedition objectives.

Throughout the South Pacific Gyre (Sites U1365–U1370), dissolved oxygen and nitrate are present throughout the entire sediment sequence. Concentration profiles of oxygen and nitrate indicate that subseafloor heterotrophic respiration is oxic and proceeds very slowly. In contrast, at Site U1371 in the upwelling zone just south of the gyre, detectable oxygen and nitrate are limited to the top and bottom of the sediment column and manganese reduction is a prominent electron-accepting process.

Geographic variation in subseafloor profiles of dissolved and solid-phase chemicals are consistent with the magnitude of organic-fueled subseafloor respiration declining from outside the gyre to the gyre center.

Microbial cell counts are lower than at all sites previously drilled. Countable cells disappear with increasing depth in the sediment at every site in the South Pacific Gyre (Sites U1365–U1370). Concentrations of dissolved oxygen and nitrate, total organic carbon, and total nitrogen stabilize as countable cells fall below the minimum detection limit. The downhole disappearance of cells and measurable organic oxidation appears to result from the disappearance of organic electron donors.

At the South Pacific Gyre sites, dissolved hydrogen concentration is low but often above detection in deep sediment. At Site U1371, where most of the sediment is anoxic, dissolved hydrogen concentration is above detection through much of the column.

High-resolution chemical and physical measurements provide the opportunity for reconstructing glacial seawater characteristics through the South Pacific Gyre. Such reconstruction will greatly contribute to understanding the global ocean-climate system.

Dissolved chemical profiles and igneous petrology indicate that basement alteration continues on the timescale of formation fluid replacement, even at the sites with oldest basement (84–120 Ma at Sites U1365 and U1366). Profiles of dissolved chemicals indicate that microbial habitability of the entire sediment sequence

and the uppermost basalt is not limited by access to electron acceptors (oxygen and nitrate) or major nutrients (carbon, nitrogen, and phosphorus).

Introduction

The nature of life in the sediment beneath mid-ocean gyres is very poorly known. Almost all sites where subseafloor sedimentary life has been studied are on ocean margins (Ocean Drilling Program [ODP] Legs 112, 180, 201, and 204 and Integrated Ocean Drilling Program [IODP] Expeditions 301, 307, and 323) or in the equatorial ocean (ODP Legs 138 and 201). Despite those studies, the extent and character of subseafloor life throughout most of the ocean remains unknown (Ocean Studies Board, 2003). This absence of knowledge is largely due to ignorance of subseafloor life in the major ocean gyres, which collectively cover most of the area of the open ocean.

The South Pacific Gyre is the ideal region for exploring the nature of subseafloor sedimentary communities and habitats in the low-activity heart of an open-ocean gyre. It is the largest of the ocean gyres and its center is farther from continents than the center of any other gyre. Surface chlorophyll concentrations and primary photosynthetic productivity in the seawater are lower in this gyre than in other regions of the world ocean (Behrenfeld and Falkowski, 1997) (Fig. F1). Its surface water is the clearest in the world (Morel et al., 2007). The sediment of this region has some of the lowest organic burial rates in the ocean (Jahnke, 1996). Our recent survey cruise demonstrated that shallow sediment of this region contains the lowest cell concentrations and lowest rates of microbial activity ever encountered in shallow marine sediment (D'Hondt et al., 2009).

The South Pacific Gyre is also ideal for testing hypotheses of the factors that limit hydrothermal circulation and chemical habitability in aging oceanic crust (sedimentary overburden, basement permeability, and decreasing basal heat flux). It contains a continuous sweep of oceanic crust with thin (1–100 m) sedimentary cover spanning thousands of kilometers and >100 m.y. of seafloor age.

The South Pacific Gyre contains the largest portion of the seafloor that has never been explored with scientific ocean drilling. Consequently, IODP Expedition 329 will advance scientific understanding across a broad front, will help to constrain the nature of crustal inputs to the subduction factory, and will constrain the origin of the Cretaceous Normal Superchron (CNS) and tectonic history of a region as large as Australia. Recovery of sedimentary interstitial waters at several of the proposed sites will provide novel constraints on glacial–interglacial pCO_2 models.

Expedition history

Expedition 329 is based on IODP drilling Proposal 662-Full3, "Life beneath the seafloor of the South Pacific Gyre" (available at **iodp.tamu.edu/scienceops/ expeditions/south_pacific_gyre_microbio.html**). Following ranking by the IODP Scientific Advisory Structure, the expedition was scheduled for the R/V *JOIDES Resolution,* operating under contract with the US Implementing Organization (USIO). The expedition started in Papeete, Tahiti, on 8 October 2010 and ended in Auckland, New Zealand, on 13 December. Further details about USIO and the facilities aboard the *JOIDES Resolution* can be found at **www.iodp-usio.org/.** Supporting site survey data for Expedition 329 are archived at the IODP Management International, Inc., Site Survey Data Bank (**ssdb.iodp.org/**). The KNOX-02RR site survey expedition report is available in this volume (see **D'Hondt et al.,** 2011).

Geological setting

Expedition 329 sites span nearly the entire width of the Pacific plate in the Southern Hemisphere between 20°S and 45°S (Fig. **F2**). This oceanic crust was accreted along at least four different plate boundaries (e.g., Pacific/Phoenix, Pacific/Antarctic, Pacific/Farallon, and Pacific/Nazca). Crustal ages range from ~100 Ma (Chron 34n) at Site U1365 to ~6 Ma (Chron 3An.1n) at alternate proposed Site SPG-7A. Calculated spreading rates range from slow–intermediate (<20 km/m.y., half-rate) to ultrafast (>80 km/m.y., half-rate).

The site locations cover a relatively wide range of crustal ages, spreading rates, and tectonic/volcanic environments. The depth and crustal age of each site correlates well with the predicted depth versus age curve (Stein and Stein, 1994), which suggests the sites are located on representative crust. Calculated spreading rates at each site are somewhat biased toward fast and ultrafast spreading rates (28–95 km/m.y., half-rate). Surprisingly, the 95 km/m.y. value is one of the fastest spreading half-rates measured globally. The abyssal hill fabric is relatively well defined for most coring sites. However, off-axis volcanism at alternate proposed Site SPG-5A and Site U1368 masked the original seafloor fabric. Sediment thickness ranges from <3 to 122–130 m and generally increases west and south of our survey area. This sediment thickness trend is consistent with greater sediment cover on older crust and on crust located farther away from the center of the gyre. The notable exception to this trend is along the northern transect on crust accreted along the Pa-

cific-Farallon spreading system and older than ~30 m.y. Sediment at each of the sites generally appears as pelagic drape, with some localized mass wasting deposits. Seismic images also reveal areas of bottom current activity occasionally resulting in localized scouring of all sediment above volcanic basement (e.g., alternate proposed Site SPG-5A).

Microbiological setting

The sedimentary communities and activities of shallow (0–8 meters below seafloor [mbsf]) South Pacific Gyre sediment are unlike those in any sediment of equal depth previously explored by scientific ocean drilling (D'Hondt et al., 2009). The survey expedition, KNOX-02RR, demonstrated that cell concentrations and organic-fueled respiration in the shallow sediment of Sites U1365–U1370 are orders of magnitude lower than concentrations in previously examined sediment of equivalent depth (Fig. F3) (D'Hondt et al., 2009). Dissolved oxygen (O_2) penetrates extremely deeply (Fig. F4A) (D'Hondt et al., 2009; Fischer et al., 2009).

These pilot results demonstrated that, at least in the shallow sediment, (1) net metabolic activities are low and oxygen is the principal net terminal electron acceptor and (2) biomass is substantially different than in any previously examined deep-sea sediment. In contrast, on the southern edge of the gyre, where sea-surface chlorophyll content is much higher, cell concentrations and dissolved chemical concentrations in the shallow (0–4 mbsf) sediment (D'Hondt et al., 2009) resemble those of ODP Site 1231 (on the northeastern edge of the gyre) (Figs. F3, F4), where most of the subseafloor interstitial water is anoxic and the community may be principally supported by oxidation of organic matter coupled to reduction of $Mn(IV)$, $Fe(II)$, and NO_3^- migrating up from the underlying basaltic aquifer (Shipboard Scientific Party, 2003; D'Hondt et al., 2004). These results suggested that biomass and microbial activity in subseafloor sediment may vary predictably with sea-surface chlorophyll content.

Seismic studies/Site survey data

From 18 December 2006 to 27 January 2007, Cruise KNOX-02RR, aboard the R/V *Revelle*, surveyed all 11 drilling sites (Fig. F1). Sediment was geophysically imaged and cored at all 11 sites. Cores from the survey are curated at the US National Science Fund–supported Rock and Core Facility at the University of Rhode Island (USA). Sites U1365–U1370 are in the central portion of the South Pacific Gyre. Site U1371 is below higher productivity water at the gyre's southern edge.

All of the sites are at a crossing point of two track lines or on a single track line immediately adjacent to a crossing point. The multibeam and seismic results are provided in figure form for each site (see D'Hondt et al., 2010).

Geophysical data collected at each site include SIM-RAD EM120 swath map bathymetry and Knudsen digitally recorded 3.5 kHz and multichannel seismic reflection. Data were collected at 4.5–6 kt with continuous GPS navigation, including at least one set of intersecting track lines. Following each geophysical survey, shallow sediment (0–8 mbsf) was recovered using gravity, piston, and multicores. At sites with water depths deeper than 4 km, this shallow sediment is principally abyssal clay capped by manganese nodules. At sites in shallower water (proposed Sites SPG-6A and SPG-7A), the shallow sediment is clayey nannofossil ooze.

All Expedition 329 drill sites were supported by seismic, navigation, and bathymetric data and classified as "1Aa" by the Site Survey Panel. The 1Aa classification indicates that all required data are in the site survey data bank and have been reviewed by the Site Survey Panel and that they image the target adequately and there are no scientific concerns of drill site location and penetration.

Scientific objectives

Our study has the following fundamental objectives:

- To document the habitats, metabolic activities, genetic composition and biomass of microbial communities in subseafloor sediment with very low total activity;
- To test how oceanographic factors (such as surface ocean productivity) control variation in sedimentary habitats, activities, and communities from gyre center to gyre margin;
- To quantify the extent to which subseafloor microbial communities of this region may be supplied with electron donors by water radiolysis, a process independent of the surface photosynthetic world; and
- To determine how basaltic basement habitats, potential activities and, if measurable, microbial communities vary with crust age and hydrologic regime (from ridge crest to abyssal plain).

We proposed to meet these objectives by

- Coring the entire sediment column at several sites along two transects in the region of the South Pacific Gyre (Figs. F1, F2);
- Coring and logging the upper 100 m of the basaltic basement at three key sites; and

- Undertaking extensive microbiological, biogeo-chemical, geological, and geophysical analyses of the cores and drill holes.

The project results address several significant questions. Are the communities in mid-gyre subseafloor sediment uniquely structured? Do they contain previously unknown organisms? What are their principal sources of metabolic energy? Do their principal metabolic activities and composition vary with properties of the surface world, such as sea-surface chlorophyll concentrations or organic flux to the seafloor? Is microbial activity is sustainable in subseafloor basalt by mineral oxidation (e.g., oxidation of iron and sulfur species in the basaltic minerals) for tens of millions of years after basalt formation? Are microbial communities recognizably present in subseafloor basalt older than 13 Ma?

These questions can be framed as hypotheses to be tested. For example, we hypothesized the following:

- A living community persists in the most organic poor sediment of the world ocean.
- Organic-fueled metabolic activity is extremely low and oxygen is the principal net terminal electron acceptor in this sediment. Consequently, the degree of anaerobic activities is far lower here than in previously examined subseafloor sediments.
- The biomass, metabolism, and composition of this subseafloor sedimentary community is distinctly different from the communities observed in organic-rich anaerobic subseafloor ecosystems on the continental margins.
- H_2 from water radiolysis is a significant electron donor for microbial respiration in the most organic-poor subseafloor sediment.
- Open flow continues in the very old basalt of the western gyre.
- Basalt oxidation may support chemolithotrophic microbial activity for 100 m.y. here.
- Biomass and activity decrease with basement age as electron donor accessibility decreases.

Even if all of the above hypotheses are falsified, the results of Expedition 329 will significantly advance understanding of the subsurface world. Postcruise research by Expedition 329 scientists will test the extent to which distinct oceanographic and geologic provinces contain distinct subseafloor habitats and distinct subseafloor communities. They will document the extent to which life in the low-activity gyre sediment depends on the surface photosynthetic world—and the extent, if any, to which it is metabolically independent of the surface world. They will place firm constraints on the potential for microbial redox activity in ancient subseafloor basalt and how that potential varies with crustal age over 100 m.y.

or more. They will place firm constraints on estimates of total subseafloor biomass and habitable space on our planet.

The results of Expedition 329 and subsequent shore-based studies will also test

- The factors that control evolution of geothermal circulation and chemical alteration in oceanic crust,
- Models of regional tectonic history,
- Geodynamo models, and
- Models of glacial–interglacial ocean-climate change.

Explanation of primary objectives

Our first primary objective is to document the habitats, metabolic activities, genetic composition, and biomass of microbial communities in subseafloor sediment with very low total activity.

Key questions are: What are the principal microbial activities in mid-gyre subseafloor sediment? What are the rates of those activities? How dense are the populations in this sediment? What are the communities active here? How do these communities and activities compare to those in subseafloor sediment with much higher levels of activity? How unique are their organisms?

Expedition 329 provides a crucial opportunity to document microbial habitats, activities, and community composition in a subseafloor sedimentary ecosystem that has never been explored by scientific ocean drilling.

The penetration of high concentrations of O_2 and NO_3^- meters into the sediment at KNOX-02RR survey sites suggested that the net rate of electron-accepting activity is even lower in the South Pacific Gyre than at Site 1231 in the Peru Basin (D'Hondt et al., 2009). Along with chemical data from Deep Sea Drilling Project (DSDP) Leg 92, these O_2 and NO_3^- profiles also suggested that the principal electron-accepting activity in the subseafloor sediment of this region may be different than at any of the sites where subseafloor sedimentary communities have been previously explored. A sequence of sites was drilled during Leg 92 at ~20°S in the northern portion of the gyre (Leinen, Rea, et al., 1986). At all Leg 92 sites where interstitial water chemistry was analyzed, dissolved NO_3^- is present throughout the entire sediment column, which is as thick as 50 m (Gieskes and Boulègue, 1986). Because NO_3^- concentrations do not significantly change with depth in the KNOX-02RR survey cores (except at Site U1371) or the Leg 92 cores, O_2 was predicted to be the principal net electron acceptor in subseafloor sediment

throughout the South Pacific Gyre (D'Hondt et al., 2009).

Quantification of subseafloor biomass in the South Pacific Gyre will place strong constraints on the size of Earth's subseafloor biomass and total biomass.

On the basis of acridine orange direct counts in subseafloor sediment of relatively high activity sites, subseafloor sedimentary biomass has been estimated to comprise one-tenth to one-third of total carbon of living biomass on Earth (Parkes et al., 2000; Whitman et al., 1998). A subsequent study of intact polar lipids estimated living archaeal biomass in subseafloor sediment to be 90 Pg (Lipp et al., 2008; Lipp and Hinrichs, 2009), equal to ~15% of Earth's living biomass. These estimates make a key assumption that needs to be tested by Expedition 329; they assume that the sites where cells were counted are representative of biomass content in the subseafloor sediment of all regions. However, most sites used for these biomass estimates are in relatively organic-rich, high-biomass sedimentary environments and therefore may not accurately represent much of the world ocean. As described earlier, cell concentrations in the KNOX-02RR cores are orders of magnitude lower than concentrations at the same depths in all previous IODP/ODP sediment (D'Hondt et al., 2009) (Fig. F3). Therefore, living subseafloor biomass may be significantly lower than 10%–30% of Earth's total biomass. Expedition 329 provides fundamental data to address this issue.

Genetic analyses of bulk sediment samples and cultured bacterial isolates from deep beneath the seafloor have demonstrated that similar subseafloor sedimentary environments separated by thousands of kilometers contain similar phylogenetic types of microbial communities. For example, hydrate-bearing sediment of the Peru margin and the northwestern US margin (Hydrate Ridge) resulted in statistically similar compositions of 16S rRNA gene clone libraries (Inagaki et al., 2006). In contrast, nearby sites with different sedimentary environments contain very different populations, suggesting that environmental factors on energetic constraints and availability may significantly affect the geographic distribution of microbial communities and their metabolic processes (Inagaki et al., 2006).

Other studies demonstrated the presence of previously undiscovered and therefore uncharacterized phylogenetic lineages in subseafloor sediment, even within a few meters of the seafloor (Sørensen et al., 2004). For example, archaeal 16S rRNA gene clone libraries from shallow sediment (≤2.1 mbsf) collected during the KNOX-02RR cruise show that the diversity of predominant archaeal components shift from *Nitrosopmilus*-related ammonia oxidizers (α-sub-

group) to physiologically unknown members of η- and υ-subgroups within the Marine Crenarchaeota Group I (Durbin and Teske, 2010).

In combination with the metabolic points described above, these genetic discoveries underscore three important points about potential community composition in subseafloor sediment of the South Pacific Gyre. First, the gyre's subseafloor microbial communities may greatly differ from those of any subseafloor environments explored to date. Second, the very low activity and potentially aerobic communities of the deepest sediment in the South Pacific Gyre are likely to contain unique and previously undiscovered microorganisms. Third, exploration of the gyre sediment may provide deep insight into community composition and structure throughout much of the open ocean, because the genetic communities of subseafloor sediment in the other major ocean gyres may resemble those of the South Pacific Gyre.

The second primary objective is to test how oceanographic factors (such as surface ocean productivity) control variation in sedimentary habitats, activities and community compositions from gyre center to gyre margin.

Key question is: How are subseafloor sedimentary activities and community compositions affected by oceanographic properties that vary predictably from gyre center to gyre margin?

Expedition 329 provides an unprecedented opportunity to document how the nature of subseafloor sedimentary life varies with oceanographic properties in the least biologically active region of the world ocean.

Interstitial water surveys of regions with higher organic fluxes to the seafloor, such as the equatorial Pacific and continental margins, suggest that the principal electron-accepting activity and the net rates of electron-accepting activities vary predictably with sea-surface chlorophyll content and organic flux to the seafloor (D'Hondt et al., 2002, 2004). These relationships appear to be principally due to reliance of subseafloor sedimentary communities on burial of photosynthesized organic matter for electron donors. Other sedimentary properties that vary with measures of oceanic productivity include sediment composition, which depends on the rate of microfossil production in the overlying water column as well as on the position of the carbonate compensation depth (CCD), and sediment thickness, which largely depends on the rate of calcium carbonate and biogenic silica production in the overlying water column.

The KNOX-02RR results (D'Hondt et al., 2009) suggest that the principal electron-accepting activity,

net rates of activities, and cell concentrations in the shallow subseafloor sediment of the South Pacific Gyre may vary with sea-surface chlorophyll content from within the gyre to outside the gyre and perhaps from site to site within it. Expedition 329 will test these predictions.

The third primary objective is to quantify the extent to which these sedimentary microbial communities may be supplied with electron donors by water radiolysis.

Key question is: To what extent does the ecosystem of organic-poor sediment depend on in situ radiolysis of interstitial water?

Expedition 329 provides an unprecedented opportunity to determine if subseafloor life in very low activity sediment is nourished to a significant extent by H_2 from in situ radiolysis of water.

Buried organic matter appears to be the principal source of electron donors in subseafloor sediment of ocean margins and the equatorial Pacific (D'Hondt et al., 2004). However, the burial flux of organic carbon is so low in the South Pacific Gyre that in situ radiolysis of water may be the principal source of electron donors there (D'Hondt et al., 2009) (Fig. F5).

Water radiolysis has been described as a possible source of energy for ecosystems in hard rock far beneath continental surfaces (Pedersen, 1996; Lin et al., 2005a). The longest-lived products of water radiolysis are the electron donor H_2 and the electron acceptor O_2 (Debierne, 1909). H_2 can be supplied by in situ radiolysis or, in theory, by transport of radiolytic H_2 from a much deeper biologically dead environment (e.g., the mantle and oceanic basement deep beneath sediment).

The potential importance of water radiolysis to subseafloor sedimentary communities can be assessed by comparing radiolytic H_2 production to organic-fueled respiration. For this comparison, in situ H_2 production by water radiolysis must be quantified from

- Logging estimates of uranium, thorium, and potassium concentrations (D'Hondt, Jørgensen, Miller, et al., 2003) or inductively coupled plasma–mass spectrometry data (Blair et al., 2007);
- Shipboard physical properties measurements (porosity and density) (D'Hondt, Jørgensen, Miller, et al., 2003); and
- A numerical model of water radiolysis (Blair et al., 2007).

Water radiolysis may provide a higher flux of electron donors than buried organic matter in gyre sediment. Organic-fueled respiration rates are much lower in this sediment than in any previously drilled regions of the world ocean. Clay-rich sediment contains much higher concentrations of radioactive elements than other types of deep-sea sediment. Furthermore, in fine-grained porous sediment, most alpha- and beta-energy production occurs within striking range of interstitial water. Consequently, clay-rich sediment will yield much higher rates of water radiolysis than other geological environments.

Quantification of rates of microbial uptake of radiolytic H_2 requires measurement of dissolved H_2 concentrations in the cored sediment (Fig. F6). The expected rate of radiolytic H_2 production is so high (D'Hondt et al., 2009) that in situ H_2 concentrations are measurable onboard if the H_2 is not biologically utilized. If H_2 is biologically utilized, its in situ concentrations will be below detection; because of its high activation enthalpy, the recombination of O_2 and H_2 does not occur at measurable rates at temperatures below 400°C. Bacterial catalysis allows this reaction on a timescale of minutes.

A number of postexpedition studies will help to further constrain the role of radiolysis in the subseafloor sediment and basalt of the South Pacific Gyre. Measurement and transport modeling of He^{-4} concentration profiles will constrain estimates of radiolysis rates independently of estimates based on abundances of radioactive elements. Postcruise experiments with sterilized samples of cored sediment and basalt plus tritium-labeled water may be used to verify rates of H_2 production by water radiolysis. Similar (unlabeled) experiments with artificial radiation sources were done by Lin et al. (2005b). Radiolysis rates may be compared to measured hydrogen turnover in sediment incubations with known numbers of microbial cells using an array of relevant electron acceptors (O_2, NO_3^-, and oxidized metals). In this way, possible rates of microbial hydrogen oxidation in the subsurface ecosystem can be constrained.

The fourth primary objective is to determine how basement habitats, potential activities and, if measurable, communities vary with crust age and hydrologic regime (from ridge crest to abyssal plain).

Key questions are: How does the habitability of subseafloor basalt change with crust age? How does this change depend on basement hydrologic evolution and mineral alteration? Do fractures remain open for flow in basalt as old as 100 Ma? What is the role of sediment cover in controlling hydrologic flow, alteration, and habitability in subseafloor basalt? Are dissolved oxidants (oxygen and nitrate) available in thinly sedimented subseafloor basalt as old as 100 Ma? Are reduced elements (e.g., iron and sulfur)

available for oxidation in basalt as old as 100 Ma? Does mineral oxidation support measurable microbial activity in this basalt?

Expedition 329 provides a unique opportunity to determine how basement habitability and microbial communities vary with crust age, sediment cover, and hydrologic conditions over 100 m.y. or more of basement history and in the most thinly sedimented region of the world ocean.

Subseafloor basalt has been proposed as the largest potential microbial habitat on Earth (Fisk et al., 1998). Glass alteration textures have been interpreted as evidence of microbial colonization in subseafloor basalt as old as 145 Ma (Fisk et al., 1998; Furnes and Staudigel, 1999). Laboratory experiments indicate that microbial communities may play an important role in basalt weathering (Staudigel et al., 1998). Other experiments with cultured isolates and biomineralogical studies using seafloor basalts suggest that microbes can receive their energy from rock weathering (e.g., oxidation of reduced iron and sulfur in minerals) (Edwards et al., 2003). A study of fluid samples from a cased borehole in 3.5 Ma basalt on the eastern flank of the Juan de Fuca ridge showed that thermophilic microbes exist in the borehole (Cowen et al., 2003; Nakagawa et al., 2006; Orcutt et al., 2011).

Despite this evidence, the nature and extent of subseafloor basaltic communities remain largely unknown and the factors that control the "metabolic habitability" of the basalt (the ability of the basalt to fuel microbial reactions) are largely unexplored. The biological significance of the textural features and the factors that control alteration and its timing in crust are not well constrained.

Metabolic habitability of subseafloor basalt ultimately depends on the supply of electron donors (including reduced Fe and S) in the basalt and hydrogen from in situ radiolysis and the supply of electron acceptors (e.g., O_2 and NO_3^-) from seawater flowing into and through the basalt. Processes that change these supplies over the basalt's lifetime include mineral alteration, which changes the supply of electron donors, and the evolution of hydrologic flow through the basalt, which changes the supply of electron acceptors.

Evolution of crust alteration and metabolic habitability

Compilation of DSDP/ODP geochemical data, mostly from the North Atlantic, suggests that oxidation of Fe and S in the upper few hundred meters of subseafloor basalt occurs principally during the first 10 m.y. after basalt formation (Bach and Edwards, 2003). During this interval, the Fe(III)/ΣFe ratio of the bulk basalt in the database increases from ~0.15 to 0.35 and most of the sulfur is oxidized (Bach and Edwards, 2003). Whether this alteration is microbially mediated or not, it changes the redox habitability of the basalt. Alteration patterns are heterogeneous within and between cores, with greatest alteration in permeable zones, such as brecciated pillows (Bach and Edwards, 2003).

Recent studies of altered basalt at ODP Site 801 (~170 Ma) showed that alteration characteristics of this ancient oceanic basement are generally similar to those observed in much younger crust (e.g., ODP Hole 504B at ~6 Ma), suggesting that most alteration takes place when oceanic crust is young (Alt et al., 1992). If oxidative alteration ceases 10–15 m.y. after basalt formation, then the oceanic crust inhabitable by mineral-oxidizing microbes is limited to basalt younger than 10–15 Ma.

Other evidence suggests that oxidative alteration need not be limited to basalt younger than 10–15 Ma. Older basalt has potential for continued redox alteration, and it probably occurs in some geochemical/hydrological regimes. Geophysical measures of matrix density suggest that about half of all intergrain-scale crustal alteration in the uppermost basalt occurs in basement older than 10–15 Ma (Jarrard et al., 2001). In the equatorial Pacific, dissolved O_2 and NO_3^- are present in basement as old as 35 Ma (D'Hondt et al., 2004). As much as 65% of the Fe remains as Fe(II) in shallow oceanic basalt older than 10 Ma (Bach and Edwards, 2003). Whether this Fe(II) continues to be oxidized at very slow rates where exposed to dissolved O_2 and NO_3^- or is physically inaccessible to oxidation remains to be determined.

Sediment thickness provides one explanation for the average change in redox alteration at 10–15 Ma. Once sedimentary cover is thick, laterally extensive, and anoxic enough to seal basement from contact with oxidized seawater, redox disequilibria (habitability) may disappear and oxidative alteration cease. Drilling basement of different ages beneath the unusually thin sediment cover in this region of the Pacific presents a unique test of this hypothesis. If a critical sediment thickness is necessary to curtail oxidative alteration, then the young (13.5 Ma), moderate (33.5 Ma), and old (84–125 Ma) basement sites drilled during Expedition 329 will exhibit more intense or differing styles of alteration relative to other fast-spreading sites of comparable age and greater sediment cover (e.g., Site 801, ~400 m of sediment at ~170 Ma; ODP Site 1256, ~200 m of sediment at 15 Ma; and Hole 504B, ~250 m of sediment at ~6 Ma). If this is the case, the basaltic environment of the South Pacific Gyre is redox habitable for many tens of millions of years after basalt formation.

Evolution of crustal hydrology and chemical habitability

The timing and distribution of shallow basement alteration is intriguingly linked to evidence of the hydrologic evolution of subseafloor basalt. Seismic velocity and macroporosity data suggest that porosity and bulk permeability of subseafloor basalt decrease rapidly during the first 10–15 m.y. after basalt formation (Jarrard et al., 2001). These decreases are thought to derive from secondary mineralization in the basalt. This mineralization reduces surface area within the basalt and may limit electron donor and nutrient availability in the basaltic aquifer.

Global compilations of heat flow data indicate that advective heat loss is high in young seafloor and decreases with increasing age until ~65 Ma, where, on average, advective heat loss ceases (Stein and Stein, 1994) (Fig. F7). Fisher and Becker (2000) explain these observations by invoking closure of small-scale permeability in basement within 10–15 m.y. but ongoing flow for 65 m.y. in large fractures and faults that fill a relatively small volume of the rock. Three mechanisms are thought responsible for limiting hydrothermal circulation in old crust:

- Buildup of laterally extensive low-permeability sediment cover that isolates the oceanic crust from overlying seawater;
- Ongoing mineralization, which decreases basement permeability with age; and
- Decreasing basal heat flux with age, which reduces the driving force for buoyant fluid flow.

Basement permeability is commonly thought to ultimately control the cessation of hydrothermal circulation (Stein and Stein, 1994; Jarrard et al., 2001). However, a growing body of evidence suggests that oceanic basalt remains permeable enough to sustain advective heat loss through its life. This evidence includes the significant variance in age-dependent heat flow averages (Stein and Stein, 1994) (Fig. F7), large variations in heat flow survey data of Cretaceous-aged basement (Von Herzen, 2004; Fisher and Von Herzen, 2005) velocity logs, macroporosity data, matrix data (Jarrard et al., 2001), present-day fluid flow within ~132 Ma basement at ODP Site 1149 (Shipboard Scientific Party, 2000), and celadonite precipitation ages that indicate low-temperature fluid circulation at the Trodos ophiolite (Gallahan and Duncan, 1994). Given these lines of evidence, the termination of the average heat flow deficit at ~65 Ma probably signifies that much of the open circulation between basaltic basement and ocean has largely stopped by then, rather than that hydrothermal flow has ended (Anderson and Skilbeck, 1981; Jacobson, 1992; Stein and Stein, 1994).

We hypothesize that old seafloor can host advective fluid and that the thin sediment cover characterizing the South Pacific Gyre facilitates fluid flow in old oceanic crust. If this hypothesis is true, the apparent waning of hydrothermal circulation at ~65 Ma is controlled by sediment thickness or declining heat flow, rather than by basement permeability. The South Pacific Gyre offers a unique opportunity to test this hypothesis because its sediment is thin and its basement relief is relatively variable. Further, this hypothesis implies large-scale permeability will be high regardless of basement age and heat flow data at the drill sites may deviate significantly from conductive values. Surface heat flow data from our recent survey (Fig. F7) and from scattered older measurements within 200 km of Sites U1365 and U1367 suggest that an active flow system may be present in the basement throughout the region of proposed drilling.

An additional implication of this hypothesis is that the supply of the dissolved electron acceptors O_2 and NO_3^- to the upper basement of the South Pacific Gyre may remain high long past the first 10–15 m.y. after basalt formation. If drilling of the lowermost sediment and the basalt shows the occurrence of these electron acceptors in the upper basement at the sites, either (1) the metabolic habitability of South Pacific Gyre basalt remains sufficient to support life for as long as 100 m.y. or (2) the metabolic habitability of this basalt is ultimately controlled by the inaccessibility of electron donors in the basalt rather than by access to electron acceptors. If the first case applies, increased oxidative alteration may be evident in crust of increasingly greater age (e.g., alteration at Site U1365 will be greater than alteration at Site U1367, which will be greater than alteration at Site U1368). If the second case applies, oxidative alteration will be similar at all three sites.

Assessment of the extent and relative importance of secondary alteration to the basaltic basement will require an integrated program of petrographic, geochemical, and borehole analyses. At hand-sample and thin section scales, we will carefully describe general alteration textures and characteristics (e.g., veins, halos, vesicle filling, mineral/matrix replacement, and glass palagonitization), principal secondary mineralogy (e.g., saponite, celadonite, calcite, Fe oxyhydroxide, etc.), and the size, distribution, and orientation of veins and other structural features in the crust. Discrete samples of the core, representing "fresh" (e.g., pristine glass), average, and end-member altered domains, will be powdered and analyzed for bulk major, trace, and volatile element chemistry, as a means of characterizing the bulk crustal compo-

sition and geochemical effects of alteration. Borehole logging and core-log integration are invaluable for reconstructing recovery gaps and estimating bulk geochemical and structural characteristics of deep basement drill sites (Barr et al., 2002; Révillon et al., 2002; Kelley et al., 2003; Pockalny and Larson, 2003). Postexpedition radiogenic isotope measurements will place important constraints on the timing of alteration at each site. For example, calcite formed during crust alteration often contains high concentrations of uranium but little to no lead, making the lead isotopic system a potentially useful calcite precipitation geochronometer, especially in old oceanic crust (Hauff et al., 2003).

Basement community composition

Drilling of the basalt sites during Expedition 329 provides a direct opportunity to test the existence and composition of microbial communities in oceanic basement of three very different ages (13.5, 33.5, and 80–125 Ma). Molecular ecological and biomineralogical studies of uncontaminated basalt from the site with youngest basement will test whether or not microbes take full advantage of the redox habitability of relatively young basalt in open exchange with the overlying ocean while analyses of samples from the sites with older basement will test whether or not ongoing oxidation of the subseafloor basalt (by occurrence of reduced Fe and supply of dissolved O_2 and NO_3^- by ongoing advection and diffusion through the sediment) sustains similar (or different) communities, albeit at slower rates of redox activity. Collectively, the study of these sites will track the compositional and functional evolution of basement microbial communities >100 m.y. in a thinly sedimented region of fast-spreading crust, where we hypothesize supply of dissolved oxidants to continue for as long as 100 m.y. (or more).

Explanation of secondary objectives

Oceanic crust inputs to the subduction factory

The altered oceanic crust at our oldest basement sites (U1365 and U1366) is outboard of the Tonga-Kermadec subduction zone. Characterizing the style and extent of alteration in this subducting plate will provide an important reference for assessing the role of altered oceanic crust in the subduction process. Of global arcs, the Tonga arc has perhaps the smallest sediment flux (Plank and Langmuir, 1998) and the altered oceanic crust in this system is proportionally more influential in the subduction process than at most other arcs. If the low sedimentation rate at this site has resulted in unusual alteration characteristics in the subducting oceanic crust, these differences

may translate into geochemically distinct signatures in the magmas produced at the Tonga arc.

Regional tectonics

Sites U1365 and U1366 are centrally located in ocean crust accreted during the CNS. The tectonic history of this Australia-sized area is poorly constrained because correlatable magnetic seafloor anomalies are not present. Although limited bathymetry data suggest a general north–south spreading direction, the actual direction(s) and the presence of a failed rift within the region are poorly constrained. Drilling and logging ocean crust at these sites would address these questions. Radiometric dating of plagioclase within the recovered basalt would provide important age constraints (Koppers et al., 2003) and structural analysis of dipping flow units with core logging data would provide a spreading direction (Pockalny and Larson, 2003). Resolving the tectonic history of this region is critical to understanding the effect of large igneous provinces on tectonic processes and whether the Ontong Java, Manihiki, and Hikurangi plateaus were created by one or multiple mantle plumes (Taylor, 2006).

Geodynamo

The causal mechanisms for the Cocos-Nazca spreading center are still debated. Some authors have proposed the presence of a strong magnetic field during superchrons (Larson and Olson, 1991; Tarduno et al., 2001), which would argue for an efficient geodynamo (i.e., large intensities during low reversal frequency). Others argue for a weak field (Loper and McCartney, 1986; Pick and Tauxe, 1993), suggesting that increased convective vigor in the core would increase the reversal rate by generating frequent instabilities. If the latter model applies, the Cocos-Nazca spreading center record is low in paleointensity but may contain frequent reversals. Further adding to this controversy, the limited number of paleointensity measurements from the Cocos-Nazca spreading center yielded very different results for different methods (Pick and Tauxe, 1993; Tarduno et al., 2001). Drilling basement at Site U1365 will provide important data and samples to test these models and methods. The paleointensity methods could be compared and the measurements would provide important data (in conjunction with the radiometric age) for the origin of the Cocos-Nazca spreading center and its relationship to the geodynamo.

Paleoceanography

Interstitial waters of the South Pacific Gyre represent a unique archive of glacial-aged water from which

relict NO_3^- can be used to test hypotheses of glacial–interglacial ocean-climate change with significantly lower uncertainty than through proxy measurements.

It has been hypothesized that changes in strength of the biological carbon pump caused the dominant variation in Earth's climate and atmospheric CO_2 over the last 1 m.y. (Broecker, 1982). We will test the two principal models of this variation by reconstructing the preformed NO_3^- content and deep ocean $\delta^{15}NO_3^-$ of the last glacial maximum (LGM) through measurement of O_2, NO_3^-, and $\delta^{15}NO_3^-$ in the interstitial fluid of gyre sediment. Our tests utilize the fact that pore fluids from depths greater than ~30–50 mbsf (e.g., at Sites U1365 and U1370) are samples of paleo–bottom water that have effectively been out of diffusive contact with the ocean since the LGM.

Relationship to previous drilling

Site U1365 is located in the western portion of the gyre, near DSDP Sites 595 and 596 (Menard, Natland, Jordan, Orcutt, et al., 1987). There are no DSDP/ODP/IODP sites near any of the other Expedition 329 sites. The closest sites were cored during Leg 92, which recovered Oligocene and younger sediment from a series of sites at 20°S (Leinen, Rea, et al., 1986). The Leg 92 sites are located beneath higher productivity waters than the central gyre (Fig. F1). The entire sediment column was cored at the Leg 92 sites; basement was encountered between 1 and 50 mbsf (with sediment depth increasing westward).

Coring-drilling strategy

Our general strategy during Expedition 329 was to core the entire sediment column multiple times at seven sites and to core the upper basement at three sites. The sites collectively underlie the full range of surface-ocean productivity conditions present in the South Pacific Gyre, ranging from the extremely low productivity conditions of the gyre center (Site U1368) to the moderately high (for open ocean) productivity at the southern edge of the gyre (Site U1371, at the northern edge of the Antarctic Convergence) (Figs. F1, F2). This series of sites is composed of two transects (Fig. F1), with the first transect centered at ~26°S, beneath the heart of the South Pacific Gyre, and the second transect centered at ~42°S in the southern portion of the gyre.

The sites in the northern sequence have been continuously far from shore and beneath the low-productivity gyre waters for many tens of millions of years (Figs. F1, F2). They provide an ideal opportunity to meet our first objective (to document the nature of life in subseafloor sediment with very low biomass and very low rates of activity). In combination with the southern transect, the northern transect is also necessary to meet our second objective (to determine how subseafloor sedimentary microbial activities and communities vary from gyre center to gyre margin).

Sites U1365 to U1371 are necessary for our third objective (to quantify the extent to which subseafloor communities in organic-poor sediment are sustained by H_2 from radiolysis of water). Sites U1365, U1370, and U1371 are particularly crucial for this objective because their sediment columns are thick enough that their dissolved He^{-4} (alpha particle) concentrations and fluxes will be measurable.

The sites in the second transect have been in the southern portion of the present gyre (Sites U1369 and U1370) or south of the gyre (Site U1371) for tens of millions of years. Particularly at Site U1371, chlorophyll-a concentrations and primary productivity are much higher than at all of the sites in the northern transect (Figs. F1, F2). This transect is necessary to meet our second objective (to document how subseafloor sedimentary microbial activities and communities vary from gyre center to gyre margin). Because Site U1371 provides an anoxic standard of comparison for the other sites, it is also crucial for documenting the potential uniqueness (or ubiquity) of the microbial communities and activities that persist in the low-activity, low-biomass sediment beneath the gyre center.

The northern sequence of sites (U1365–U1368) is placed on basaltic basement of steadily increasing age from east to west (Fig. F2). Basaltic basement ranges in age from 7 to as much as 125 Ma (Site U1365). Basement age of the southern sites ranges from 39 to 73 Ma. Their water depths generally follow the classic curve (Parsons and Sclater, 1977) of increasing water depth with increasing basement age (Fig. F2). These sites are necessary to meet our fourth objective (to document the evolution of basalt hydrology and its implications for metabolic habitability and microbial communities in ocean crust under very thin sediment cover).

Expedition synthesis

Sediment

Expedition 329 sites are located along two transects, hinged in the center of the South Pacific Gyre (Figs. F1, F2). The first transect progresses from the western edge of the gyre (Site U1365) to the gyre center (Site U1368). The second transect goes from the gyre center (Site U1368) through the southern gyre edge

(Site U1370) to the northern edge of the upwelling region south of the gyre (Site U1371).

The dominant lithology is zeolitic metalliferous clay at the deeper water sites on older basement (58 to ≤120 Ma) within the gyre (Sites U1365, U1366, U1369, and U1370) (Figs. F2, F8). Manganese nodules occur at the seafloor and intermittently within the upper sediment column at these sites. Chert and porcellanite layers are pronounced in the lower half of the sediment column at Sites U1365 and U1366. The dominant lithology is carbonate ooze at Site U1368, the site on youngest basement (13.5 Ma) and, consequently, in the shallowest water. At Site U1371, which lies on relatively old basaltic basement (71.5–73 Ma) just south of the gyre, the dominant lithology is siliceous ooze, although metalliferous zeolitic clay dominates the lowest portion of this sediment column.

The dominant lithology shifts from clay to carbonate ooze at depth in two of the sites (Fig. F8). At Site U1367, the transition from clay to carbonate at 6–7 mbsf marks the time that the site subsided beneath the CCD as the underlying basement cooled with age. At Site U1370, carbonate ooze is the dominant lithology for a short interval deposited during planktonic foraminiferal Zone P1. This foraminifer-bearing interval is most simply interpreted as resulting from the CCD diving to greater water depth than the water depth of this site during the early Paleocene interval of low planktonic carbonate production.

Sediment thickness is generally very low throughout the gyre (Fig. F8). When sites of broadly similar age are compared (Site U1366, 84–120 Ma; Site U1369, 58 Ma; Site U1370; 74–80 Ma; and Site U1371, 71.5–73 Ma), thickness of the sediment column generally increases with increasing distance from the gyre center (Figs. F1, F2, F8).

Sedimentary microbial communities and habitability

Throughout the South Pacific Gyre (Sites U1365–U1370), dissolved oxygen and dissolved nitrate are present throughout the entire sediment column (Fig. F9), indicating that microbial respiration is oxic throughout the column, as predicted by D'Hondt et al. (2009) and Fischer et al. (2009). The concentration profiles of oxygen and nitrate demonstrate subseafloor O_2 loss and NO_3^- production indicating that the subseafloor rate of microbial respiration is generally extremely low.

In contrast, at Site U1371 in the upwelling zone just south of the gyre (Fig. F1), detectable dissolved oxygen and dissolved nitrate are limited to just below the sediment/water interface and just above the sedi-

ment/basalt interface. Between these interfaces the sediment is anoxic. Very high concentrations of dissolved (presumably reduced) manganese indicate that manganese reduction is a prominent electron-accepting process throughout most of this sediment column, with perhaps very short intervals of iron reduction as suggested by minor peaks in dissolved iron concentration associated with local minima in dissolved manganese concentration. The rapid drop of dissolved oxygen and nitrate below their detection limits at the upper and lower edges of this sediment column and the relatively high concentrations of dissolved phosphate within this column suggest that the subseafloor rate of microbial respiration is much higher at this site than at the sites located in the gyre.

Geographic variation in subseafloor profiles of dissolved oxygen, dissolved nitrate, dissolved phosphate, dissolved inorganic carbon (DIC), total solid-phase organic carbon (TOC), and total solid-phase nitrogen are consistent with the magnitude of organic-fueled subseafloor respiration declining from outside the gyre (Site U1371) to gyre margins (Sites U1365 and U1370) to gyre center (Site U1368) (Figs. F1, F9, F10).

At all sites located within the gyre (Sites U1365–U1370), microbial cell counts are three or more orders of magnitude lower than at the same sediment depths in all sites previously cored by scientific ocean drilling (Fig. F11). Microbial cell counts are generally higher at Site U1371 than at the sites within the gyre (Sites U1365–U1370) but are lower than at all other sites previously drilled.

At all sites in the gyre, TOC and total nitrogen decline rapidly with depth in the upper sediment column and are generally constant at greater depth (Fig. F10). In contrast, at Site U1371 TOC and total nitrogen are generally much higher than at the other sites at all depths.

Countable cells disappear within the upper sediment column at every site in the gyre. Dissolved oxygen content, dissolved nitrate concentration, TOC, and total nitrogen stabilize as countable cells disappear. The downhole disappearance of countable cells and measurable oxygen reduction appears to result from the disappearance of organic electron donors.

Dissolved oxygen, dissolved nitrate, dissolved phosphate, and DIC are present throughout the entire sediment column at all sites in the gyre (Sites U1365–U1370) (Fig. F9), indicating that microbial life is not limited by availability of electron acceptors or major nutrients (carbon, nitrogen, and phosphorus) in this sedimentary environment. At Site U1371, dissolved oxygen is absent from most of the sedi-

ment column, but the dissolved manganese concentration profile suggests that manganese reduction occurs through most of the sequence. Dissolved sulfate, dissolved nitrate, dissolved phosphate, and DIC are present throughout the entire sediment column at Site U1371, indicating that microbial life is not limited by availability of electron acceptors or major nutrients in this sedimentary environment either.

Dissolved hydrogen concentration is below detection in the upper sediment column of all sites within the gyre (Fig. F10). At most sites, it rises above detection with increasing depth. Because dissolved H_2 is continually produced by in situ water radiolysis, the presence of dissolved H_2 in many samples suggests that hydrogen-utilizing microbial activity is impaired or absent at sample depths where H_2 concentration is detectable and oxygen is present. At Site U1371, which is anoxic throughout most of the sediment column, dissolved hydrogen concentration is low, but above detection limits through much of the column, with slightly higher values at the base of the column. In the deepest sediment at that site, the apparent coexistence of dissolved oxygen, dissolved manganese, and dissolved hydrogen suggests that microbial activity at that depth is insufficient to fully remove either oxygen or the electron donors, manganese and hydrogen.

The sulfate anomaly profile and the occurrence of disseminated pyrite in the upper 10 m of sediment at Site U1371 suggest that sulfate and manganese reduction co-occur within the column.

Paleoceanography

High-resolution measurements of dissolved chloride and nitrate concentrations, as well as formation factor, provide the opportunity for reconstruction of glacial seawater characteristics through the South Pacific Gyre. Given the importance of this region to ocean circulation, such reconstruction will greatly contribute to understanding of the global ocean-climate system.

Basalt

The uppermost basaltic basement at Site U1365 is composed of lava flows, whereas the uppermost basement at Sites U1367 and U1368 is primarily composed of pillow basalt.

Basalt alteration

Alteration in lava flow units, as evident at Site U1365, appears to be strongly controlled by lithologic structure, with most alteration focused at the

flow boundaries (Fig. F12). In contrast, alteration in pillow lava units (the dominant lithologies at Sites U1367 and U1368) appears to be more evenly distributed.

At all sites, the presence of dissolved oxygen in the lowermost sediment at below–deep water concentrations (Fig. F9) suggests that either (1) basement oxidation has occurred since seawater migrated into the formation or (2) oxygen has been lost to the overlying sediment along the flow path.

At the sites with oldest basement, alteration of the basement basalt continues on the timescale of formation fluid replacement. Natural gamma radiation (NGR) core logs, downhole NGR logs (Site U1368), and chemical analyses of the rock demonstrate that potassium has been consistently taken up during basalt alteration at all three sites where the basaltic basement was drilled (Sites U1365, U1367, and U1368). At the sites with deepest sediment (Site U1365, where basalt was drilled, plus Sites U1370 and U1371, where basalt was not drilled), dissolved potassium concentrations are noticeably lower in the deepest sediment than in the shallow sediment (Fig. F13), indicating that (1) dissolved potassium fluxes into the underlying basalt and (2) basalt alteration continues despite the great age of basement at all three sites (84–120, 74–79.5, and 71.5–73, respectively).

At all three sites where basement was cored by rotary core barrel (RCB) (Sites U1365, U1367, and U1368), secondary minerals provide evidence of both oxidative alteration (iron oxyhydroxide and celadonite) and oxygen-poor alteration (saponite and secondary sulfides). Some samples have undergone multiple stages of alteration. Late vein infills suggest that alteration may be continuous or at least occur intermittently throughout the life of the ocean crust. At Site U1365, the presence in the lowermost sediment of dissolved Mg at below-deepwater concentrations and dissolved Ca at above-deepwater concentrations indicates that basalt-water interaction in the form of Mg exchange for Ca has occurred since seawater migrated into the formation. This exchange may continue to drive late-stage calcite precipitation, despite the great age of basement at this site (80–120 Ma).

Habitability of basaltic basement

Profiles of dissolved oxygen, DIC, dissolved nitrate, and dissolved phosphate in the lowermost sediment at each site indicate that if microbial life is present in the uppermost basalt (Fig. F9), it is not limited by access to electron acceptors (oxygen and nitrate) or major nutrients (carbon, nitrogen, and phosphorus).

Past microbial activity?

Tubelike microscale weathering features occur in altered glass from Site U1365 (Fig. F14). They are arranged in discrete clusters or in masses adjacent to or near fractures and iron oxyhydroxide within the glass. Similar features have been observed in marine basaltic glass elsewhere and attributed to microbial origin (e.g., Fisk et al., 1998).

Technical advances

Expedition 329 used a wide range of instruments and techniques that have not been used often on scientific ocean drilling expeditions. Details of their Expedition 329 application are provided in the "Methods" chapter (Expedition 329 Scientists, 2011), particularly in the "Biogeochemistry," "Microbiology," and "Physical properties."

Two technical approaches were used by the Expedition 329 Scientific Party on an experimental basis, with the intention of refining them for future application. The first of these techniques was a new method of cell counting using flow cytometry (Morono et al., 2011). The second was use of NGR core logging for shipboard quantification of absolute concentrations of ^{238}U-series elements, ^{232}Th-series elements, and potassium (M. Vasilyev and R. Harris, unpubl. data)

Preliminary scientific assessment

Expedition 329 had the following four fundamental objectives:

- To document the habitats, metabolic activities, genetic composition and biomass of microbial communities in subseafloor sediment with very low total activity.
- To test how oceanographic factors (such as surface ocean productivity, sedimentation rate, and distance from shore) control variation in sedimentary habitats, activities and community compositions from gyre center to gyre margin.
- To quantify the extent to which subseafloor microbial communities of this region may be supplied with electron donors (energy sources) by water radiolysis, a process independent of the surface photosynthetic world.
- To determine how basement habitats, potential activities and, if measurable, microbial communities vary with crust age and hydrologic regime (from ridge crest to abyssal plain).

The expedition made major strides toward fulfilling all of these objectives.

Shipboard biogeochemistry, lithostratigraphy, microbiology, and physical properties studies documented many fundamental aspects of subseafloor sedimentary habitats, metabolic activities, and biomass in this very low activity sedimentary ecosystem. Documentation of genetic composition and additional aspects of sedimentary habitability and biomass must await shore-based study.

Shipboard biogeochemical and cell-enumeration results have also significantly improved understanding of how oceanographic factors control variation in subseafloor sedimentary habitats, activities, and biomass from gyre center to gyre margin. Postexpedition studies are necessary to improve understanding of the underlying mechanisms and to test how oceanographic factors control variation in community composition.

Shipboard studies have quantified the availability of dissolved hydrogen throughout the sediment column and taken the samples necessary to quantify in situ rates of radiolytic hydrogen production. Postexpedition analyses of these samples are required to quantify these rates and their distribution throughout the sediment column of each site.

Shipboard biogeochemical, petrological, and physical properties data document first-order patterns of basement habitability and potential microbial activities. A broad range of postexpedition studies will be necessary to further constrain habitability and to test how microbial community structure varies with basement age, water-rock interactions, and hydrologic regime.

Site summaries

During Expedition 329 we drilled and/or cored in 42 holes at 7 sites ranging from 3749 to 5707 meters below sea level (mbsl). We cored 1321.8 m of sediment and basalt and recovered 1168.8 m of core (Table T1). Downhole logs were collected in one hole.

Site U1365

The scientific objectives at Site U1365 (proposed Site SPG-1A) are

- To document the nature of subseafloor life in very old (>100 Ma) and slowly accumulating organic-poor sediments;
- To test how oceanographic factors (such as surface ocean productivity, sedimentation rate and distance from shore) control variation in sedimentary habitats, activities, and community compositions from gyre center to gyre margin;
- To quantify the extent to which subseafloor microbial communities in organic-poor sediment are sustained by H_2 from radiolysis of water; and

- To determine how basement habitats, potential activities, and, if measurable, communities vary with basalt age and hydrologic regime (from ridge crest to abyssal plain).

Site U1365 (5695 mbsl) is centrally located in ocean crust formed during the CNS. The tectonic history of this Australia-sized area is poorly constrained because correlatable magnetic seafloor anomalies are not present. Consequently, radiometric dating of the recovered basalt will provide important constraints on the tectonic and volcanic history of this region.

The complete sedimentary succession was recovered by the advanced piston corer (APC) in Hole U1365A. Excluding a drilled-over chert interval in the lower sediment column, complete successions were also recovered from Holes U1365B and U1365C. Core recovery in the underlying basalt was unusually high (75%). However, slow penetration (<1 m/h) allowed us to drill only ~50 m of basalt, preventing us from reaching sufficient depth below seafloor to deploy downhole logging tools.

Principal results

Sediment

The sedimentary succession at Site U1365 is composed of three lithologic units. Unit I consists of medium-brown zeolitic metalliferous pelagic clay (0–44 mbsf). Unit II consists of porcellanite and chert (44–65 mbsf). Unit III consists of dark brown metalliferous clay (65–75 mbsf) (Fig. F15).

Microbial cell counts are three or more orders of magnitude lower than at the same sediment depths in all sites previously cored by scientific ocean drilling and decline to near the minimum detection limit (MDL) at 15 mbsf. They are above the MDL (1.4×10^3 cells/cm^3) in many samples (and below the MDL in many other samples) for the remainder of Unit I (Fig. F16). Because the chert cannot be disaggregated, the presence or absence of cells cannot be determined in Unit II. Cell counts are consistently below the MDL in the metalliferous clay at the base of the sediment column (Unit III).

Dissolved oxygen is present throughout the entire sediment column at Site U1365. It declines most rapidly in the first several meters of the sediment column and then declines at increasingly lower rates with increasing depth in Unit I (Fig. F17A). We could not measure its concentration in the chert and porcellanite of Unit II. Its concentration is essentially constant throughout Unit III.

Dissolved nitrate, dissolved phosphate, and DIC are also present throughout the sediment column. The increase in dissolved nitrate concentration (from ~35 to 45 µM) over the uppermost 20 mbsf is consistent with nitrate production by oxygen-fueled reduction of organic matter (Fig. F17B). Below the chert-dominated interval, dissolved nitrate concentration approximates the present deepwater value.

Dissolved hydrogen concentration is below detection throughout most of the sediment column (with the exception of a 30 nM peak centered at 30 mbsf).

The concentration of total nitrogen declines rapidly in the first 10 mbsf from 0.05 to 0.01 wt%. It then declines more slowly until it drops consistently beneath its MDL (~0.007 wt%) at 38 mbsf. Consistently, TOC declines rapidly over the first few meters below seafloor (from ~0.2 to 0.05 wt%) and remains below 0.05 wt% for the remainder of the sediment column (Fig. F18).

Basalt

The drilled sequence of basement rock is composed of a series of massive basalt flows (Fig. F12). Massive flows at the top of deep-sea basement are unusual in ocean drilling history (e.g., ODP Site 1256 and Site 1243 [interpreted as a lava pond]). The low-temperature alteration is similar to alteration in the uppermost basalt at other ocean drilling sites (Menard, Natland, Jordan, Orcutt, et al., 1987; Laverne et al., 1996; Teagle et al., 1996; Teagle, Alt, Umino, Miyashita, Banerjee, Wilson, and the Expedition 306/312 Scientists, 2006).

Relationships between igneous unit boundaries and alteration indicate that alteration at Site U1365 is strongly controlled by the structure of the basalt (Fig. F12). Ingress of seawater, secondary mineral precipitation, and wall-rock interaction is primarily restricted to regions between lava flows. A direct relationship between visual observations of alteration and NGR-based potassium content (Fig. F12) indicates that NGR can provide a more accurate and quantitative approach to estimating alteration extent than visual interpretation alone.

Secondary minerals provide evidence of both oxidative and oxygen-poor alteration. Some samples have undergone several stages of vein opening and halo emplacement. Minerals indicative of oxygen-poor alteration are most prevalent toward the base of the drilled basalt column.

Tubelike microscale weathering features occur in altered glass and discrete clusters or masses adjacent to fractures and iron oxyhydroxide (Fig. F14). Similar features have been observed in marine basaltic glass elsewhere and attributed to microbial origin (Fisk et al., 1998).

Multiple episodes of late-stage calcite precipitation and vein infill have occurred at Site U1365. These late fills suggest that alteration may be continuous or

at least occur intermittently during the life of the ocean crust. Dissolved concentrations of magnesium and calcium in the lowermost sediment indicate that basalt-water interaction in the form of Mg exchange for Ca has occurred since seawater migrated into the formation. This exchange may continue to drive late-stage calcite precipitation.

General results

Downhole temperature was measured using the advanced piston corer temperature tool. Six measurements give a least-squares thermal gradient of 76°C/km. This result closely agrees with the thermal gradient observed by site survey cruise KNOX-02RR of 74°C/km (D'Hondt et al., 2011). The heat flow of 61 mW/m² is typical for crust of this age. Bottom water temperature is 1.22°C and temperature at the sediment/basement interface is estimated to be 6.8°C. These temperatures are well within the range inhabited by psychrophilic microbes.

A wide range of microbiology and biogeochemistry experiments was initiated shipboard. Experiments on major microbial processes and cultivation of viable microbes were initiated on samples taken at selected depths ranging from near the sediment/water interface to nearly 50 m into the basaltic basement. Subsamples for shore-based biogeochemical and molecular ecological studies were routinely taken from all of the distinct lithologic units.

Site U1366

The scientific objectives at Site U1366 (proposed Site SPG-2A) are

- To document the habitats, metabolic activities, genetic composition, and biomass of microbial communities in subseafloor sediment with very low total activity;
- To test how oceanographic factors control variation in sedimentary habitats, activities, and community compositions from gyre center to gyre margin;
- To quantify the extent to which these sedimentary microbial communities may be supplied with electron donors by water radiolysis; and
- To assess from pore water chemistry how basement habitats and potential activities vary in the underlying basalt with crust age and sediment thickness (from ridge crest to abyssal plain).

Site U1366 (5129 mbsl) is located in ocean crust formed during the CNS. The complete sedimentary succession, from seafloor to underlying basalt, was recovered by APC coring in Hole U1366F. Partial suc-

cessions, from seafloor to various depths, were also recovered from Holes U1366B–U1366E.

Principal results

The sediment at Site U1366 is primarily clay and is assigned to two lithologic units: zeolitic metalliferous pelagic clay (Unit I) and metalliferous clay (Unit II) (Fig. F19). The principal components of the sediment are smectite, mica-group members, phillipsite, and red-brown to yellow-brown semiopaque oxide (RSO). Manganese nodules are relatively common at the seafloor and at depth in Unit I. The nodules generally produce peaks in NGR, magnetic susceptibility, and gamma ray attenuation density. Both clay and zeolite exhibit overall trends of decreasing abundance with increasing depth.

NGR core logging can be used to quantify in situ concentrations of potassium, ^{238}U-series isotopes and ^{232}Th-series isotopes (Fig. F20). Prominent NGR features at Site U1366 include (1) a pronounced peak in ^{238}U-series isotopes just below the seafloor and (2) NGR peaks associated with manganese nodules, which were temporarily removed from the core for additional NGR logging. The manganese nodules (at the seafloor and at depth) do not contribute to the ^{238}U-isotope peak just below the seafloor.

Cell counts for Site U1366 sediment are three or more orders of magnitude lower than at the same depths in all sediment cored gathered by previous scientific ocean drilling expeditions. Cell counts range from below the MDL (1.4×10^3 cells/cm³) to nearly 10^4 cells/cm³. They do not exhibit any consistent trend with depth (Fig. F21).

The concentration of total nitrogen declines steadily from 0.04 wt% at the seafloor to below detection at 15 mbsf. TOC declines downhole to ~0.03 wt% at 10.75 mbsf (Fig. F22).

Dissolved oxygen is present throughout the entire sediment column. Its concentration drops rapidly by 20 µM in the uppermost 3 mbsf and declines linearly with depth to ~110 µM at the sediment/basalt interface. Over the uppermost ~10 mbsf, dissolved nitrate and DIC increase slightly in concentration (from ~35 to ~40 µM and ~2.5 to ~2.7 mM, respectively) (Fig. F23A, F23B). Both are relatively stable for the remainder of the sediment column. These gradual increases are consistent with oxygen-fueled reduction of organic matter in the first 10 mbsf.

Dissolved hydrogen concentration is below detection throughout the uppermost 15 m of the sediment column but rises by several tens of nannomolar as the basaltic basement is approached.

Chloride concentrations increase monotonically from ~550 mM to reach a maximum of ~570 mM in the lowermost 5 m of the sediment column (a 3% increase) (Fig. **F23C**). This increase is most likely due to relict glacial seawater and, possibly, hydration of the underlying basement.

A wide range of microbiology and biogeochemistry experiments was initiated shipboard. Experiments on major microbial processes and cultivations of viable microbes were initiated on samples taken at selected depths ranging from near the sediment/water interface to the sediment/basement contact. Subsamples for shore-based biogeochemical and molecular ecological studies were routinely taken from all of the distinct lithologic units.

Site U1367

Site U1367 (proposed Site SPG-4A) was selected as a drilling target because (1) its microbial activities and cell counts were expected to be characteristic of a setting midway between the western gyre edge and the gyre center, and (2) its basement age renders it a reasonable location for documenting microbial habitability and testing the extent of basalt alteration and openness to flow in a thinly sedimented region of ~33.5 Ma basaltic basement.

The principal objectives at Site U1367 are

- To document the habitats, metabolic activities, genetic composition, and biomass of microbial communities in subseafloor sediment with very low total activity;
- To test how oceanographic factors control variation in sedimentary habitats, activities, and community compositions from gyre center to gyre margin;
- To quantify the extent to which these sedimentary microbial communities may be supplied with electron donors by water radiolysis; and
- To determine how habitats, potential activities and, if measurable, communities in subseafloor basalt vary with crust age and hydrologic regime (from ridge crest to abyssal plain).

Site U1367 (4289 mbsl) is located in ocean crust formed during magnetic polarity Chron 13n (33.3–33.7 Ma; Gradstein et al., 2004). The complete sedimentary succession, from seafloor to underlying basalt, was recovered by APC coring in Holes U1367B–U1367E. The sediment/basalt contact varies by a few meters from hole to hole. The lowermost sediment and fragments of the underlying basalt were recovered by RCB coring in Hole U1367F. Core recovery of the basalt was unusually low (11%). Continuous fall-in of basaltic debris forced us to terminate the hole early, preventing us from reaching sufficient depth below seafloor to deploy downhole logging tools.

Principal results

Sediment

The sediment at Site U1367 is composed of 5.5–7 m of pelagic clay (lithologic Unit I) overlying ~16 m of Oligocene carbonate ooze (Unit II) (Fig. **F24**). The principal components of the clay are smectite and mica-group members, phillipsite (a zeolite), and RSO. The ooze is composed mainly of coccolithophores and RSO, accompanied by foraminifers. The clay and ooze differ significantly in several physical properties, including porosity, bulk density, electrical conductivity, magnetic susceptibility, and NGR. The transition from clay to ooze is gradual. The depth of the sediment/basalt interface varies by ~3 m from hole to hole. Although unit thickness and composition vary from hole to hole, general sediment composition is very similar in each hole.

Microbial cell counts decline rapidly from ~10^5 cells/cm³ at 0.15 mbsf to the MDL (10^3 cells/cm³) at 2 mbsf. Cell counts are mostly below the MDL throughout the remaining sediment column.

The concentration of total nitrogen declines to below detection (from 0.03% to 0.0%) in the uppermost 7 mbsf. TOC declines from 0.17 to 0.02 wt% over the same interval.

Dissolved nitrate, dissolved phosphate, and DIC are present throughout the sediment column (Fig. **F25**). Dissolved oxygen also occurs throughout the column. Dissolved hydrogen concentration is below detection in most of the clay but above detection in most samples of the carbonate.

Basalt

The recovered sequence of basement rock is composed of pillow basalt fragments with prominent chill margins. Secondary mineralization and wallrock interaction is limited in the recovered basalt. However, it is likely that the most altered portions of the basalt were not recovered.

A wide range of microbiology experiments was initiated shipboard. Experiments on major microbial processes and cultivations of viable microbes were initiated on samples taken at selected depths ranging from near the sediment/water interface to ~30 m into the basaltic basement. Subsamples were routinely taken from all of the distinct lithologic units for postcruise molecular assays and microbiological experiments.

Site U1368

Site U1368 (proposed Site SPG-6A) was selected as a drilling target because (1) its microbial activities and cell counts were expected to be characteristic of the gyre center and (2) its basement age renders it a reasonable location for testing the extent of microbial habitability and basalt alteration in a thinly sedimented region of ~13.5 Ma basaltic basement.

The principal objectives at Site U1368 are

- To document the habitats, metabolic activities, genetic composition, and biomass of microbial communities in subseafloor sediment with very low total activity;
- To test how oceanographic factors control variation in sedimentary habitats, activities, and community compositions from gyre center to gyre margin;,
- To quantify the extent to which these sedimentary microbial communities may be supplied with electron donors by water radiolysis; and
- To determine how habitats, potential activities, and, if measurable, communities in subseafloor basalt vary with crust age and hydrologic regime (from ridge crest to abyssal plain).

Site U1368 (3740 mbsl) is located in ocean crust formed during magnetic polarity Chron 5ABn (13.4–13.6 Ma; Gradstein et al., 2004). Most or all of the sedimentary succession was recovered by APC coring in Holes U1368B–U1368E. Basalt fragments were recovered from the basal cores of Holes U1368B and U1368D. The uppermost ~100 m of basalt was cored using RCB in Hole U1368F. Approximately 60 m of the basaltic basement was logged with both the triple combination and Formation MicroScanner tool string.

Principal results

Sediment

The sediment at Site U1368 is 15–16 m thick and consists of calcareous ooze, pelagic clay, and lithic sand. (Fig. F26). An additional 1 m of volcaniclastic breccia was recovered from an interval between basalt flows, 80 m below the upper sediment/basalt interface. The principal components of the ooze are calcareous nannofossils accompanied by RSO and foraminifers. Planktonic foraminiferal biostratigraphy indicates that the calcareous ooze spans from the middle Miocene to the middle Pliocene. Clay minerals are in relatively low abundance throughout the sediment. The lowermost sediment contains one to three sandy intervals that collectively contain a wide variety of minerals, including albite-anorthite, ankerite, augite, calcite, chlorite, hematite, and ti-

tanomagnetite. The volcaniclastic breccia contains altered basaltic lithic and vitric grains.

Microbial cell counts decline rapidly from 10^5 to 10^6 cells/cm^3 just below the seafloor to slightly more than 10^3 cells/cm^3 at ~5 mbsf. Cell counts hover near the MDL (10^3 cells/cm^3) for the remainder of the sediment column.

The concentration of total nitrogen declines to below detection in the uppermost 10 cm below seafloor. TOC declines to 0.03 wt% over the uppermost 0.5 mbsf and remains low for the remainder of the sediment column.

Dissolved nitrate, dissolved phosphate, DIC, and dissolved oxygen are present throughout the sediment column. Dissolved hydrogen concentration is below detection for the first 9.4 mbsf but above detection in half of the samples at greater depth (Fig. F27).

Basalt

The recovered sequence of basement rock is composed of pillow basalt fragments with prominent chill margins.

Estimates of potassium content derived from downhole NGR logging agree closely with potassium concentration estimates derived from NGR logging of whole-round cores (Fig. F28).

A wide range of microbiology experiments was initiated shipboard. Experiments on major microbial processes and cultivations of viable microbes were initiated on samples from selected depths ranging from near the sediment/water interface to ~100 m into the basaltic basement. Subsamples were routinely taken from all of the distinct lithologic units for postcruise molecular assays and microbiological experiments.

Site U1369

Site U1369 (proposed Site SPG-10A) was selected as a drilling target because (1) its microbial activities and cell counts were expected to be characteristic of midway between gyre center and the southern gyre edge and (2) its basement age renders it a reasonable location for testing the extent of sediment-basement interaction in a thinly sedimented region of ~58 Ma basaltic basement.

The principal objectives at Site U1369 are

- To document the habitats, metabolic activities, genetic composition, and biomass of microbial communities in subseafloor sediment with very low total activity;
- To test how oceanographic factors control variation in sedimentary habitats, activities, and

community compositions from gyre center to gyre margin;

- To quantify the extent to which these sedimentary microbial communities may be supplied with electron donors by water radiolysis; and
- To determine how sediment-basement exchange and potential activities in the basaltic basement vary with basement age and hydrologic regime (from ridge crest to abyssal plain).

Site U1369 is located in the South Pacific Gyre at 5277 mbsl. Basement age is estimated from extrapolated magnetic models and changes in spreading rate recorded by neighboring magnetic profiles. Our best estimate of the crustal age is ~58 Ma and corresponds to magnetic polarity Chron 25r (57.2–58.4 Ma; Gradstein et al., 2004). The sedimentary succession was recovered by APC coring in Holes U1369B, U1369C, and U1369E. Basalt fragments were recovered from the basal cores of these holes.

Principal results

Sediment

The sediment at Site U1369 consists of ~16 m of zeolitic metalliferous clay. The sediment is massive in texture and contains visible burrows throughout. The principal components of the clay are phillipsite, RSO, and clay (Fig. F29). Manganese nodules were recovered from the sediment/water interface and from deeper in the sediment column. Micro- and nannofossils are almost completely absent. The sediment/basalt interface consists of vitric sand overlying altered basalt. Sediment thickness and composition are fairly uniform from hole to hole.

Microbial cell counts decline rapidly from ~10^5 cells/cm^3 just below the seafloor to ~10^3 cells/cm^3 at ~2 mbsf (Fig. F30). Cell counts are below the MDL (~10^3 cells/cm^3) for the remainder of the sediment column.

Total nitrogen and TOC decrease rapidly from near the seafloor to ~3 mbsf and are extremely low for the remainder of the sediment column.

Dissolved oxygen, dissolved nitrate, dissolved phosphate, and DIC are present throughout the sediment column (Fig. F31). Dissolved hydrogen concentration is consistently low throughout the column.

A wide range of microbiology experiments was initiated shipboard. Experiments on major microbial processes and cultivations of viable microbes were initiated with samples from selected depths ranging from near the sediment/water interface to the sediment/basalt interface. Subsamples were routinely taken from all of the distinct lithologic units for postcruise molecular assays and microbiological experiments.

Site U1370

Site U1370 (proposed Site SPG-11B) was selected as a drilling target because (1) its microbial activities and cell counts were expected to be characteristic of midway between gyre center and the southern gyre edge and (2) its basement age renders it a reasonable location for testing the extent of sediment-basement interaction in a moderately sedimented region of 74–80 Ma basaltic basement.

The principal objectives at Site U1370 are

- To document the habitats, metabolic activities, genetic composition, and biomass of microbial communities in subseafloor sediment with low total activity;
- To test how oceanographic factors control variation in sedimentary habitats, activities, and community compositions from gyre center to gyre margin;
- To quantify the extent to which these microbial communities may be supplied with electron donors by water radiolysis; and
- To determine how sediment-basement exchange and potential activities in the basaltic basement vary with basement age and hydrologic regime (from ridge crest to abyssal plain).

Site U1370 is located in the South Pacific Gyre at 5074 mbsl. The coring site is located within magnetic polarity Chron 33n, so the crustal age may range from 73.6 to 79.5 Ma (Gradstein et al., 2004). The sedimentary succession was recovered by APC coring in Holes U1370D, U1370E, and U1370F. Altered basaltic fragments were recovered from the basal cores of Holes U1370D and U1370F.

Principal results

Sediment

The sediment at Site U1370 is ~70 m thick. The dominant lithology is dark brown zeolitic metalliferous pelagic clay (Fig. F32). The principal components of the clay are RSO, phillipsite, and smectite. Lithologic Unit I lies between the sediment/water interface and the top of a nannofossil ooze (Unit II) at ~61 mbsf. Unit II is a relatively short (30–290 cm) pale yellow interval predominantly composed of coccolithophores, with trace phillipsite, and clay. Unit III is a thin clay interval containing 88% RSO and 12% clay that directly overlays the basaltic basement. Although volcanic glass is locally abundant (~43%) in Unit I, its overall abundance is only 7%, and it is completely absent in Units II and III. A large, fragmented manganese nodule was recovered in Hole U1370D at 10 mbsf, and fragments of a manganese-encrusted hardground were in recovered in Hole U1370F at 52 mbsf.

Overall sediment structure at Site U1370 is massive, although occasional laminations and thin beds are visible in the lower half of Unit I. *Planolites* (horizontal) burrows are faintly visible in most of the clay and *Trichichnus* (vertical) burrows blend the upper and lower contacts of the nannofossil ooze and the overlying and underlying clay. Sediment thickness and composition are uniform from hole to hole.

The nannofossil ooze was deposited during early Paleocene foraminiferal Zone P1. Its occurrence in this deep-sea clay sequence is attributed to deepening of the CCD and lysocline during the interval of decreased planktonic carbonate precipitation that followed the end-Cretaceous mass extinction (D'Hondt, 2005).

Microbial cell counts were above the MDL (~10^3 cells/cm³) throughout much of the sediment column.

The dissolved oxygen and nitrate profiles at Site U1370 (Fig. **F33**) exhibit much greater curvature than the profiles at previous Expedition 329 sites. Dissolved oxygen concentration decreases sharply in the uppermost several meters below seafloor and then more gradually to 40 mbsf. Below that depth, it decreases monotonically from ~10 μM to a few micromolar at the sediment/basalt interface. The rate of increase in dissolved nitrate concentration from surface sediment to 20 mbsf is higher than at previous sites (U1365–U1369), suggesting that organic nitrogen oxidation in the sediment is greater here than at those sites. The changes in dissolved oxygen and nitrate throughout the upper sediment column are attributed to oxygen consuming organic oxidation by sedimentary microbes.

Basalt

Dissolved potassium concentration declines nearly linearly with depth in the sediment (Fig. **F34**), indicating a sink for dissolved potassium in the underlying basaltic basement. This sink is inferred to be basalt alteration (clay formation).

A wide range of microbiology experiments was initiated shipboard. Experiments on major microbial processes and cultivations of viable microbes were initiated with samples taken at selected depths ranging from near the sediment/water interface to the sediment/basalt interface. Subsamples were routinely taken from all of the distinct lithologic units for postcruise molecular assays and microbiological experiments.

Site U1371

Site U1371 (proposed Site SPG-12A) was selected as a drilling target because (1) its microbial activities and cell counts were expected to be characteristic of the upwelling region just south of the gyre and (2) its basement age renders it a reasonable location for testing the extent of sediment-basement interaction in a moderately sedimented region of 71.5–73 Ma basaltic basement.

The principal objectives at Site U1371 are

- To document the nature of life in moderately slowly accumulating sediments of great age (as old as 73 Ma), where the surface ocean is characterized by moderate mean chlorophyll content (<3 mg/m³);
- To determine the extent to which basement age, thermal regime, and chemical transport through the 73 Ma basaltic basement affect microbial communities and biogeochemical processes in the sediment and the extent to which chemical transport and microbial activities in the sediment affect the alteration and habitability of the basaltic basement;
- To provide a much higher activity standard of comparison for the sites within the gyre (Sites U1365–U1370); and
- To test the extent to which life in this sediment may be supplied with an electron donor (dissolved hydrogen) by radiolysis of water.

Site U1371 is located in the South Pacific Gyre at 5301 mbsl. The coring site is located within magnetic polarity Chron 32n.2n, so the crustal age may range from 71.5 to 72.9 Ma (Gradstein et al., 2004). Based on a tectonic reconstruction of the region by Larson et al. (2002), the crust was accreted along the Pacific-Phoenix spreading center at ~73 Ma. The sedimentary succession was recovered by APC coring in Holes U1371D–U1371F. Additional mudline cores were recovered in Holes U1371B, U1371C, U1371G, and U1371H. Altered basaltic fragments were recovered from the basal core of Hole U1371F.

Principal results

Sediment

The sediment at Site U1371 consists of ~130 m of diatom ooze and pelagic clay, divided into two lithologic units based on their sharply contrasting mineralogy (Fig. **F35**). Unit I is ooze with average diatom and clay content of 56% and 17%, respectively. It is 104–107 m thick and contains numerous ash layers and multiple thin hardgrounds. Unit II is a blend of clay (32%), zeolite (30%), and RSO (15%). The transition from ooze to clay constitutes the upper 5 m of Unit II; this portion of Unit II contains as much as 26% diatoms. Other minor sedimentary components at Site U1371 include quartz, pyrite, manganese ox-

ide/hydroxide, radiolarians, spicules, and silicoflagellates.

The clay-bearing diatom ooze and pelagic clay at Site U1371 form interbedded intervals of highly fossiliferous and clay-rich layers. Bioturbation is a prominent feature of the sediment, causing diffuse boundaries on most beds. Overall sediment thickness and composition appear to be broadly uniform from hole to hole.

Microbial cell counts were above the MDL (~10^3 cells/cm³) throughout much of the sediment column.

Profiles of dissolved chemicals clearly indicate that most of the sediment column is anoxic, with thin oxic zones at the top and bottom of the column (Fig. **F36**). Manganese is a prominent net electron acceptor throughout most of the column. Dissolved oxygen concentration decreases rapidly within the first meter below seafloor and is below detection by ~5 mbsf. Below that depth, it is indistinguishable from zero until to a few meters above the sediment/basalt interface, when it rises to a few micromolar. Dissolved oxygen content generally matches sediment color, with dissolved oxygen present in the brown sediment at the top and bottom of the column but indistinguishable from zero throughout the gray sediment that characterized most of the column. Dissolved nitrate disappears within 2.5 mbsf but reappears above the sediment/basalt interface, from 105 to 120 mbsf (the deepest sample analyzed for nitrate). Dissolved ammonium rises from 0.35 μM at 0.15 mbsf to a maximum of ~55 μM between 30 and 65 mbsf and then decreases slightly to 40 μM at 97 mbsf (no deeper samples were analyzed for ammonium). Dissolved manganese strongly increases to ~360 μM in the uppermost 3 mbsf, exhibits four broad maxima and three local minima within the column, and decreases to ~70 μM at ~128 mbsf. Redox potential, measured by electrode, broadly mirrors the dissolved iron (Fe) profile, with positive potential and low dissolved Fe at the top and bottom of the sediment column, but generally low potential and high dissolved Fe content throughout most of the column. Three minima in redox potential within the column correspond to local maxima in dissolved Fe concentration.

Throughout the sediment column, concentrations of dissolved phosphate and DIC are much higher at Site U1371 than at equivalent sediment depths at the sites within the gyre (Sites U1365–U1370). Concentrations of these chemical species peak a few meters below seafloor.

Shipboard studies of Site U1371 found at least four additional results of note. First, the presence of py-

rite in the uppermost 0–10 m of the sediment column suggests that sulfate and iron reduction have occurred in the near-seafloor zones of oxygen, nitrate, and manganese reduction. Second, the sulfate anomaly profile suggests that sulfate reduction and manganese reduction may broadly co-occur within the column. Third, dissolved oxygen and dissolved manganese appear to coexist for at least 13 m in the lowermost sediment column. Fourth, dissolved oxygen and dissolved hydrogen also appear to coexist in the lowermost sediment column. Postcruise studies will test (1) the co-occurrence of sulfate reduction, iron reduction, and other redox processes in this sediment column and (2) explanations of the co-occurrence of dissolved oxygen, manganese, and hydrogen deep in the column.

Basalt

The presence of dissolved oxygen, nitrate, phosphate, and DIC in the lowermost sediment indicates that life is not inhibited in the upper basaltic basement by absence of electron acceptors, major nutrients, or carbon.

Dissolved potassium concentration declines with depth in the sediment, indicating a sink for dissolved potassium in the underlying basaltic basement. This sink is inferred to be basalt alteration (clay formation).

A wide range of microbiology and biogeochemistry experiments was initiated shipboard. Experiments on major microbial processes and cultivations of viable microbes were initiated with samples taken at selected depths ranging from near the sediment/water interface to the sediment/basalt interface. Subsamples were routinely taken from all of the distinct lithologic units for postcruise molecular assays and microbiological experiments.

References

Alt, J.C., France-Lanord, C., Floyd, P.A., Castillo, P., and Galy, A., 1992. Low-temperature hydrothermal alteration of Jurassic ocean crust, Site 801. *In* Larson, R.L., Lancelot, Y., et al., *Proc. ODP, Sci. Results,* 129: College Station, TX (Ocean Drilling Program), 415–427. **doi:10.2973/odp.proc.sr.129.132.1992**

Anderson, R.N., and Skilbeck, J.N., 1981. Oceanic heat flow. *In* Emiliani, C. (Ed.), *The Sea* (Vol. 7): *The Oceanic Lithosphere:* New York (Wiley), 489–524.

Bach, W., and Edwards, K.J., 2003. Iron and sulfide oxidation within the basaltic ocean crust: implications for chemolithoautotrophic microbial biomass production. *Geochim. Cosmochim. Acta,* 67(20):3871–3887. **doi:10.1016/S0016-7037(03)00304-1**

Barr, S.R., Révillon, S., Brewer, T.S., Harvey, P.K., and Tarney, J., 2002. Determining the inputs to the Mariana

Subduction Factory: using core-log integration to reconstruct basement lithology at ODP Hole 801C. *Geochem., Geophys., Geosyst.,* 3(11):8901. doi:10.1029/2001GC000255

Behrenfeld, M.J., and Falkowski, P.G., 1997. Photosynthetic rates derived from satellite-based chlorophyll concentration. *Limnol. Oceanogr.,* 42(1):1–20.

Blair, C.C., D'Hondt, S., Spivack, A.J., and Kingsley, R.H., 2007. Radiolytic hydrogen and microbial respiration in subsurface sediments. *Astrobiology,* 7(6):951–970. doi:10.1089/ast.2007.0150

Broecker, W.S., 1982. Ocean chemistry during glacial time. *Geochim. Cosmochim. Acta,* 46(10):1689–1705. doi:10.1016/0016-7037(82)90110-7

Cowen, J.P., Giovannoni, S.J., Kenig, F., Johnson, H.P., Butterfield, D., Rappé, M.S., Hutnak, M., and Lam, P., 2003. Fluids from aging ocean crust that support microbial life. *Science,* 299(5603):120–123. doi:10.1126/science.1075653

Debierne, A., 1909. Radioactivitié: sur la decomposition de l'eau par les sel de radium. *C. R. Acad. Sci.,* 148:703–705.

D'Hondt, S., 2005. Consequences of the Cretaceous/Paleogene mass extinction for marine ecosystems. *Annu. Rev. Ecol. Evol. Syst.,* 36(1):295–317. doi:10.1146/annurev.ecolsys.35.021103.105715

D'Hondt, S., Abrams, L.J., Anderson, R., Dorrance, J., Durbin, A., Ellett, L., Ferdelman, T., Fischer, J., Forschner, S., Fuldauer, R., Goldstein, H., Graham, D., Griffith, W., Halm, H., Harris, R., Harrison, B., Hasiuk, F., Horn, G., Kallmeyer, J., Lever, M., Meyer, J., Morse, L., Moser, C., Murphy, B., Nordhausen, A., Parry, L., Pockalny, R., Puschell, A., Rogers, J., Schrum, H., Smith, D.C., Soffientino, B., Spivack, A.J., Stancin, A., Steinman, M., and Walczak, P., 2011. KNOX-02RR: drilling site survey—life in subseafloor sediments of the South Pacific Gyre. *In* D'Hondt, S., Inagaki, F., Alvarez Zarikian, C.A., and the Expedition 329 Scientists, *Proc. IODP,* 329: Tokyo (Integrated Ocean Drilling Program Management International, Inc.). doi:10.2204/iodp.proc.329.112.2011

D'Hondt, S., Inagaki, F., and Alvarez Zarikian, C., 2010. South Pacific Gyre Microbiology. *IODP Sci. Prosp.,* 329. doi:10.2204/iodp.sp.329.2010

D'Hondt, S., Jørgensen, B.B., Miller, D.J., Batzke, A., Blake, R., Cragg, B.A., Cypionka, H., Dickens, G.R., Ferdelman, T., Hinrichs, K.-U., Holm, N.G., Mitterer, R., Spivack, A., Wang, G., Bekins, B., Engelen, B., Ford, K., Gettemy, G., Rutherford, S.D., Sass, H., Skilbeck, C.G., Aiello, I.W., Guerin, G., House, C.H., Inagaki, F., Meister, P., Naehr, T., Niitsuma, S., Parkes, R.J., Schippers, A., Smith, D.C., Teske, A., Wiegel, J., Naranjo Padillo, C., and Solis Acosta, J.L., 2004. Distributions of microbial activities in deep subseafloor sediments. *Science,* 306(5705):2216–2221. doi:10.1126/science.1101155

D'Hondt, S., Rutherford, S., and Spivack., A.J., 2002. Metabolic activity of the subsurface life in deep-sea sediments. *Science,* 295(5562):2067–2070. doi:10.1126/science.1064878

D'Hondt, S., Spivack, A.J., Pockalny, R., Ferdelman, T.G., Fischer, J.P., Kallmeyer, J., Abrams, L.J., Smith, D.C.,

Graham, D., Hasiuk, F., Schrum, H., and Stancine, A.M., 2009. Subseafloor sedimentary life in the South Pacific Gyre. *Proc. Natl. Acad. Sci. U. S. A.,* 106(28):11651–11656. doi:10.1073/pnas.0811793106

D'Hondt, S.L., Jørgensen, B.B., Miller, D.J., et al., 2003. *Proc. ODP, Init. Repts.,* 201: College Station, TX (Ocean Drilling Program). doi:10.2973/odp.proc.ir.201.2003

Durbin, A.M., and Teske, A., 2010. Sediment-associated microdiversity within the Marine Group I Crenarchaeota. *Environ. Microbiol. Rep.,* 2(5):693–703. doi:10.1111/j.1758-2229.2010.00163.x

Edwards, K.J., Rogers, D.R., Wirsen, C.O., and McCollom, T.M., 2003. Isolation and characterization of novel psychrophilic, neutrophilic, Fe-oxidizing, chemolithoautotrophic alpha- and gamma-Proteobacteria from the Deep Sea. *Appl. Environ. Microbiol.* 69(5):2906–2913. doi:10.1128/AEM.69.5.2906-2913.2003

Expedition 329 Scientists, 2011. Methods. *In* D'Hondt, S., Inagaki, F., Alvarez Zarikian, C.A., and the Expedition 329 Scientists, *Proc. IODP,* 329: Tokyo (Integrated Ocean Drilling Program Management International, Inc.). doi:10.2204/iodp.proc.329.102.2011

Fischer, J.P., Ferdelman, T.G., D'Hondt, S., Røy, H., and Wenzhöfer, F., 2009. Oxygen penetration deep into the sediment of the South Pacific gyre. *Biogeosciences,* 6:1467–1478. http://www.biogeosciences.net/6/1467/2009/bg-6-1467-2009.pdf

Fisher, A.T., and Becker, K., 2000. Channelized fluid flow in oceanic crust reconciles heat-flow and permeability data. *Nature (London, U. K.),* 403(6765):71–74. doi:10.1038/47463

Fisher, A.T., and Von Herzen, R.P., 2005. Models of hydrothermal circulation within 106 Ma seafloor: constraints on the vigor of fluid circulation and crustal properties, below the Madeira Abyssal Plain. *Geochem., Geophys., Geosyst.,* 6(11):Q11001. doi:10.1029/2005GC001013

Fisk, M.R., Giovannoni, S.J., and Thorseth, I.H., 1998. Alteration of oceanic volcanic glass: textural evidence of microbial activity. *Science,* 281(5379):978–980. doi:10.1126/science.281.5379.978

Furnes, H., and Staudigel, H., 1999. Biological mediation in ocean crust alteration: how deep is the deep biosphere? *Earth Planet. Sci. Lett.,* 166(3–4):97–103. doi:10.1016/S0012-821X(99)00005-9

Gallahan, W.E., and Duncan, R.A., 1994. Spatial and temporal variability in crystallization of celadonites with the Troodos ophiolite, Cyprus: implications for low-temperature alteration of the oceanic crust. *J. Geophys. Res., [Solid Earth],* 99(B2):3147–3161. doi:10.1029/93JB02221

Gieskes, J.M., and Boulègue, J., 1986. Interstitial water studies, Leg 92. *In* Leinen, M., Rea, D.K., et al., *Init. Repts. DSDP,* 92: Washington, DC (U.S. Govt. Printing Office), 423–429. doi:10.2973/dsdp.proc.92.124.1986

Gradstein, F.M., Ogg, J.G., and Smith, A.G. (Eds.), 2004. *A Geologic Time Scale 2004:* Cambridge (Cambridge Univ. Press). http://cambridge.org/uk/catalogue/catalogue.asp?isbn=9780521781428

Hauff, F., Hoernle, K., and Schmidt, A., 2003. Sr-Nd-Pb composition of Mesozoic Pacific oceanic crust (Site

1149 and 801, ODP Leg 185): implications for alteration of ocean crust and the input into the Izu-Bonin-Mariana subduction system. *Geochem., Geophys., Geosyst.,* 4(8):8913. doi:10.1029/2002GC000421

Inagaki, F., Nunoura, T., Nakagawa, S., Teske, A., Lever, M., Lauer, A., Suzuki, M., Takai, K., Delwiche, M., Colwell, F.S., Nealson, K.H., Horikoshi, K., D'Hondt, S., and Jørgensen, B.B., 2006. Biogeographical distribution and diversity of microbes in methane hydrate-bearing deep marine sediments on the Pacific Ocean margin. *Proc. Natl. Acad. Sci. U. S. A.,* 103(8):2815–2820. doi:10.1073/pnas.0511033103

Jacobson, R.S., 1992. Impact of crustal evolution on changes of the seismic properties of the uppermost ocean crust. *Rev. Geophys.,* 30(1):23–42. doi:10.1029/91RG02811

Jahnke, R.A., 1996. The global ocean flux of particulate organic carbon: areal distribution and magnitude. *Global Biogeochem. Cycles,* 10(1):71–88. doi:10.1029/95GB03525

Jarrard, R.D., Abrams, L.J., Pockalny, R.A., Larson, R.L., and Hirono, T., 2001. Physical properties of upper oceanic crust: ODP Hole 801C and the waning of hydrothermal circulation. *Eos, Trans. Am. Geophys. Union,* 82(47)(Suppl.):V21C-0980. (Abstract) http://www.agu.org/meetings/fm01/waisfm01.html

Kelley, K.A., Plank, T., Ludden, J., and Staudigel, H., 2003. Composition of altered oceanic crust at ODP Sites 801 and 1149. *Geochem., Geophys., Geosyst.,* 4(6)8910. doi:10.1029/2002GC000435

Koppers, A.A.P., Staudigel, H., and Duncan, R.A., 2003. High-resolution $^{40}Ar/^{39}Ar$ dating of the oldest oceanic basement basalts in the western Pacific basin. *Geochem., Geophys., Geosyst.,* 4(11):8914. doi:10.1029/2003GC000574

Larson, R.L., and Olson, P., 1991. Mantle plumes control magnetic reversal frequency. *Earth Planet. Sci. Lett.,* 107(3–4):437–447. doi:10.1016/0012-821X(91)90091-U

Larson, R.L., Pockalny, R.A., Viso, R.F., Erba, E., Abrams, L.J., Luyendyk, B.P., Stock, J.M., and Clayton, R.W., 2002. Mid-Cretaceous tectonic evolution of the Tongareva triple junction in the southwestern Pacific Basin. *Geology,* 30(1):67–70. doi:10.1130/0091-7613(2002)030<0067:MCTEOT>2.0.CO;2

Laverne, C., Belarouchi, A., and Honnorez, J., 1996. Alteration mineralogy and chemistry of the upper oceanic crust from Hole 896A, Costa Rica rift. *In* Alt, J.C., Kinoshita, H., Stokking, L.B., and Michael, P.J. (Eds.), *Proc. ODP, Sci. Results,* 148: College Station, TX (Ocean Drilling Program), 151–170. doi:10.2973/odp.proc.sr.148.127.1996

Leinen, M., Rea, D.K., et al., 1986. *Init. Repts. DSDP,* 92: Washington, DC (U.S. Govt. Printing Office). doi:10.2973/dsdp.proc.92.1986

Lin, L.-H., Hall, J., Lippmann-Pipke, J., Ward, J.A., Sherwood Lollar, B., DeFlaun, M., Rothmel, R., Moser, D., Gihring, T.M., Mislowack, B., and Onstott, T.C., 2005. Radiolytic H_2 in continental crust: nuclear power for deep subsurface microbial communities. *Geochem., Geo-*

phys., Geosyst., 6(7):Q07003. doi:10.1029/2004GC000907

Lin, L.-H., Slater, G.F., Sherwood Lollar, B., Lacrampe-Couloume, G., and Onstott, T.C., 2005. The yield and isotopic composition of radiolytic H_2, a potential energy source for the deep subsurface biosphere. *Geochim. Cosmochim. Acta,* 69(4):893–903. doi:10.1016/j.gca.2004.07.032

Lipp, J.S., and Hinrichs, K.-U., 2009. Structural diversity and fate of intact polar lipids in marine sediments. *Geochim. Cosmochim. Acta,* 73(22):6816–6833. doi:10.1016/j.gca.2009.08.003

Lipp, J.S., Morono, Y., Inagaki, F., and Hinrichs K.-U., 2008. Significant contribution of Archaea to extant biomass in marine subsurface sediments. *Nature (London, U. K.),* 454(7207):991–994. doi:10.1038/nature07174

Loper, D.E., and McCartney, K., 1986. Mantle plumes and the periodicity of magnetic field reversals. *Geophys. Res. Lett.,* 13(13):1525–1528. doi:10.1029/GL013i013p01525

Menard, H.W., Natland, J.H., Jordan, T.H., Orcutt, J.A., et al., 1987. *Init. Repts. DSDP,* 91: Washington, DC (U.S. Govt. Printing Office). doi:10.2973/dsdp.proc.91.1987

Morel, A., Gentili, B., Claustre, H., Babin, M., Bricaud, A., Ras, J., and Tiéche, F., 2007. Optical properties of the "clearest" natural waters. *Limnol. Oceanogr.,* 52(1):217–229.

Morono, U., Kallmeyer, J., Inagaki, F., and the Expedition 329 Scientists, 2011. Preliminary experiment for cell count using flow cytometry. *In* D'Hondt, S., Inagaki, F., Alvarez Zarikian, C.A., and the Expedition 329 Scientists, *Proc. IODP,* 329: Tokyo (Integrated Ocean Drilling Program Management International, Inc.). doi:10.2204/iodp.proc.329.110.2011

Nakagawa, S., Inagaki, F., Suzuki, Y., Steinsbu, B.O., Lever, M.A., Takai, K., Engelen, B., Sako, Y., Wheat, C.G., Horikoshi, K., and Integrated Ocean Drilling Program Expedition 301 Scientists, 2006. Microbial community in black rust exposed to hot ridge-flank crustal fluids. *Appl. Environ. Microbiol.,* 72(10):6789–6799. doi:10.1128/AEM.01238-06

Ocean Studies Board and Earth and Life Studies, 2003. *Enabling Ocean Research in the 21st Century: Implementation of a Network of Ocean Observatories*: Washington, DC (National Academies Press). http://www.nap.edu/openbook.php?isbn=0309089905

Orcutt, B.N., Bach, W., Becker, K., Fisher, A.T., Hentscher, M., Toner, B.M., Wheat, C.G., and Edwards, K.J., 2011. Colonization of subsurface microbial observatories deployed in young ocean crust. *ISME J.,* 5(4):692–703. doi:10.1038/ismej.2010.157

Parkes, R.J., Cragg, B.A., and Wellsbury, P., 2000. Recent studies on bacterial populations and processes in subseafloor sediments: a review. *Hydrogeol. J.,* 8(1):11–28. doi:10.1007/PL00010971

Parsons, B., and Sclater, J.G., 1977. An analysis of the variation of ocean floor bathymetry and heat flow with age. *J. Geophys. Res., [Solid Earth],* 82:803–827. doi:10.1029/JB082i005p00803

Pedersen, K., 1996. Microbial life in granite rock [presented at the 1996 International Symposium on Subsurface Microbiology (ISSN-96), Davos, Switzerland, 15–21 September 1996].

Pick, T., and Tauxe, L., 1993. Geomagnetic paleointensities during the Cretaceous normal superchron measured using submarine basaltic glass. *Nature (London, U. K.),* 366(6452):238–242. doi:10.1038/366238a0

Plank, T., and Langmuir, C.H., 1998. The chemical composition of subducting sediment and its consequences for the crust and mantle. *Chem. Geol.,* 145(3–4):325–394. doi:10.1016/S0009-2541(97)00150-2

Pockalny, R.A., and Larson, R.L., 2003. Implications for crustal accretion at fast spreading ridges from observations in Jurassic oceanic crust in the western Pacific. *Geochem., Geophys., Geosyst.,* 4(1):8903. doi:10.1029/2001GC000274

Révillon, S., Barr, S.R., Brewer, T.S., Harvey, P.K., and Tarney, J., 2002. An alternative approach using integrated gamma-ray and geochemical data to estimate the inputs to subduction zones from ODP Leg 185, Site 801. *Geochem., Geophys., Geosyst.,* 3(12):8902. doi:10.1029/2002GC000344

Shipboard Scientific Party, 2000. Site 1149. *In* Plank, T., Ludden, J.N., Escutia, C., et al., *Proc. ODP, Init. Repts.,* 185: College Station, TX (Ocean Drilling Program), 1–190. doi:10.2973/odp.proc.ir.185.104.2000

Shipboard Scientific Party, 2003. Explanatory notes. *In* D'Hondt, S.L., Jørgensen, B.B., Miller, D.J., et al., *Proc. ODP, Init. Repts.,* 201: College Station, TX (Ocean Drilling Program), 1–103. doi:10.2973/odp.proc.ir.201.105.2003

Smith, W.H.F., and Sandwell, D.T., 1997. Global sea floor topography from satellite altimetry and ship depth soundings. *Science,* 277(5334):1956–1962. doi:10.1126/science.277.5334.1956

Sørensen, K.B., Lauer, A., and Teske, A., 2004. Archaeal phylotypes in a metal-rich and low-activity deep subsurface sediment of the Peru Basin, ODP Leg 201, Site 1231. *Geobiology,* 2(3):151–161. doi:10.1111/j.1472-4677.2004.00028.x

Staudigel, H., Yayanos, A., Chastain, R., Davies, G., Verdurmen, E.A.T., Schiffman, P., Bourcier, R., and De Baar, H., 1998. Biologically mediated dissolution of volcanic glass in seawater. *Earth Planet. Sci. Lett.,* 164(1–2):233–244. doi:10.1016/S0012-821X(98)00207-6

Stein, C.A., and Stein, S., 1994. Constraints on hydrothermal heat flux through the oceanic lithosphere from global heat flow. *J. Geophys. Res., [Solid Earth],* 99(B2):3081–3095. doi:10.1029/93JB02222

Tarduno, J.A., Cottrell, R.D., and Smirnov, A.V., 2001. High geomagnetic intensity during the mid-Cretaceous from Thellier analyses of single plagioclase crystals. *Science,* 291(5509):1779–1783. doi:10.1126/science.1057519

Taylor, B., 2006. The single largest oceanic plateau: Ontong Java–Manihiki–Hikurangi. *Earth Planet. Sci. Lett.,* 241(3–4):372–380. doi:10.1016/j.epsl.2005.11.049

Teagle, D.A.H., Alt, J.C., Bach, W., Halliday, A.N., and Erzinger, J., 1996. Alteration of upper ocean crust in a ridge-flank hydrothermal upflow zone: mineral, chemical, and isotopic constraints from Hole 896A. *In* Alt, J.C., Kinoshita, H., Stokking, L.B., and Michael, P.J. (Eds.), *Proc. ODP, Sci. Results,* 148: College Station, TX (Ocean Drilling Program), 119–150. doi:10.2973/odp.proc.sr.148.113.1996

Teagle, D.A.H., Alt, J.C., Umino, S., Miyashita, S., Banerjee, N.R., Wilson, D.S., and Expedition 309/312 Scientists, 2006. *Proc. IODP,* 309/312: Washington, DC (Integrated Ocean Drilling Program Management International, Inc.). doi:10.2204/iodp.proc.309312.2006

Von Herzen, R.P., 2004. Geothermal evidence for continuing hydrothermal circulation in older (>60 Ma) ocean crust. *In* Davis, E.E., and Elderfield, H. (Eds.) *Hydrogeology of the Oceanic Lithosphere:* Cambridge (Cambridge Univ. Press), 414–450.

Whitman, W.B., Coleman, D.C., and Wiebe, W.J., 1998. Prokaryotes: the unseen majority. *Proc. Natl. Acad. Sci. U. S. A.,* 95(12):6578–6583. doi:10.1073/pnas.95.12.6578

Figure F1. Map of annual chlorophyll-a (Chl-a) concentrations overlain by Expedition 329 site locations (white circles) and undrilled alternate site locations (gray circles). White lines indicate basement age in 10 m.y. increments. As illustrated by paleoposition histories of Sites U1365 (survey Site SPG-1A) and U1371 (survey Site SPG-12) (black lines), paleopositions determined with a fixed hotspot reference frame indicate that Sites U1365–U1369 have been in the gyre for tens of millions of years and Site U1371 has been at the gyre margin for tens of millions of years.
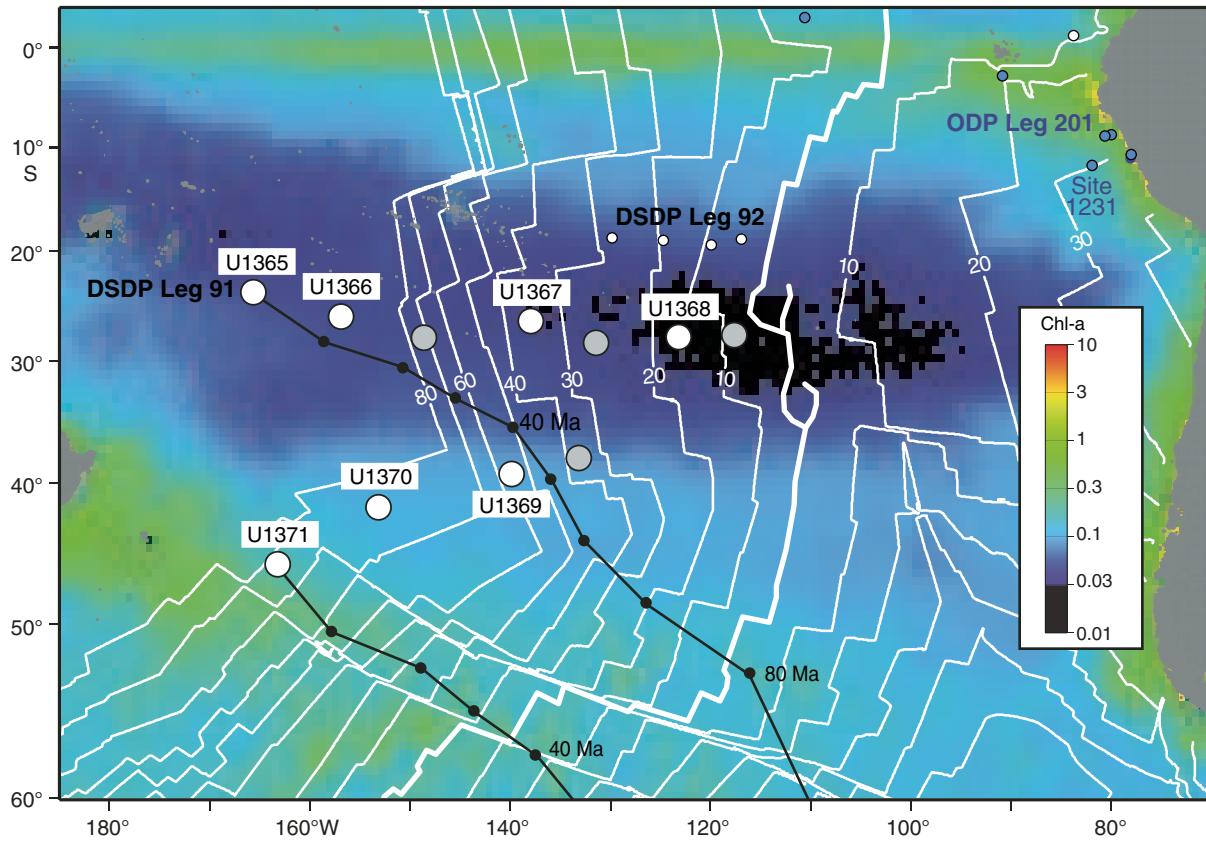
Figure F2. South Pacific seafloor bathymetry map (Smith and Sandwell, 1997) illustrating tectonic setting and location of sites drilled during Expedition 329 (large white circles) and undrilled alternate sites (gray circles). Small white circles mark nearest DSDP drill sites; blue circles mark nearest ODP drill sites.
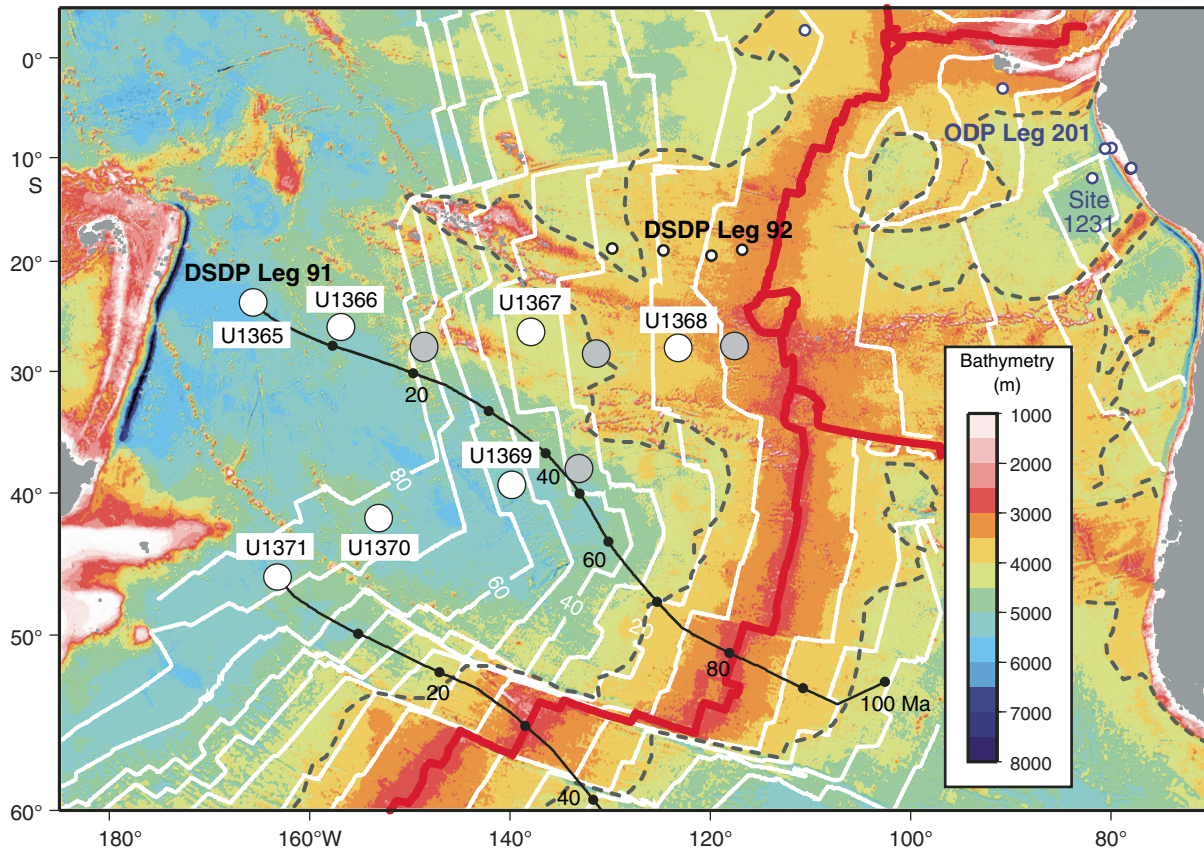
Figure F3. Subseafloor cell concentrations in shallow sediment at Expedition 329 drilling sites (open circles indicate data from sites within the South Pacific Gyre; open triangles indicate data from just outside the gyre). and at all previously counted ODP/IODP sites (solid circles) (D'Hondt et al., 2009). Site U1371 is the only KNOX-02RR survey site at which concentrations approach previous ODP/IODP values.
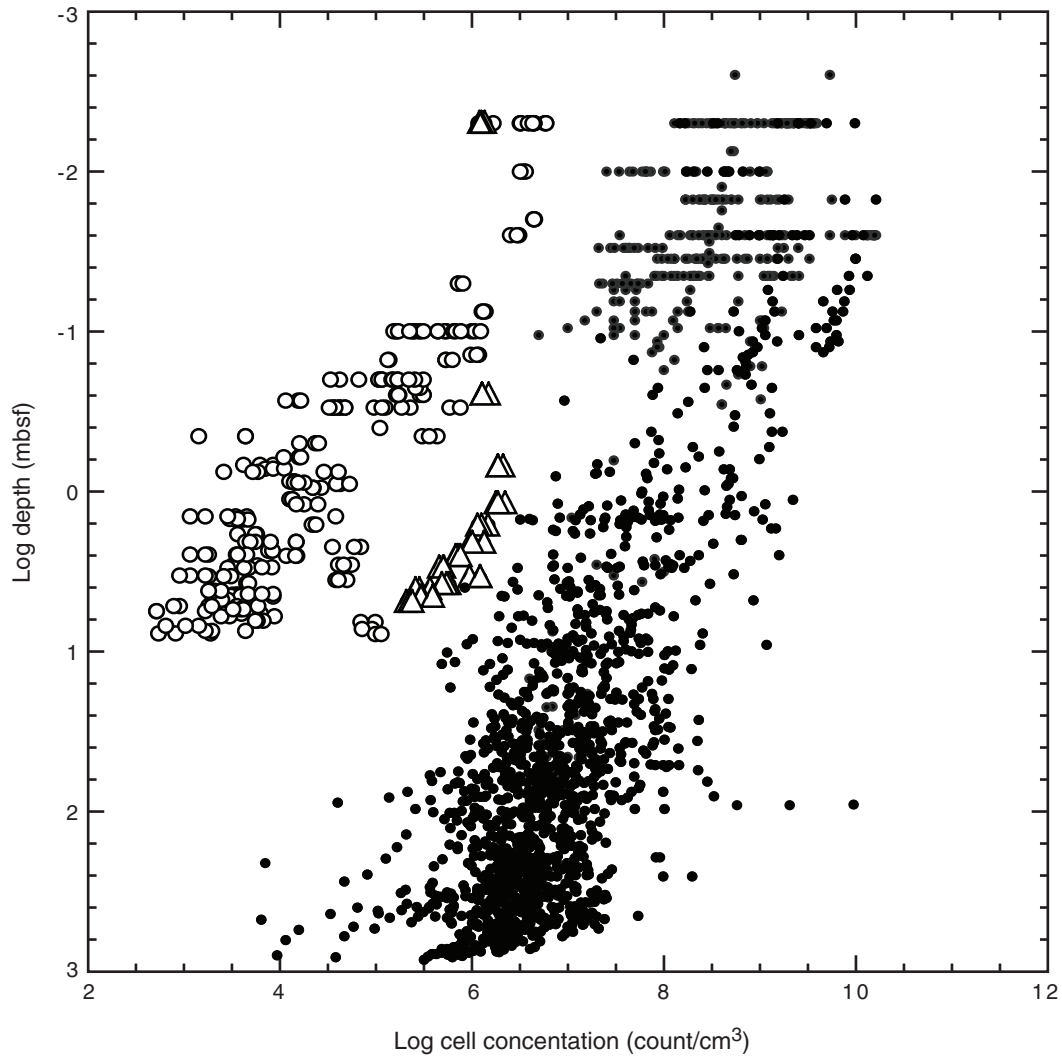
Figure F4. Dissolved (**A**) oxygen (O₂) and (**B**) nitrate (NO₃⁻) profiles in the shallow sediment at KNOX-02RR survey sites (D'Hondt et al., 2009).
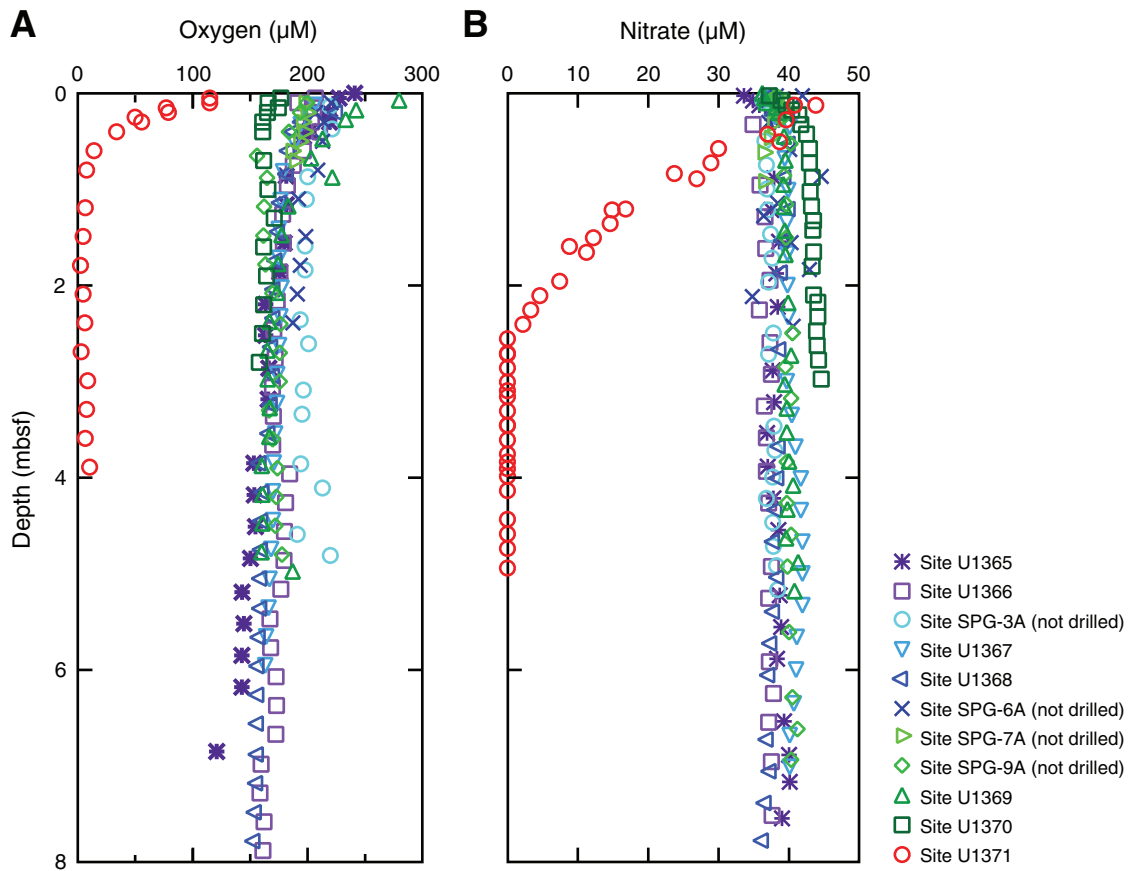
Figure F5. Model for relative rates of organic carbon (OC) oxidation and radiolytic H_2 oxidation with depth. Dotted pink line indicates maximum depth below seafloor cored curing KNOX-02RR survey. Radiolytic H_2 may provide more than half of the electron donors at some proposed sites (D'Hondt et al., 2009). Because OC is oxidized at highest rates in the youngest sediment, at some depth below seafloor (dashed blue line) microbial oxidation of radiolytic H_2 may exceed oxidation of buried organic carbon. At still greater depth (solid green line), reactive organic matter may be depleted and radiolytic H_2 may be the sole electron donor. These predictions can only be tested by drilling the entire sediment column.
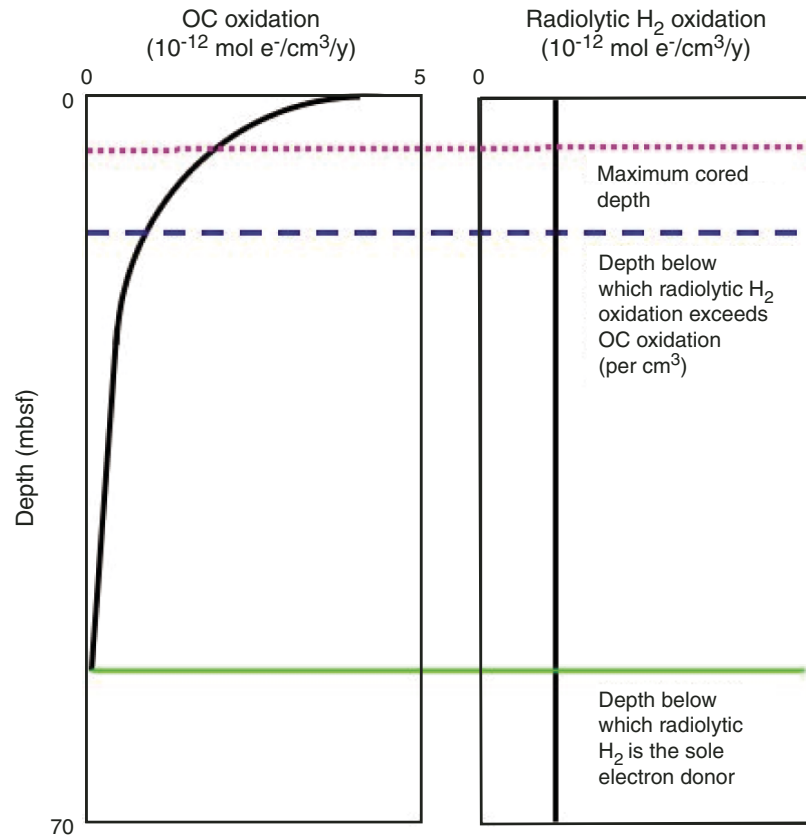
Figure F6. Models of radiolytic H_2 concentrations with depth. If H_2 is microbially oxidized, its concentration will be below our detection limit. Pink line indicates concentrations measured at Site U1370 during KNOX-02RR site survey (below detection limit of 3.5×10^{-8} M). Other lines indicate predicted concentrations if the H_2 is not oxidized (e.g., if sediment is sterile), but radioactivity and porosity are constant throughout the sediment (blue line corresponds to diffusive loss of H_2 to both overlying ocean and underlying basement aquifer, red line corresponds to diffusive loss to the overlying ocean with basement impermeable to chemical exchange). The constancy of radioactivity and porosity with depth and the concentrations of dissolved H_2 at depth can only be tested by drilling to basement.
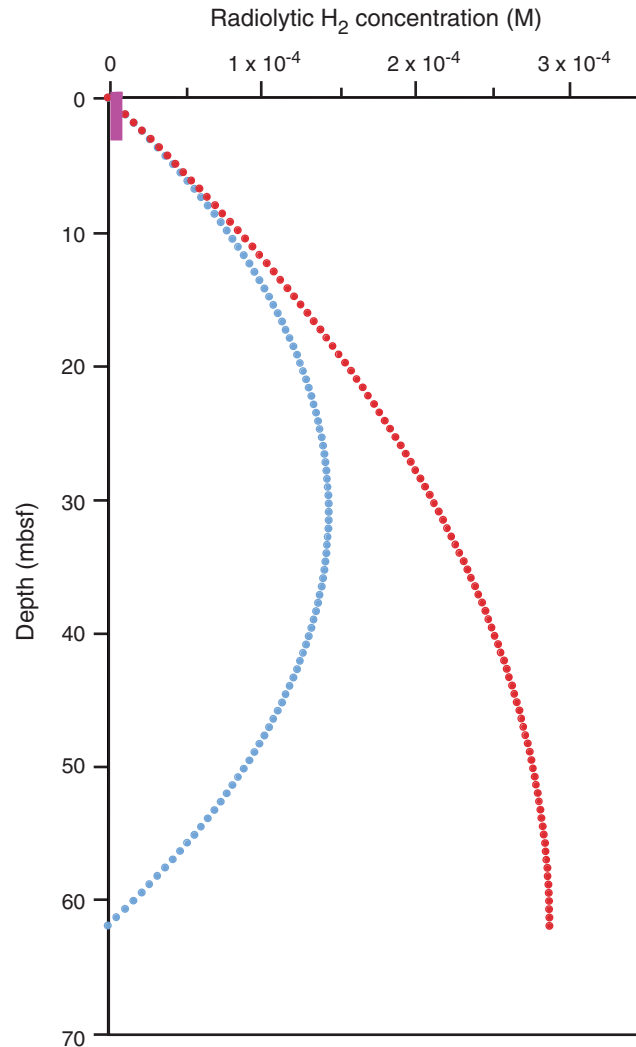
Figure F7. Surface heat flow data from KNOX-02RR survey sites (**D'Hondt et al.,** 2011) superimposed on the compilation data of Stein and Stein (1994). Red circles indicate primary drilling sites, light blue circles mark site survey sites, red arrows indicate primary sites for basement drilling. Heavy black line indicates expected heat flow for conductive crust in the absence of advection. No KNOX-02RR data are available for Sites U1370 or U1371 because of technical failure and thermistor loss. Proposed Sites SPG3, SPG6, and SPG9 were not drilled during Expedition 329.
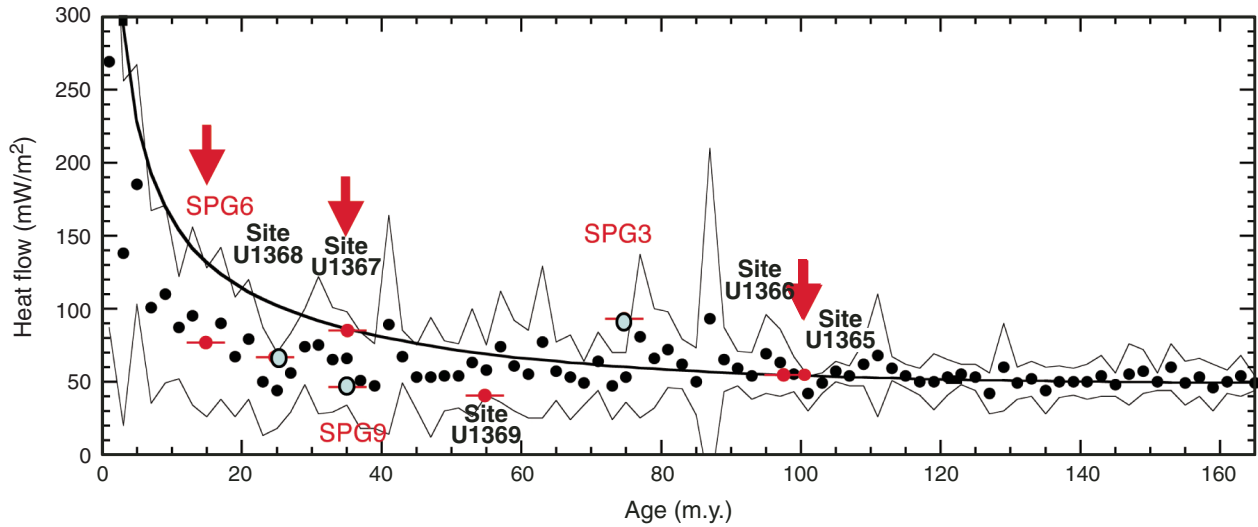
Figure F8. Representative lithologic columns, Sites U1365–U1371.
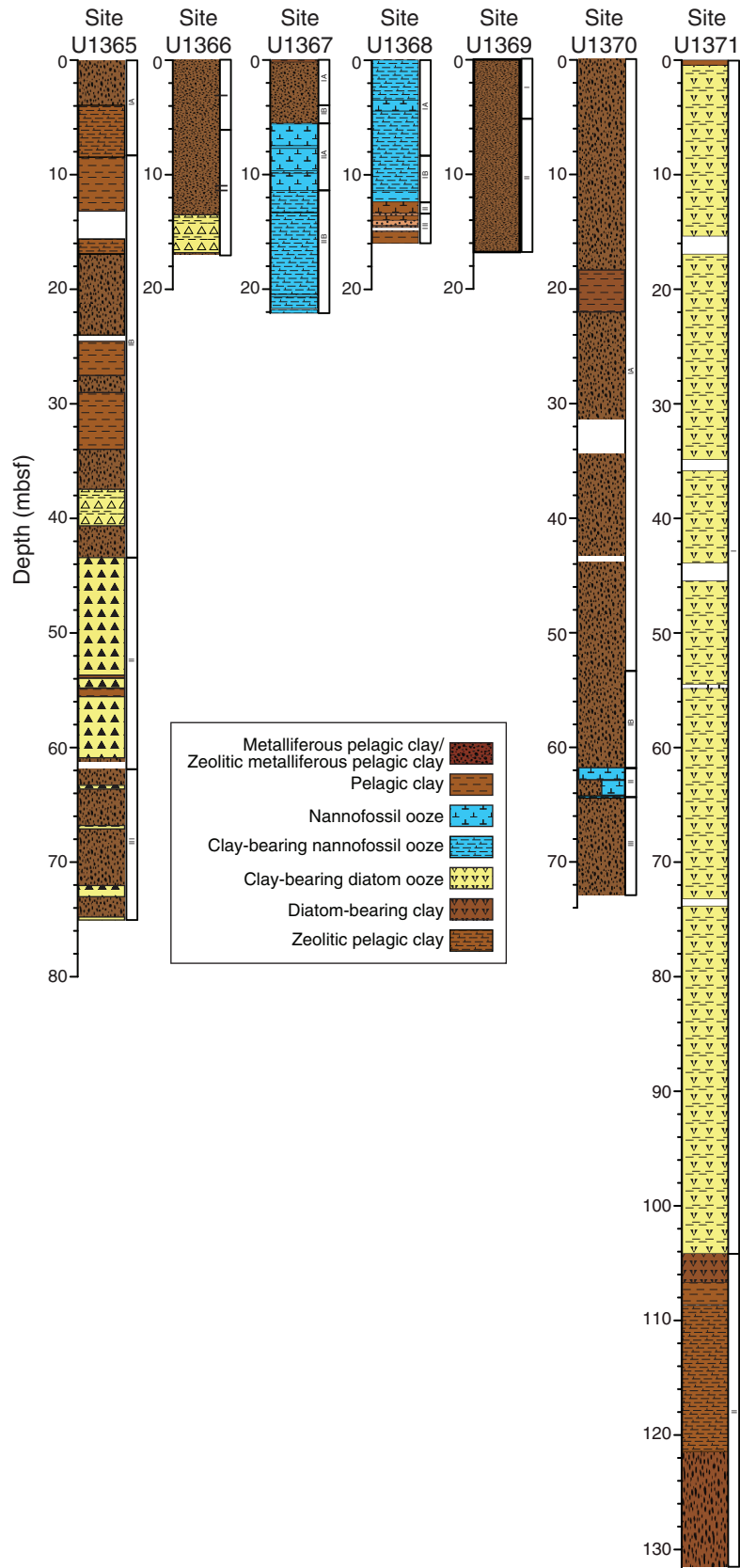
Figure F9. Plots of dissolved chemicals vs. depth, Sites U1365–U1371. DIC = dissolved inorganic carbon.
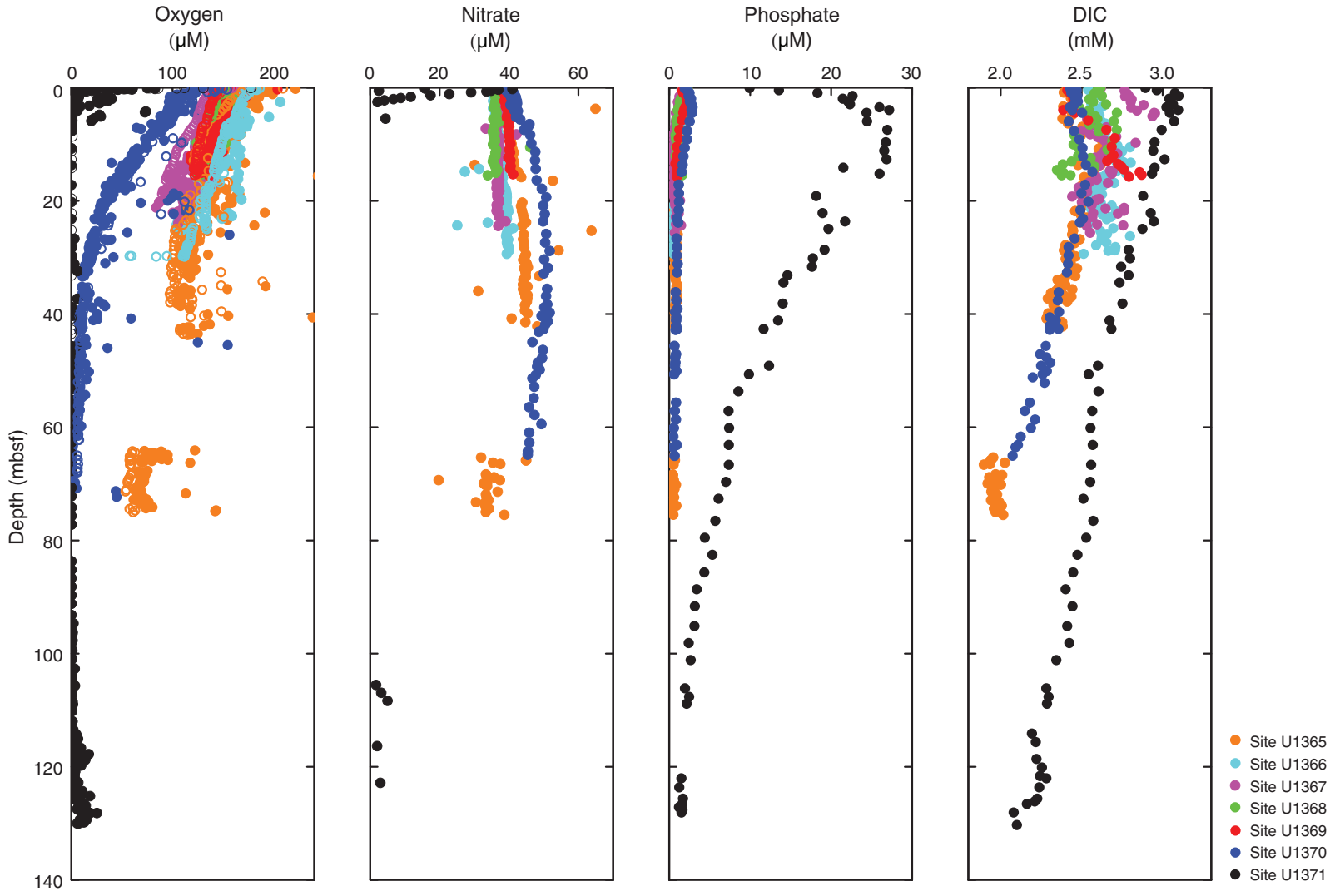
Figure F10. Plots of electron donor concentrations vs. depth, Sites U1365–U1371. TOC = total organic carbon (solid phase), TN = total nitrogen (solid-phase organic).
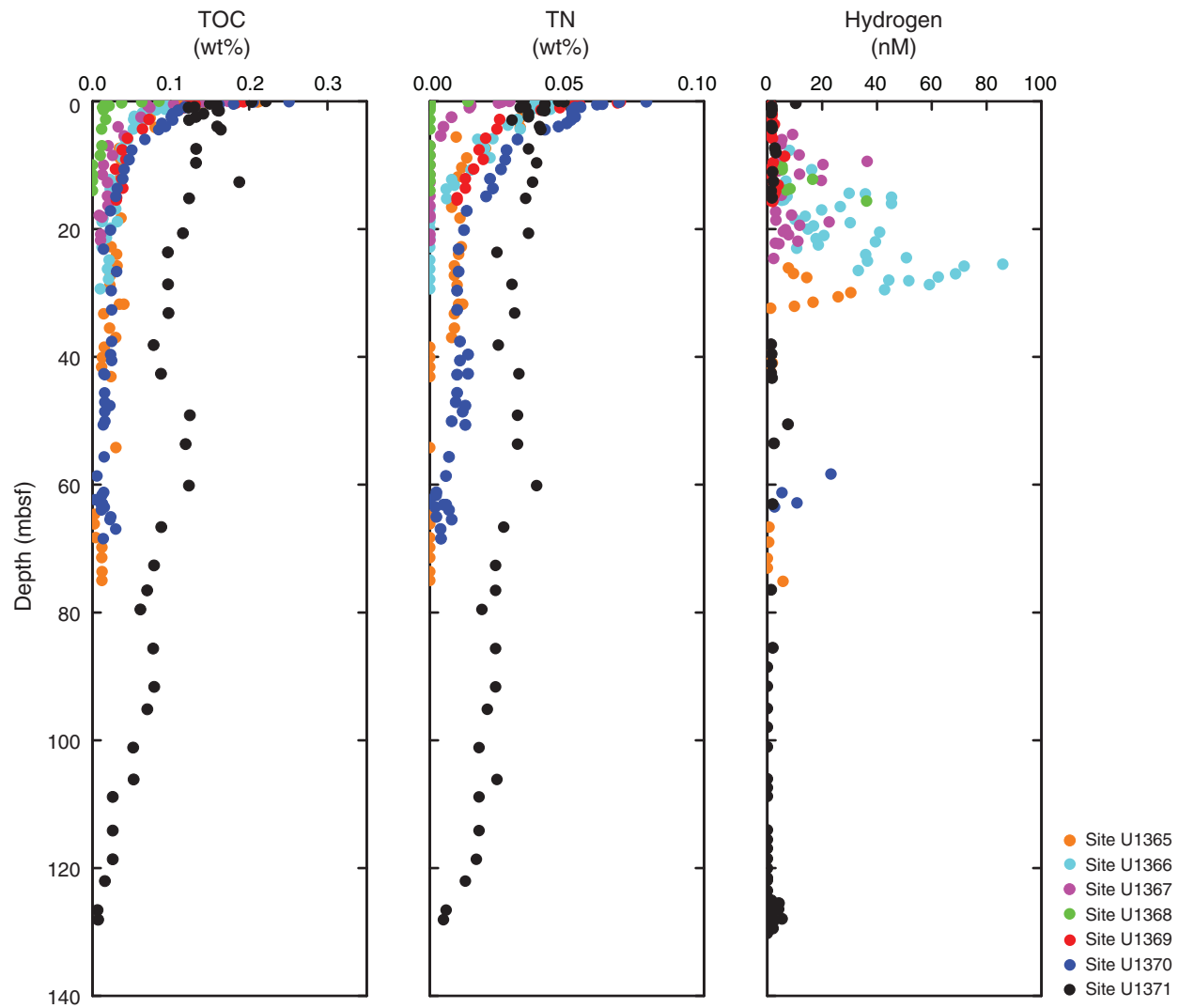
Figure F11. Plot of microbial cell counts vs. depth, Sites U1365–U1371. Minimum detection limit (MDL) is indicated by the red line.
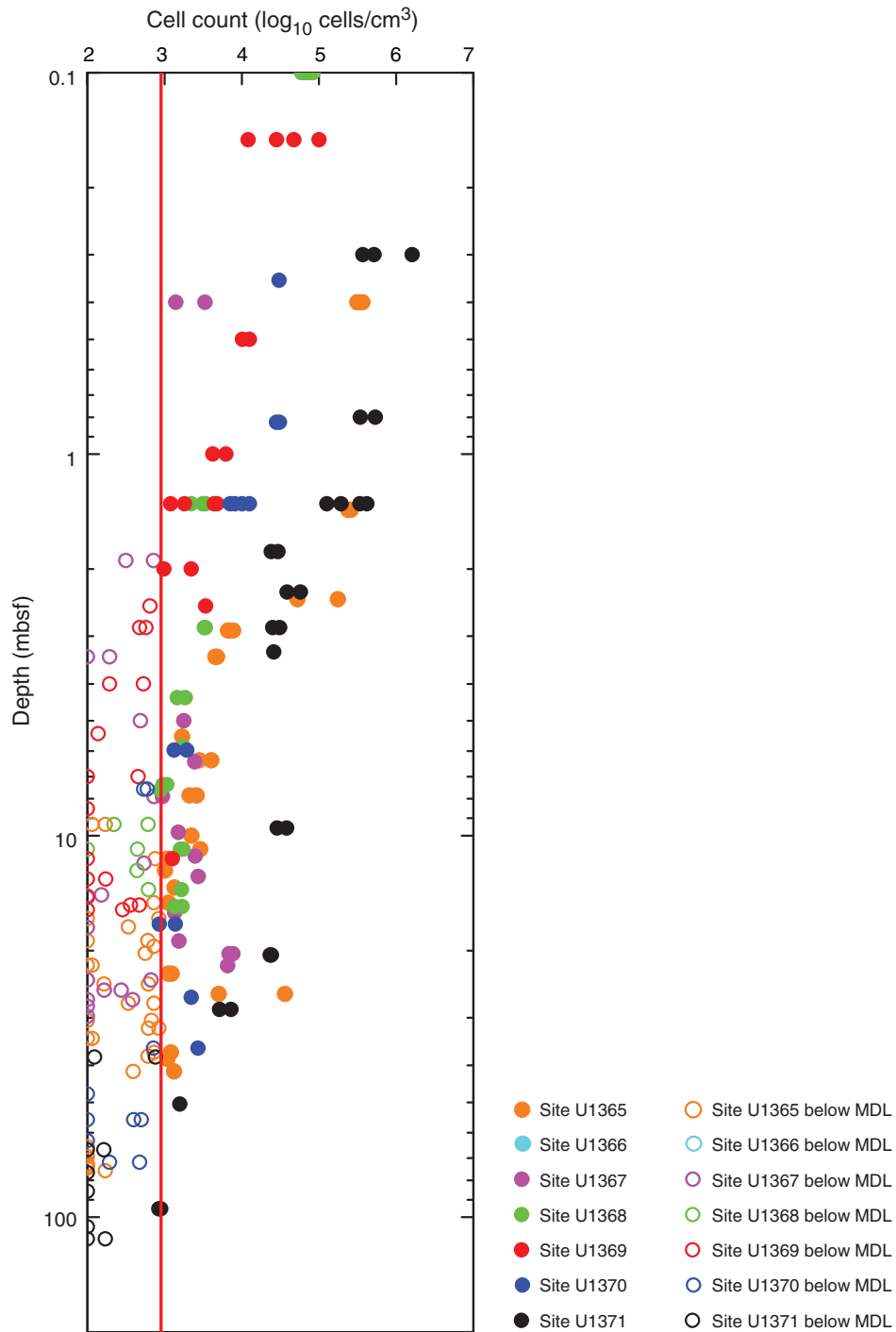
Figure F12. Illustration of relationship between igneous units, visually observed alteration intensity, and potassium content (determined by NGR core logging), Hole U1365E.
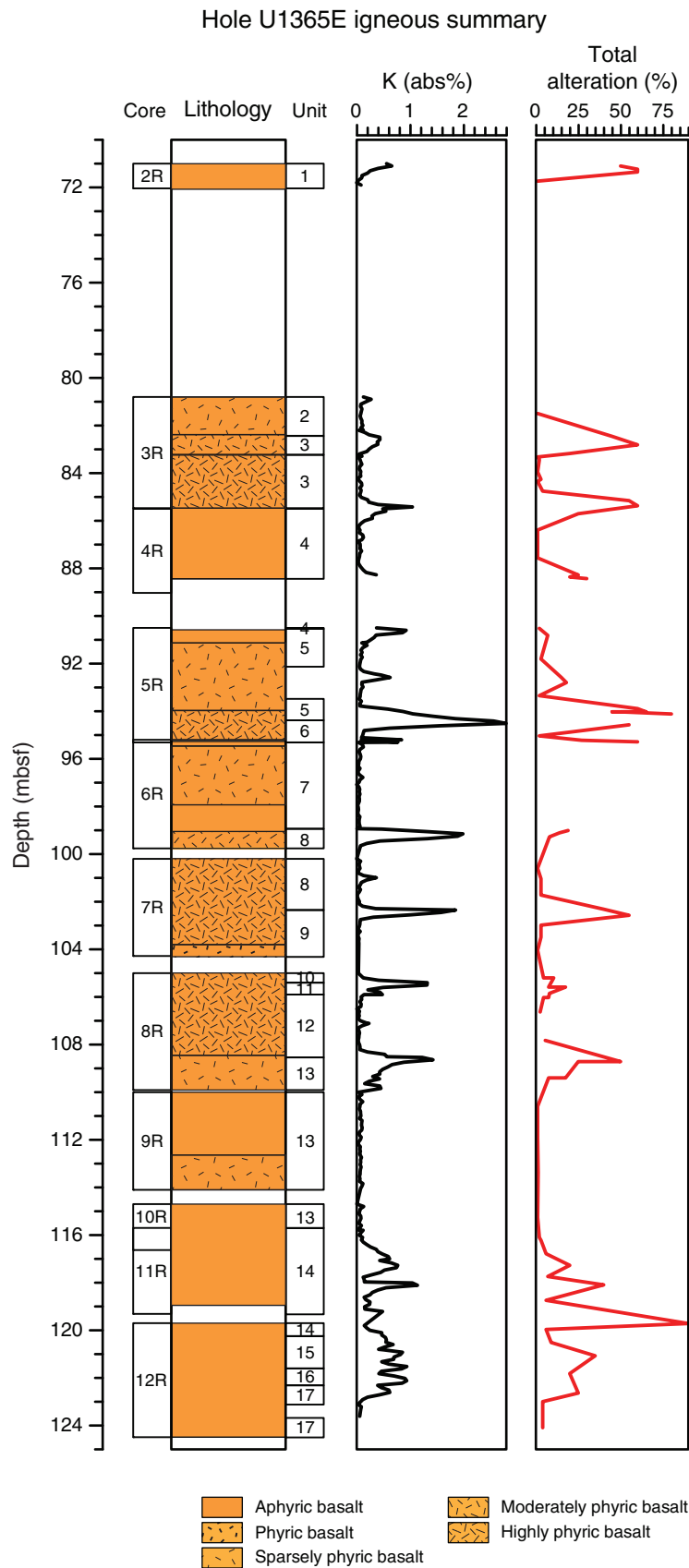
Figure F13. Plot of dissolved potassium, Sites U1365, U1370, and U1371.
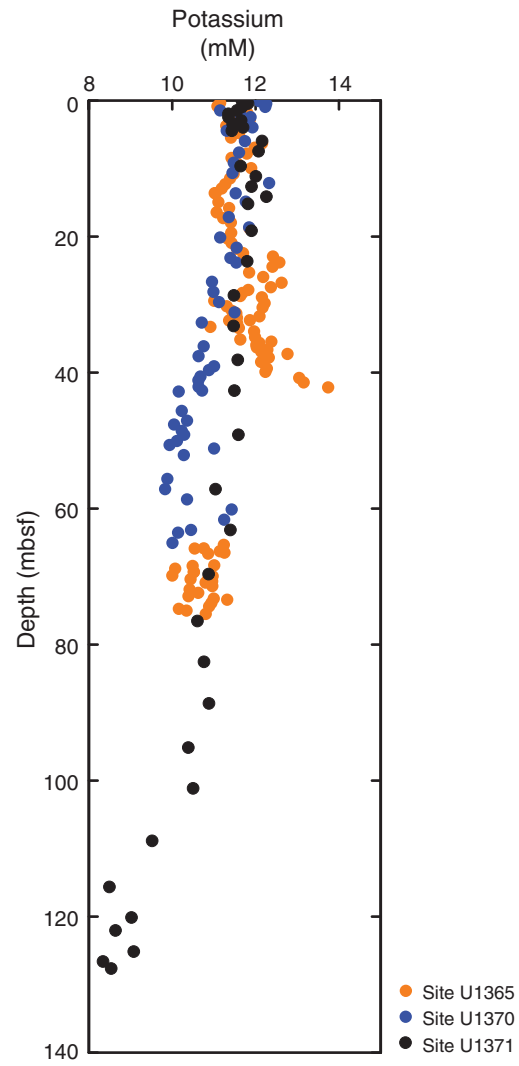
Figure F14. Photomicrograph of potential biogenic alteration features within a hyaloclastite breccia, Site U1365. Altered basaltic glass with tubelike micro-scale weathering features (Sample 329-U1365E-8R-4, 3–6 cm; hyaloclastite breccia). Fe-ox = iron oxyhydroxide. Plane-polarized light; 700× magnification.
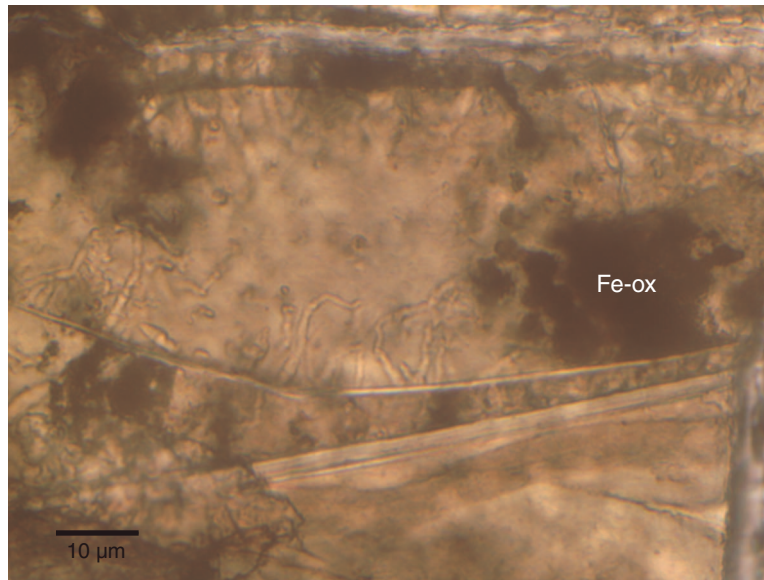
Figure F15. Summary of lithologic units and modal composition of minerals at Site U1365 based on the complete coring recovery of Hole U1365A. RSO = red-brown to yellow-brown semiopaque oxide.
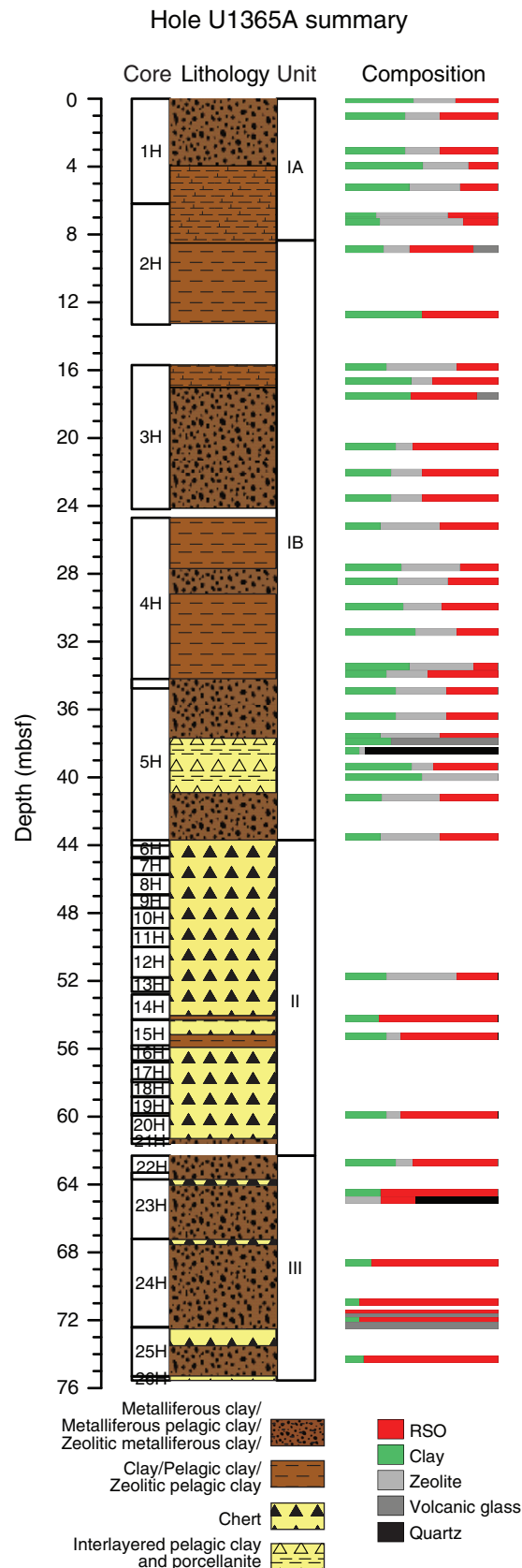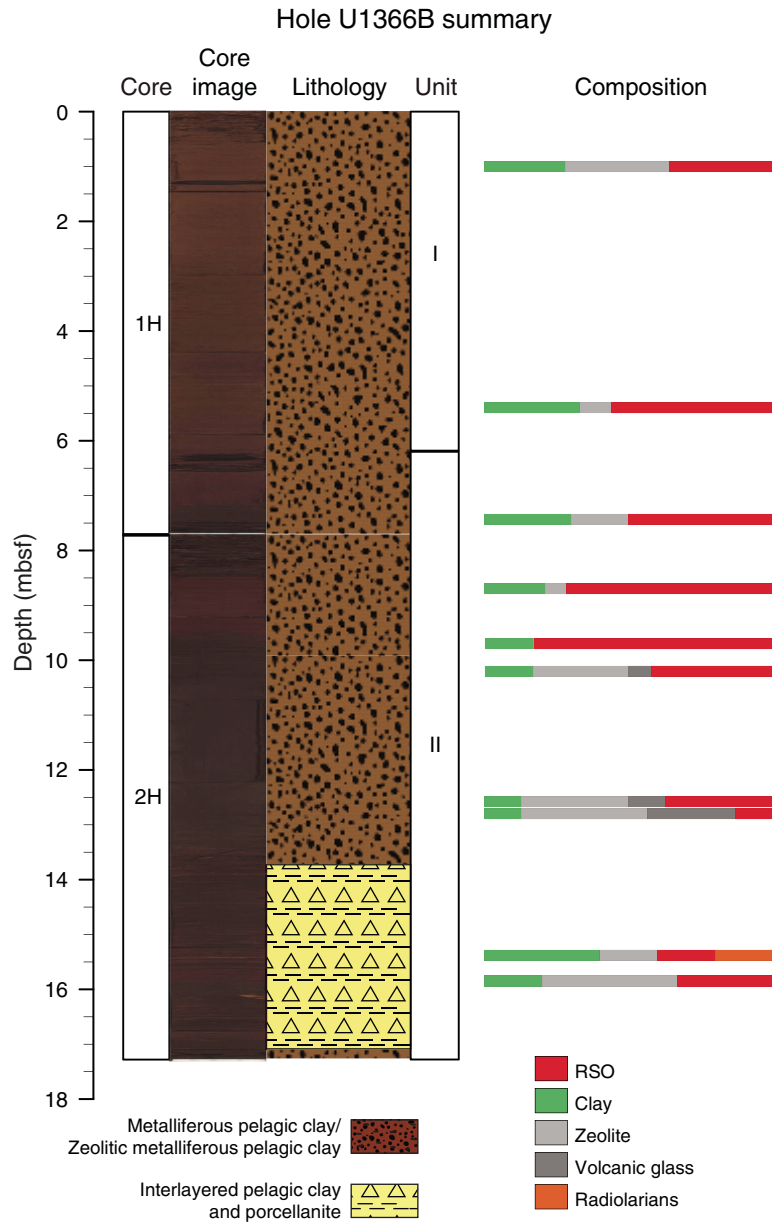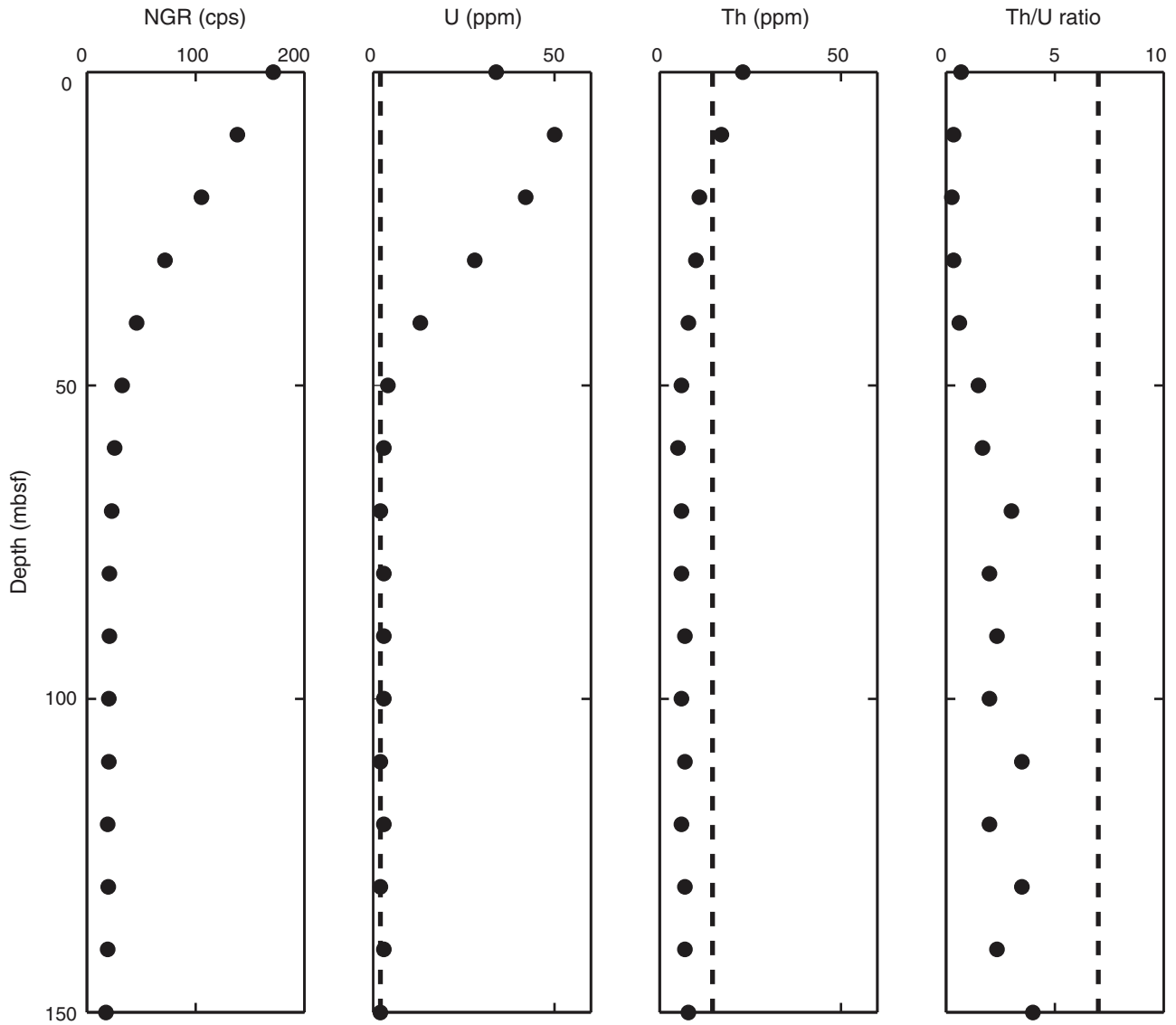
Figure F16. Plot of microbial cell count, Site U1366. Cell counts below the blank are shown as 10^2 cells/cm^3 in order to present them in the graph. Solid circles = microbial cell abundances quantified by epifluorescence microscopy (direct counts), open circles = cell counts below minimum detection limit (red line).
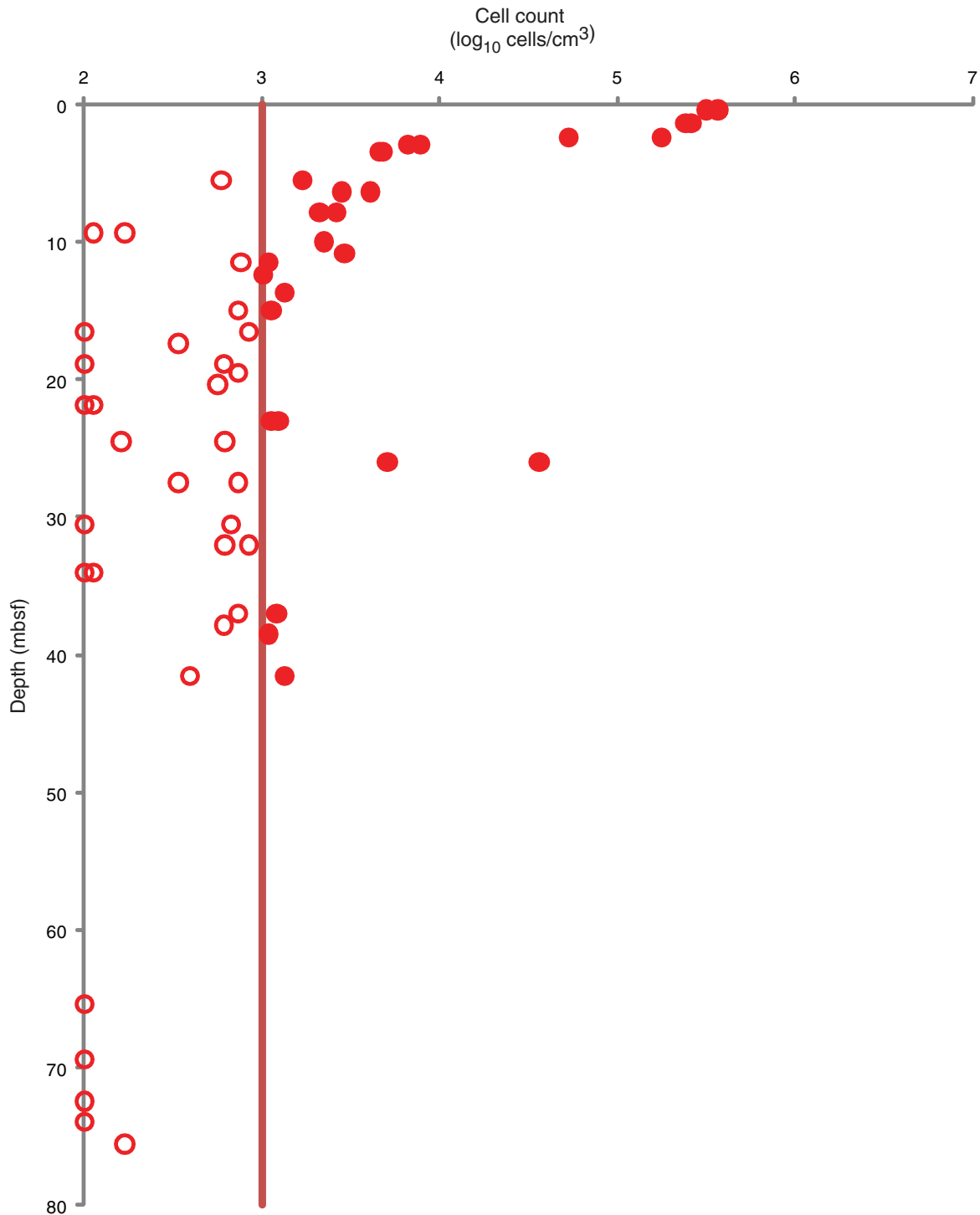
Figure F17. Plots of dissolved oxygen and dissolved nitrate, Site U1365. **A.** Dissolved oxygen concentrations on all cores. The figure includes measurements from core intervals that were observed before or during measurement to be compromised by core disturbance (flow-in, seawater intrusion, etc.). They are included to illustrate effects of core disturbance on dissolved oxygen measurements. **B.** Dissolved nitrate concentrations.
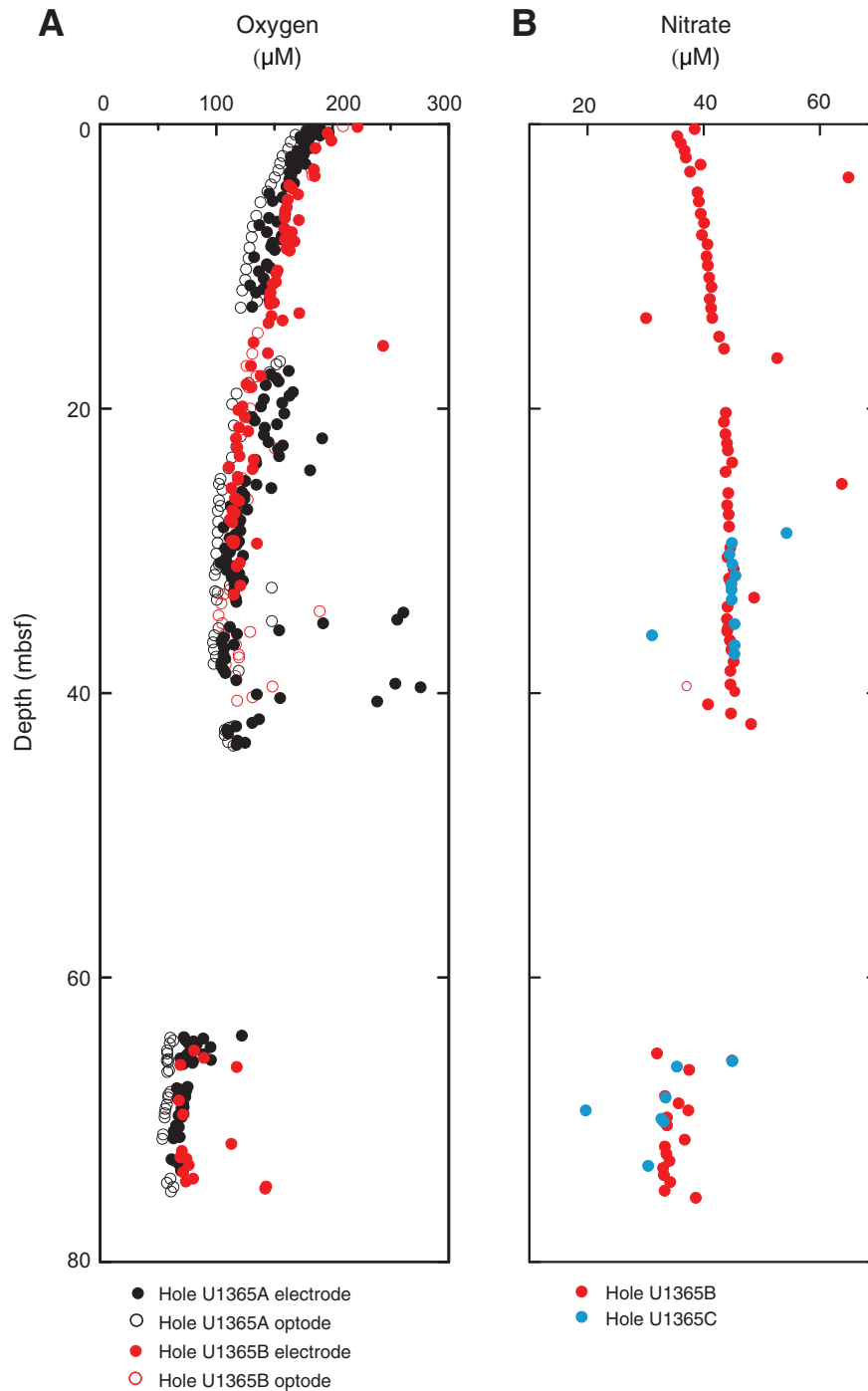
Figure F18. Plots of solid-phase nitrogen (TN) and total organic carbon (TOC) content, Hole U1365A.
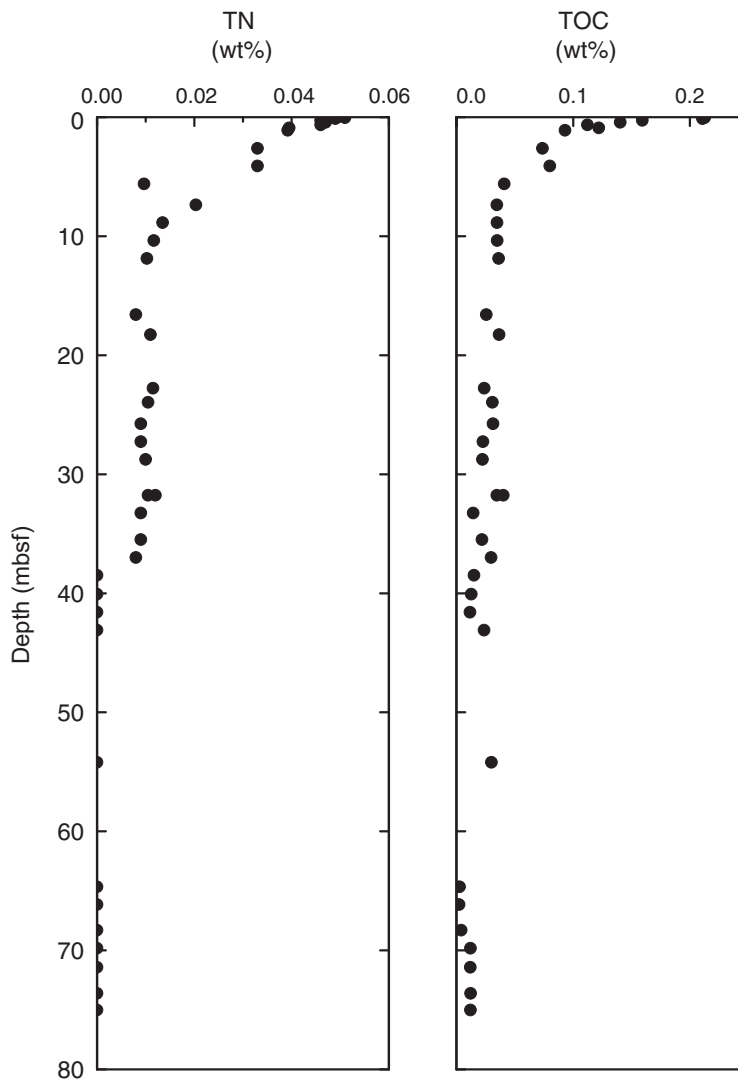
Figure F19. Summary of lithologic units and modal composition of minerals at Site U1366 based on the complete coring recovery of Hole U1366B. RSO = red-brown to yellow-brown semiopaque oxide.

Figure F20. Plots of natural gamma radiation (NGR) core logs from the uppermost 1.5 m of Hole U1366E. Each data point is integrated over 20 cm. Dashed lines show manganese nodule concentrations of ^{238}U-series isotopes, ^{232}Th-series isotopes, and their ratio.

Figure F21. Plot of microbial cell counts, Site U1366. Cell counts below the blank are shown as 10^2 cells/cm^3 in order to present them in the graph. Solid circles = microbial cell abundances quantified by epifluorescence microscopy (direct counts), open circles = direct counts below minimum detection limit (red line).
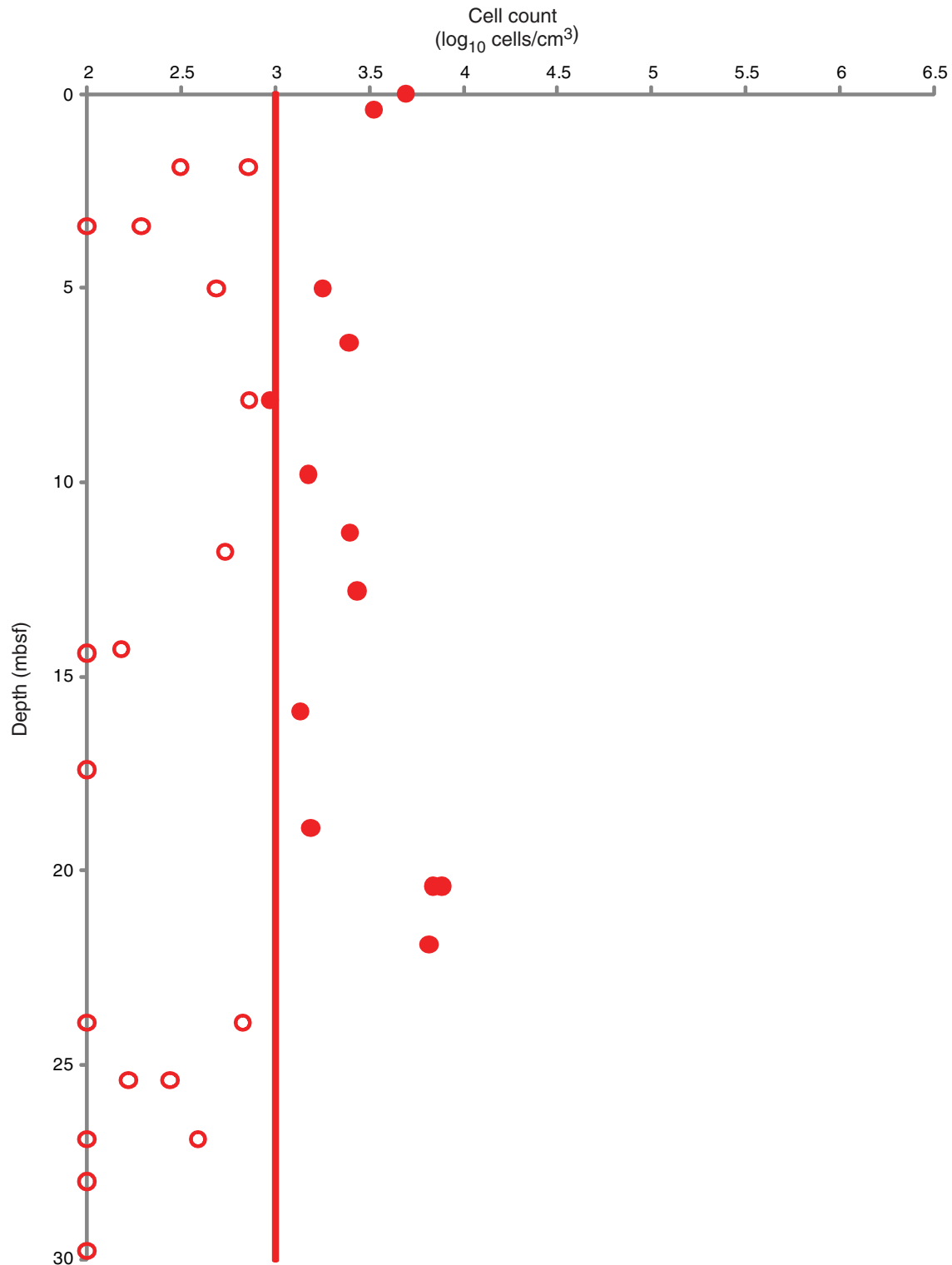
Figure F22. Plots of solid-phase nitrogen (TN) and total organic carbon (TOC) content, Holes U1366D and U1366F. WTF = whole round taken fast.
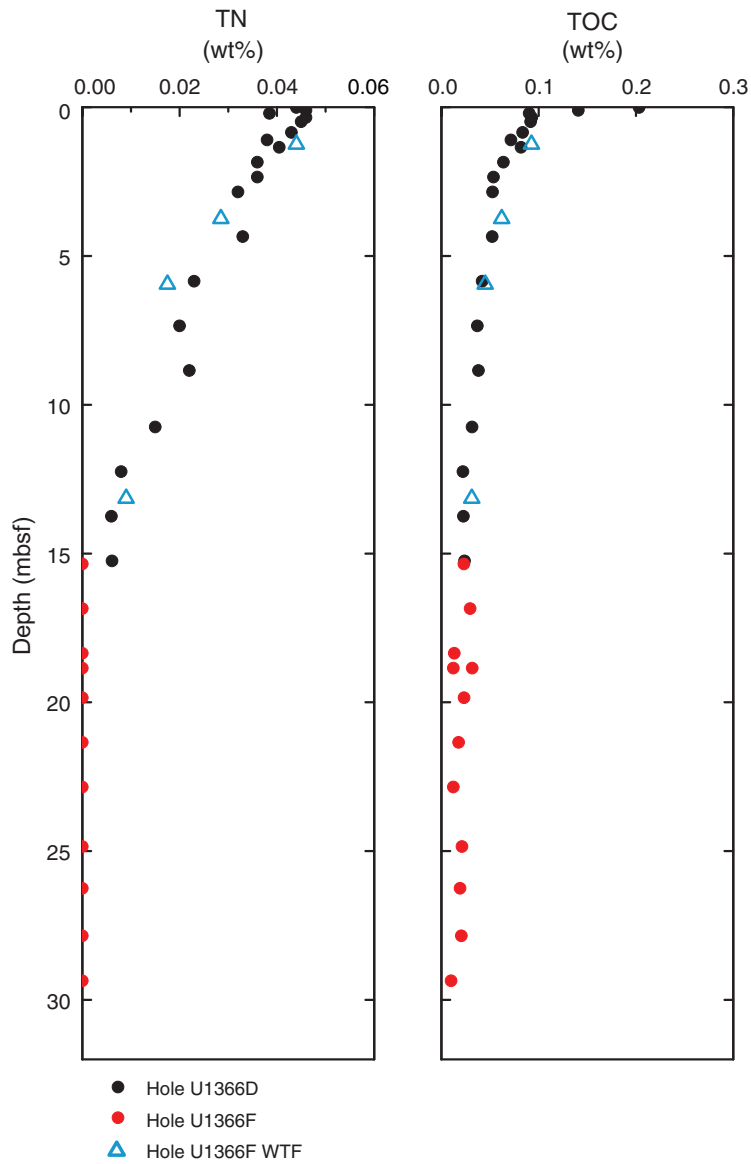
Figure F23. Profiles of (**A**) dissolved nitrate, (**B**) dissolved inorganic carbon (DIC), and (**C**) dissolved chloride concentrations, Holes U1366D and U1366F. Circles = samples taken as whole rounds in Hold Deck core refrigerator, WSS = whole round stored shorter (samples taken as whole rounds in the Hold Deck refrigerator and immediately delivered to the Geochemistry Laboratory for squeezing interstitial water).
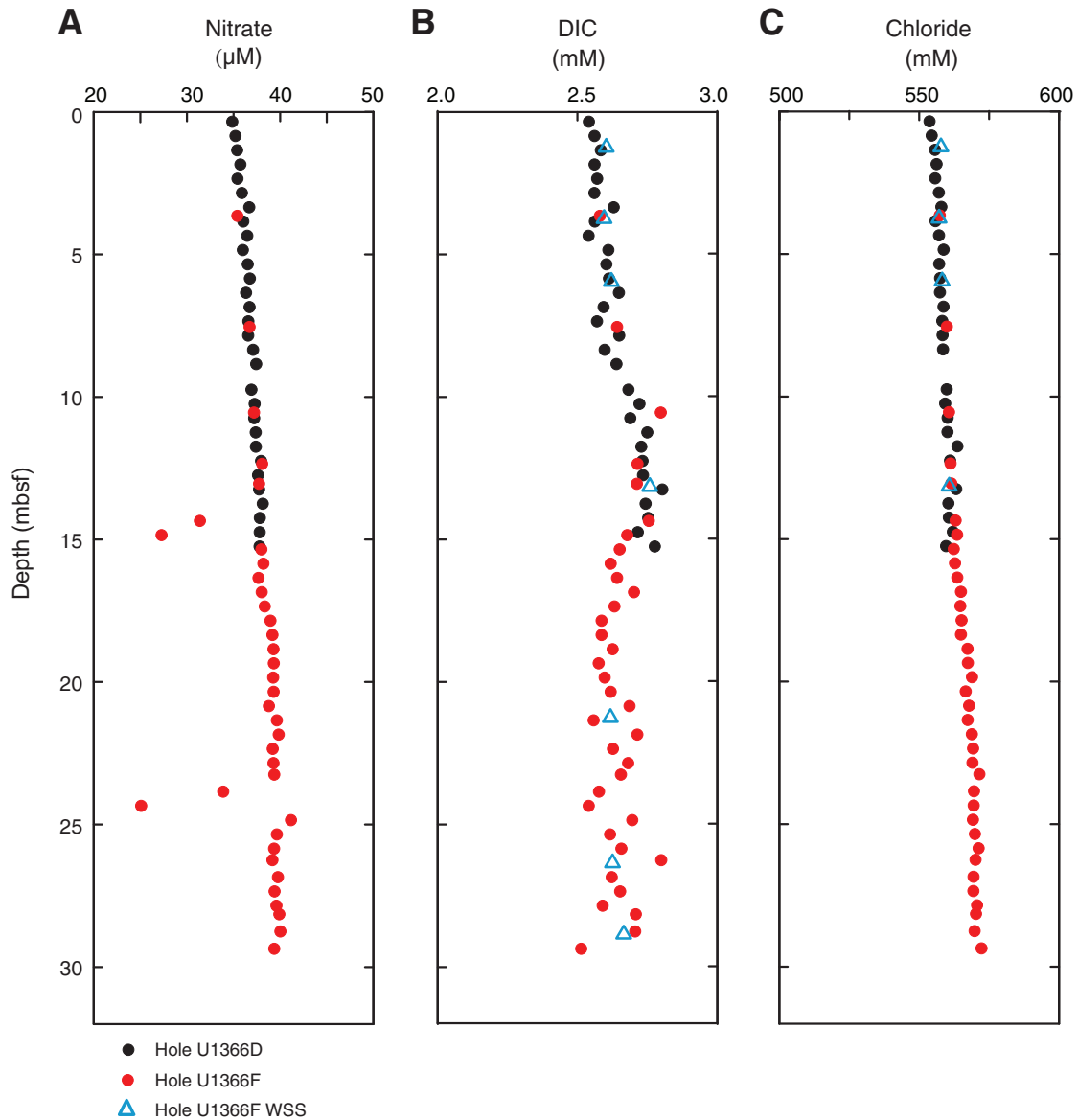
Figure F24. Summary of lithologic units and modal composition of minerals, Hole U1367B. RSO = red-brown to yellow-brown semiopaque oxide.
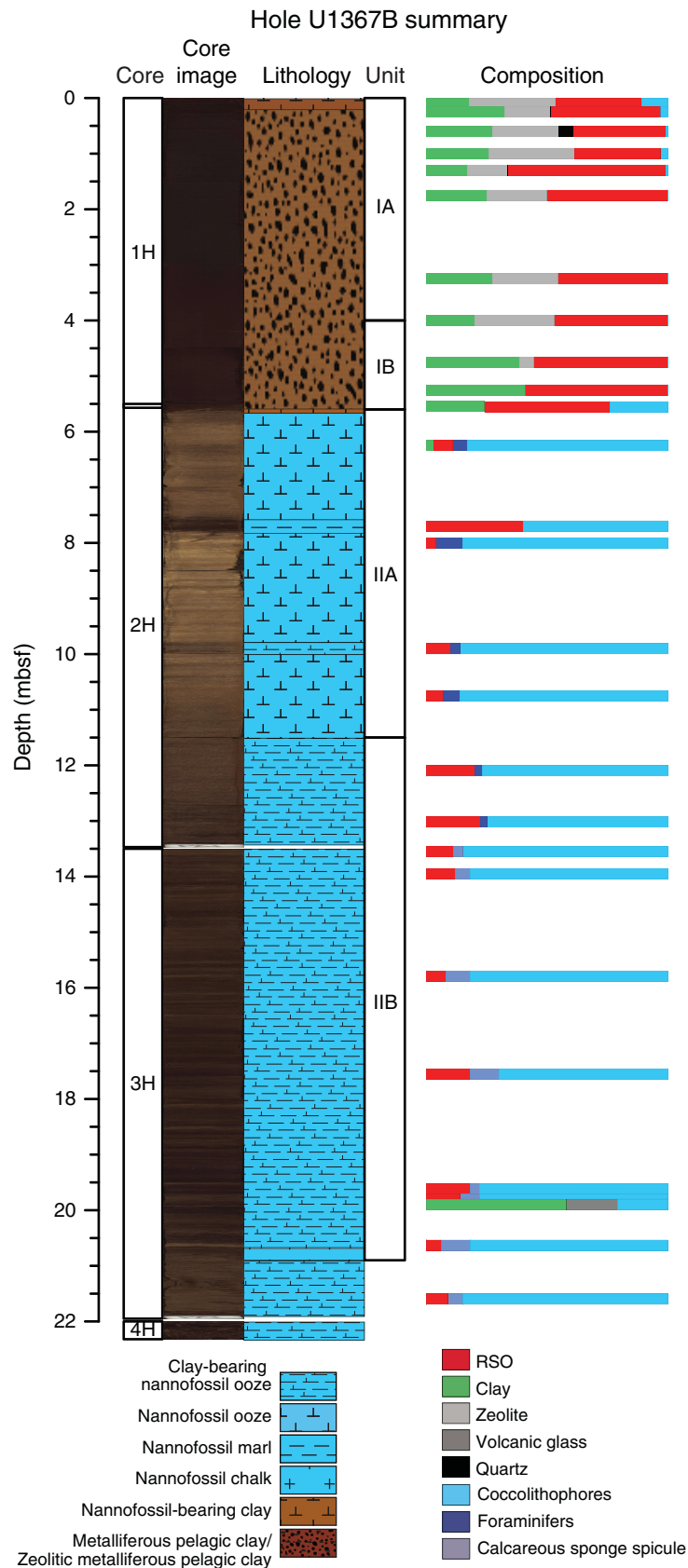
Figure F25. Plots of dissolved chemical concentrations, Holes U1366C and U1366D. DIC = dissolved inorganic carbon. Circles = samples taken as whole rounds in the Hold Deck core refrigerator, triangles = samples taken as whole rounds directly from the catwalk and immediately delivered to Geochemistry Laboratory for squeezing interstitial water.
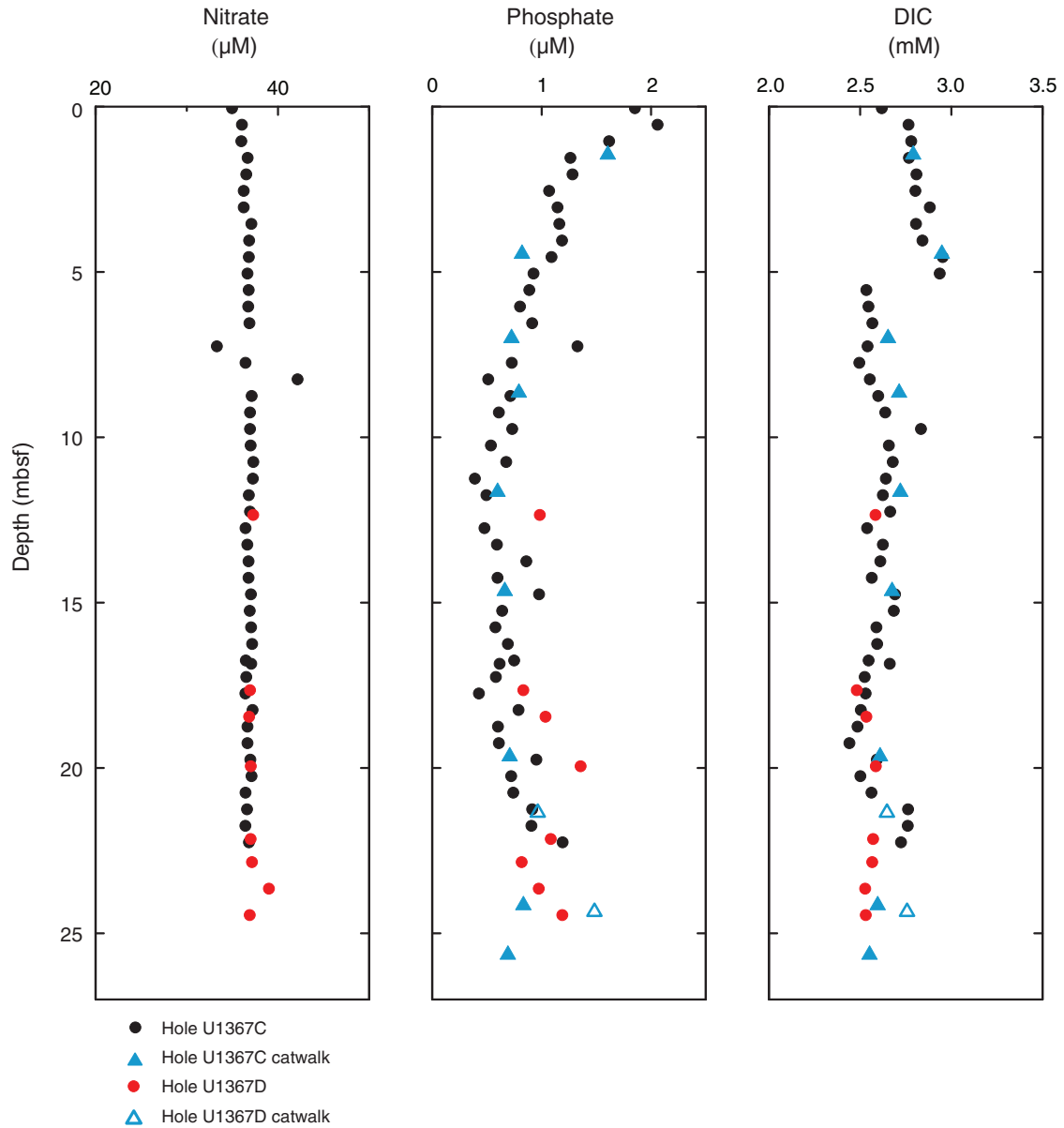
Figure F26. Summary of lithologic units and modal composition of minerals, Hole U1368B. RSO = red-brown to yellow-brown semiopaque oxide.
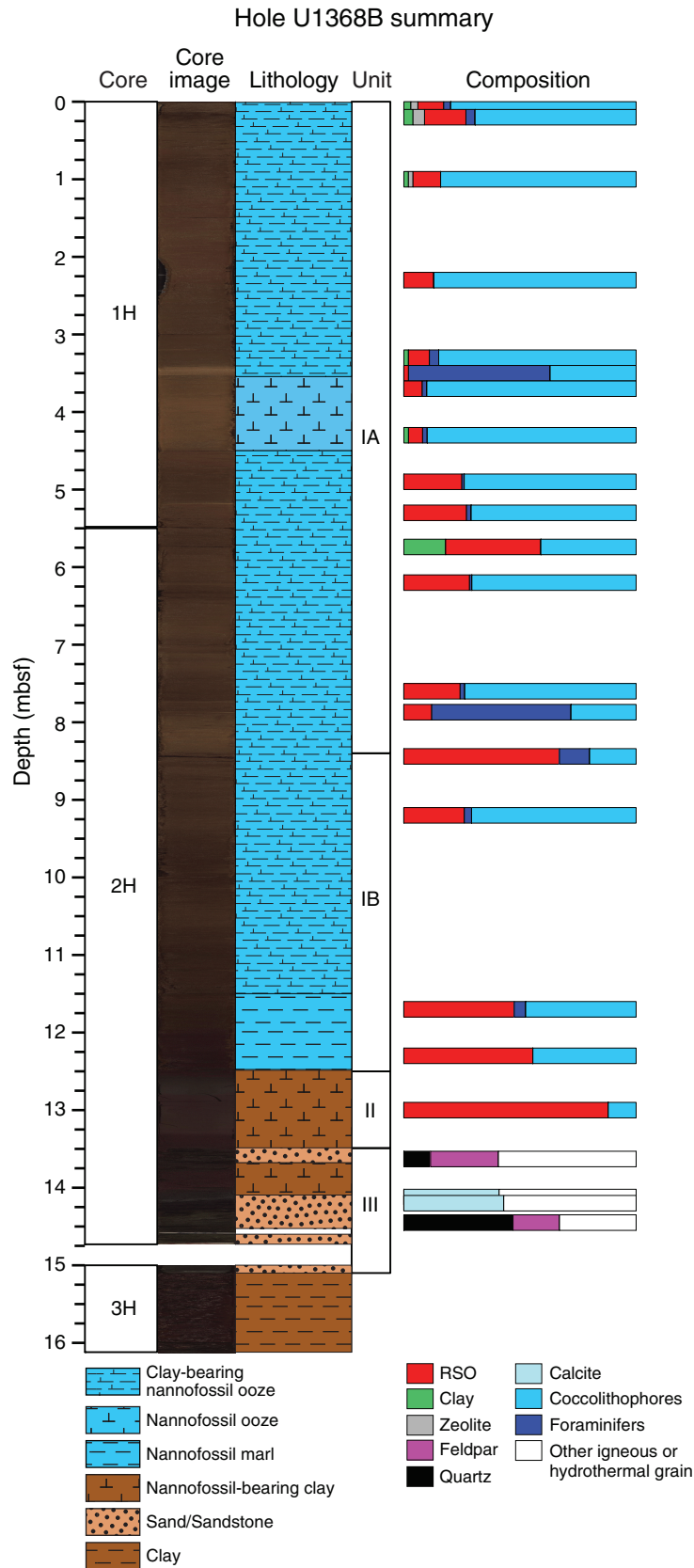
Figure F27. Plot of dissolved hydrogen, Hole U1368C. Circles = samples taken as whole rounds in the core refrigerator of the Hold Deck, triangles = samples taken as whole rounds directly from the catwalk.
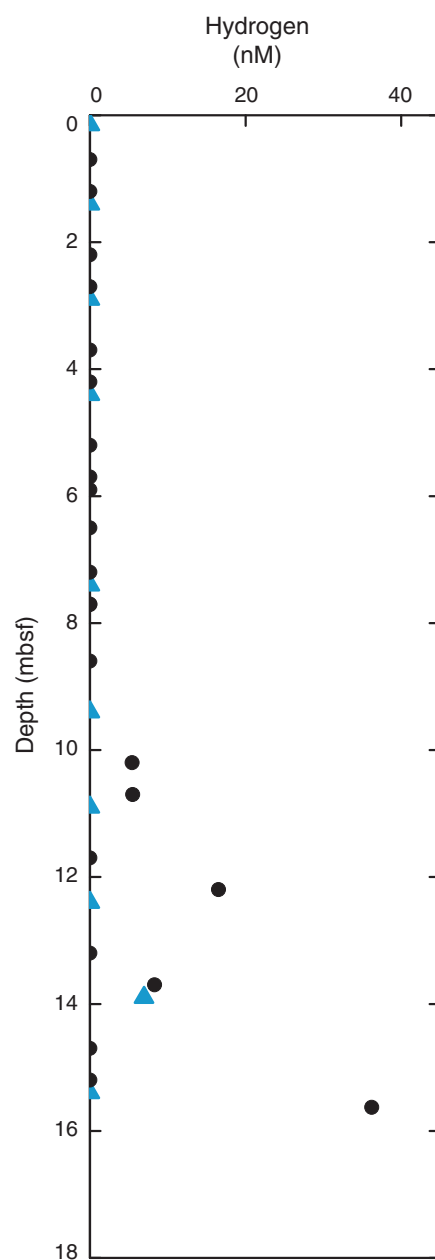
Figure F28. Profile of downhole NGR-based potassium concentration (purple) vs. whole-round core NGR-based potassium concentration (green), Site U1368.

Figure F29. Summary of lithologic units and modal composition of minerals, Hole U1369B. RSO = red-brown to yellow-brown semiopaque oxide.
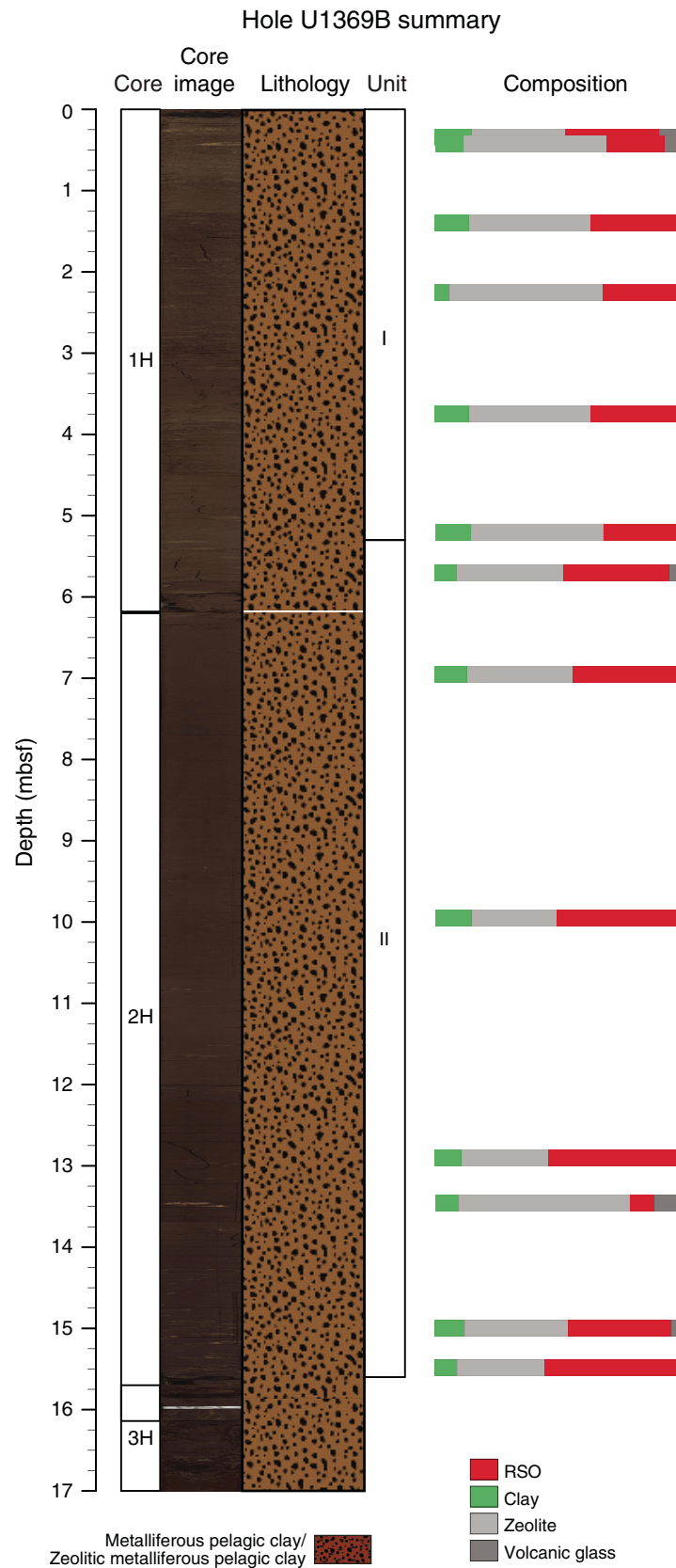
Figure F30. Plot of microbial cell counts, Site U1369. Cell counts below the blank are shown as 10^2 cells/cm^3 in order to present them in the graph. Solid circles = microbial cell abundances quantified by epifluorescence microscopy (direct counts), open circles = direct counts below minimum detection limit (red line).
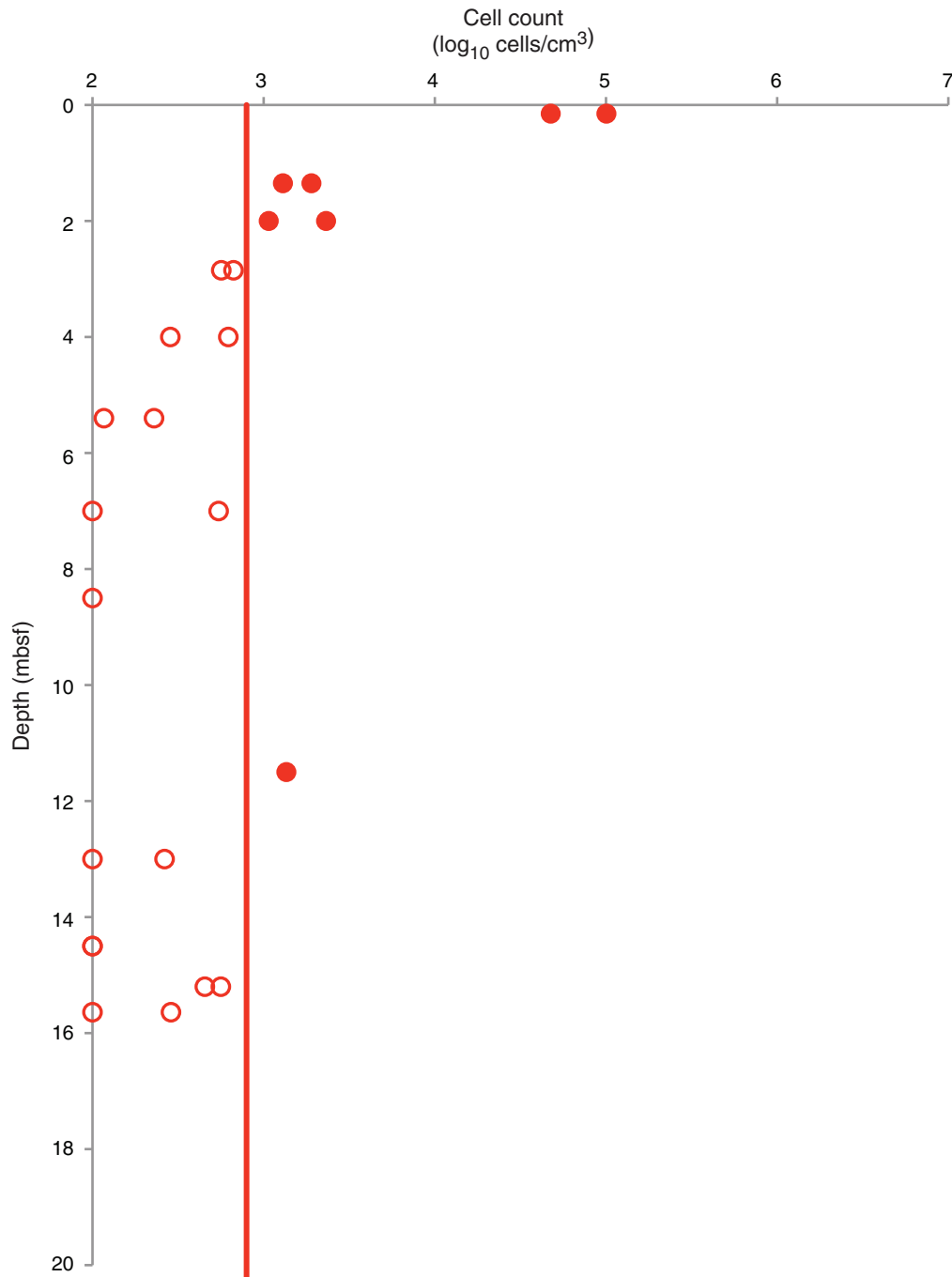
Figure F31. Plots of dissolved chemical concentrations, Site U1369. DIC = dissolved inorganic carbon.

○ Hole U1369B optode
● Hole U1369B electrode
● Hole U1369C electrode
● Hole U1369E electrode
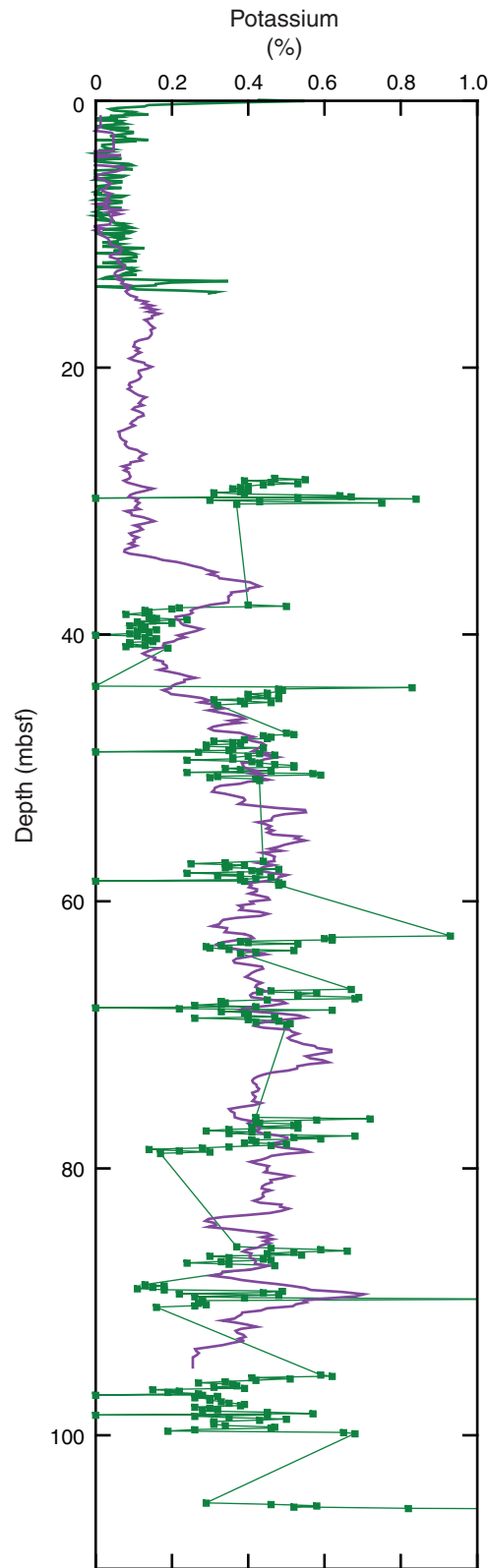
● Hole U1369C
▲ Hole U1369C catwalk
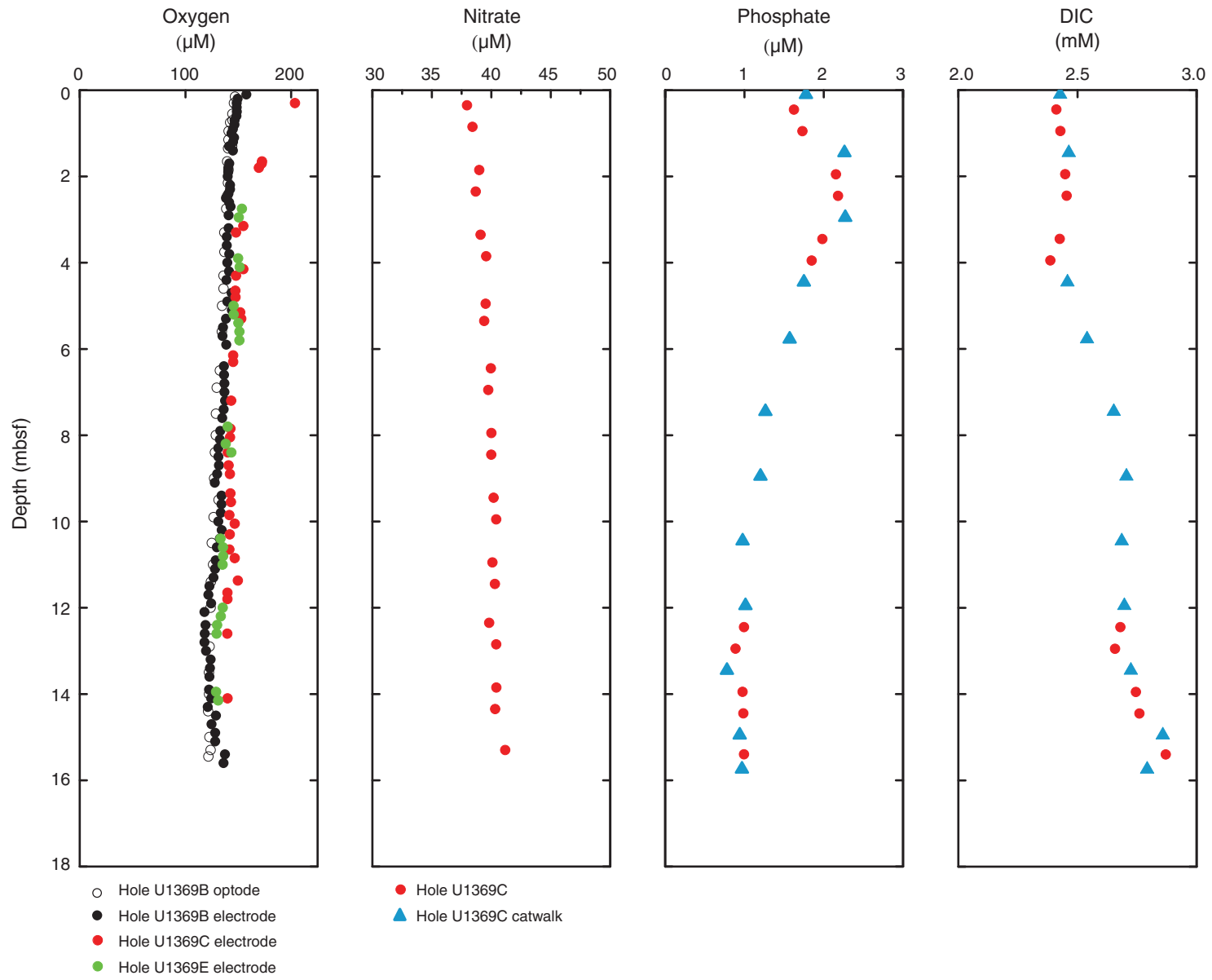
Figure F32. Summary of lithologic units and modal composition of minerals, Hole U1370D. RSO = red-brown to yellow-brown semiopaque oxide.
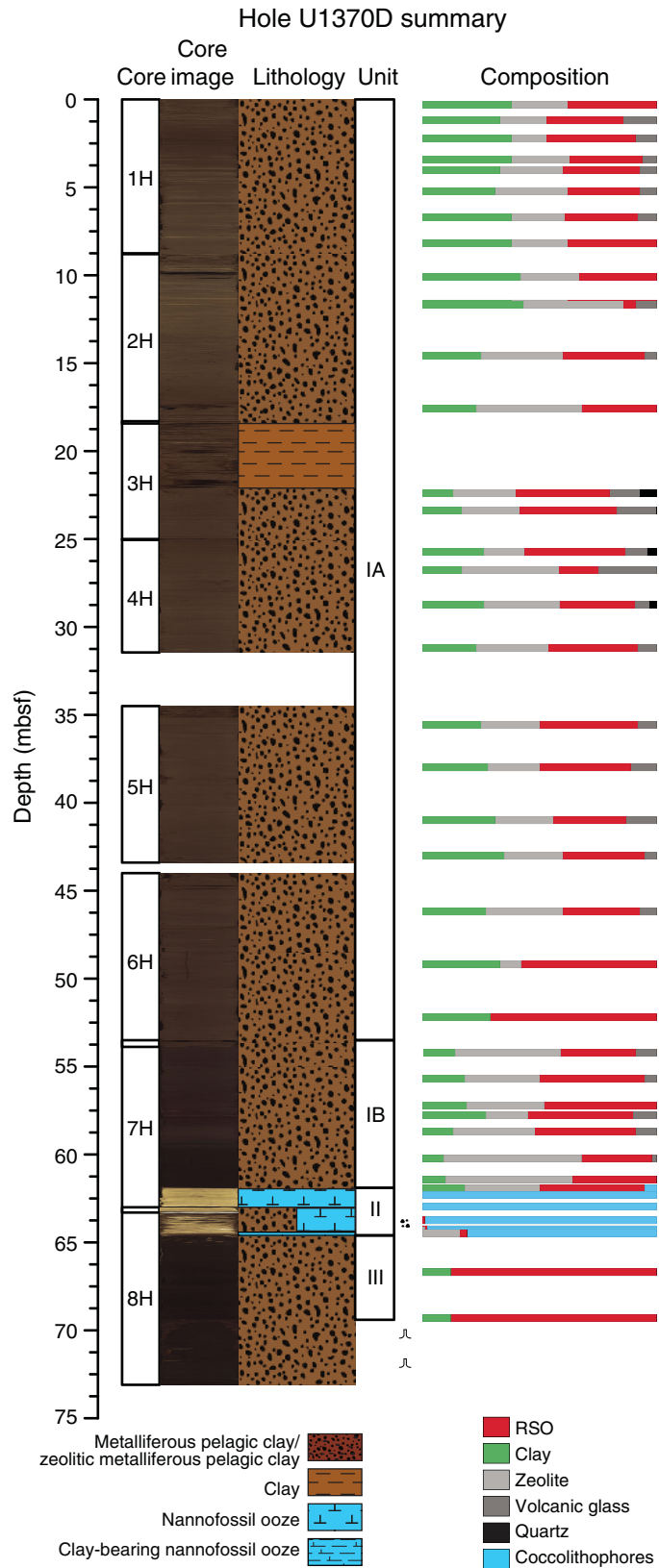
Figure F33. Plots of (**A**, **B**) dissolved oxygen and (**C**) dissolved nitrate, Site U1370.
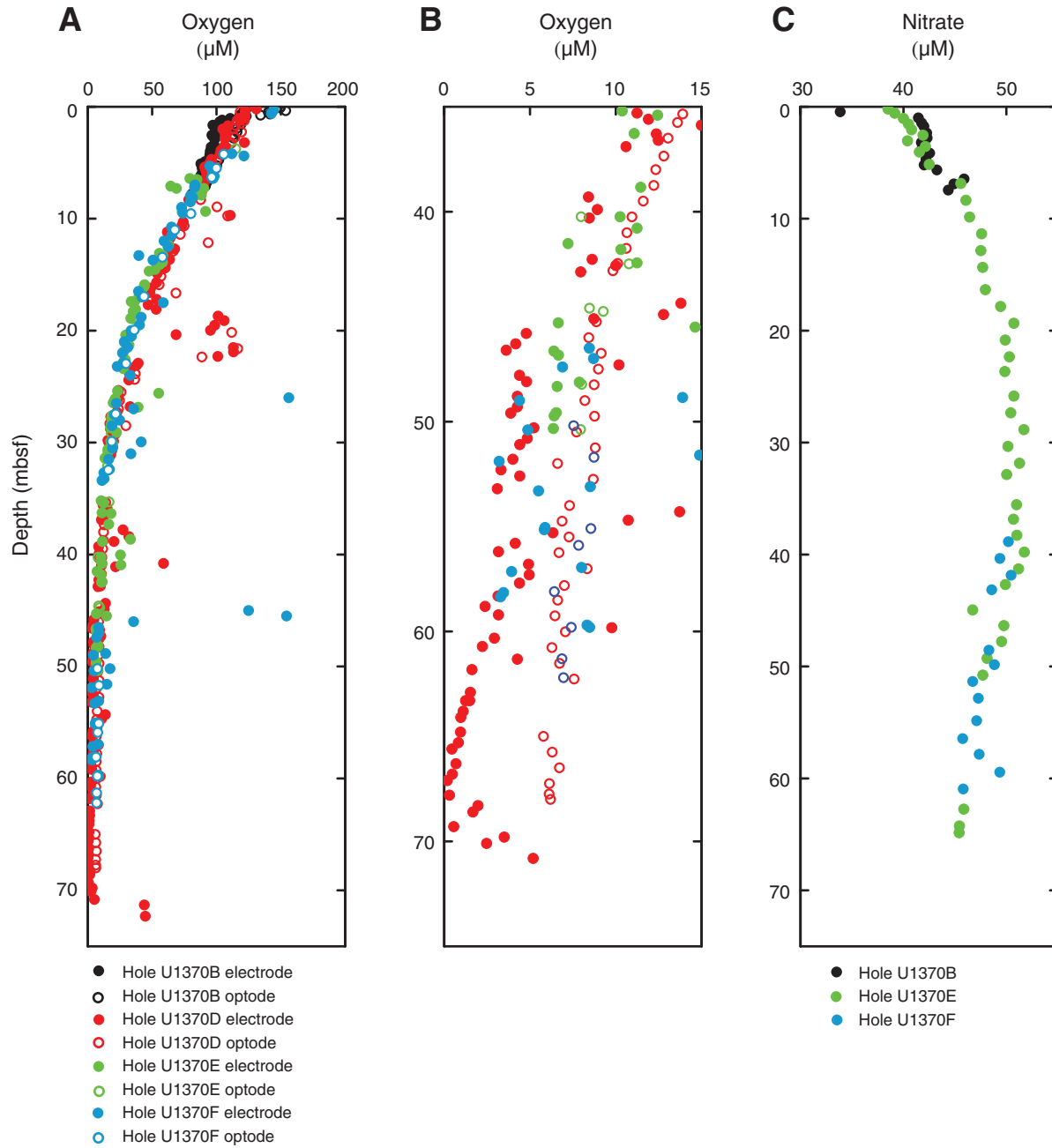
Figure F34. Plot of dissolved potassium, Site U1370. IC = ion chromatograph, ICP = inductively coupled plasma–atomic emission spectroscopy.
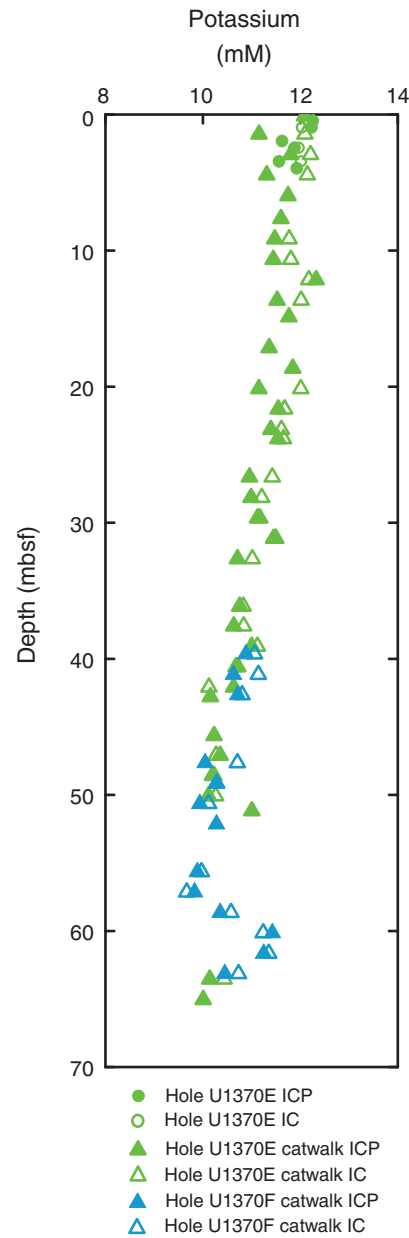
Figure F35. Summary of lithologic units and modal composition of minerals, Hole U1371D. RSO = red-brown to yellow-brown semiopaque oxide.


Hole U1371D summary
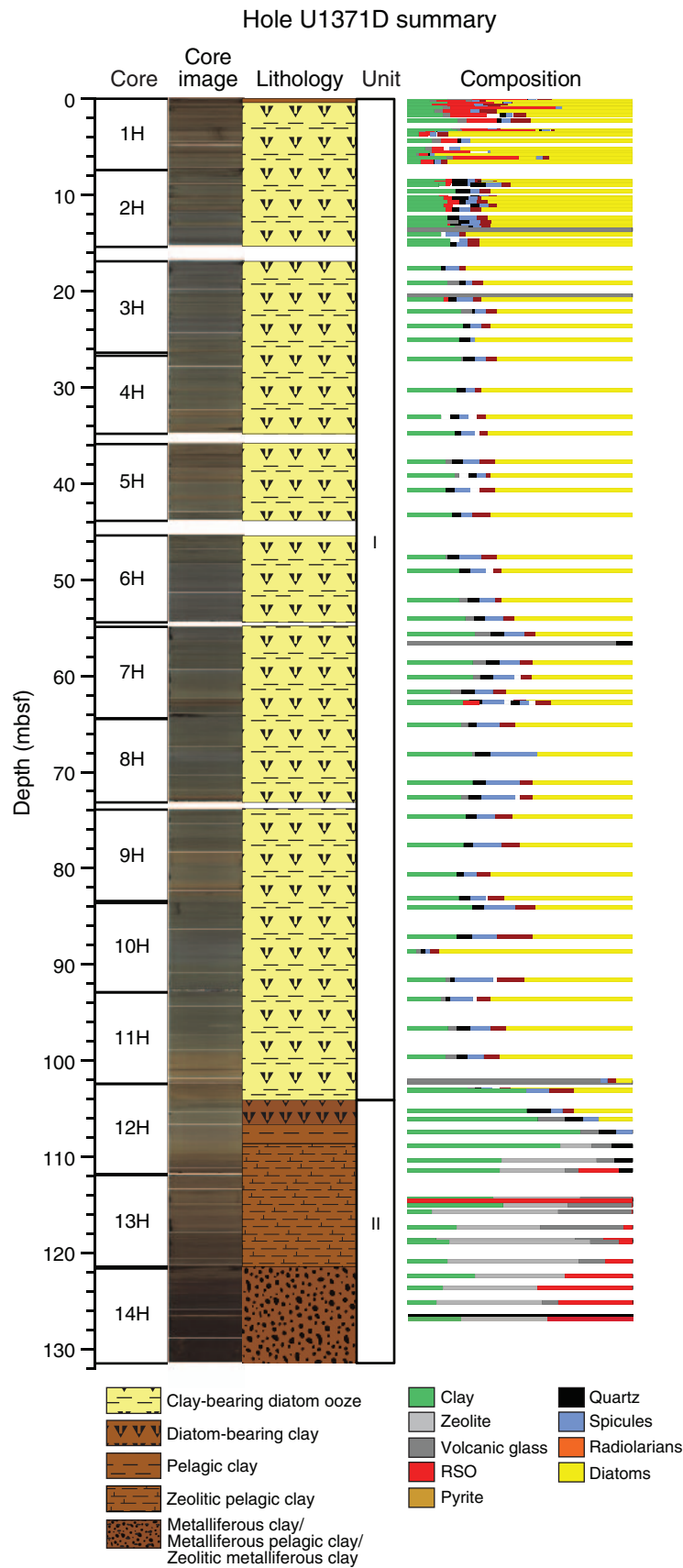
Figure F36. Plots of dissolved chemical concentrations and redox potential, Site U1371.

Hole U1371B optode
Hole U1371B electrode
Hole U1371C optode
Hole U1370C electrode
Hole U1371D optode
Hole U1370D electrode
Hole U1370F electrode
Hole U1371H optode
Hole U1370H electrode

Hole U1371D
Hole U1371E
Hole U1371E catwalk

Hole U1371F
Hole U1371H

Table T1. Operations summary, Expedition 329. (Continued on next page.)

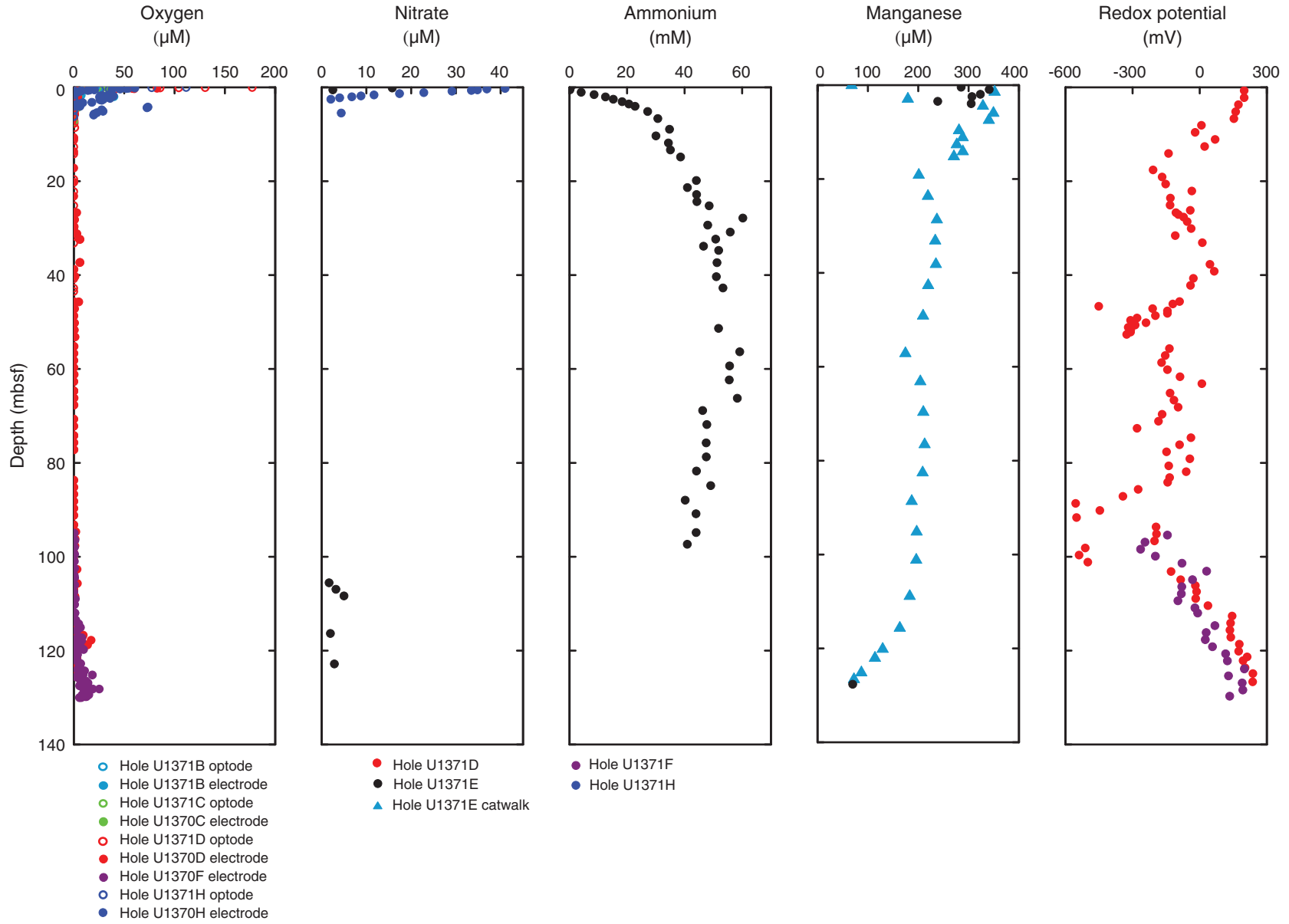| Hole	Latitude	Longitude	Water depth (mbsf)	Penetration (m)	Cored (m)	Recovered (m)	Recovery (%)	Drilled (m)	Cores (N)	Time on hole (h)	Time on site (days)	Comments
U1365A	23°51.0493′S	165°38.6624′W	5695.6	75.5	75.5	74.06	98	0	26	80.25		Washdown hole - No cores
U1365B	23°51.0388′S	165°38.6629′W	5694.7	75.6	54.6	55.79	102	21	8	22		
U1365C	23°51.0377′S	165°38.6502′W	5696.7	74.8	48.8	39.67	81	26	8	21.75		
U1365D	23°51.0359′S	165°38.6381′W	5693.7	19	19	18.89	99	0	2	16		
U1365E	23°51.0489′S	165°38.6420′W	5693.7	124.2	53.2	39.66	75	71	11	144.75		
		Site U1365 totals:		369.1	251.1	228.07	91	118	55	284.75	11.86	
U1366A	26°03.0945′S	156°53.6591′W	5135	17.8	0	0	0	17.8	0	10.5		Washdown hole - No cores
U1366B	26°03.0950′S	156°53.6714′W	5130.8	17.2	17.2	17.31	101	0	2	4.25		
U1366C	26°03.0845′S	156°53.6700′W	5129.5	25	25	25.42	102	0	3	4.25		
U1366D	26°03.0850′S	156°53.6652′W	5126.1	20.9	20.9	18.86	90	0	4	6.25		
U1366E	26°03.0843′S	156°53.6825′W	5127.8	4.7	4.7	4.71	100	0	1	0.75		
U1366F	26°03.0836′S	156°53.6937′W	5127	30.1	30.1	30.15	100	0	4	18		
		Site U1366 totals:		115.7	97.9	96.45	98.6	17.8	14	44	1.83	
U1367A	26°28.8972′S	137°56.3646′W	4290.9	21.2	0	0	0	21.2	0	9.25		Washdown hole - No cores
U1367B	26°28.8966′S	137°56.3777′W	4288.9	22.3	22.3	22.31	100	0	4	6.5		
U1367C	26°28.8860′S	137°56.3783′W	4288.2	26.7	26.7	27.01	101	0	4	5.25		
U1367D	26°28.8861′S	137°56.3659′W	4288.1	25.5	25.5	24.54	96	0	4	7		
U1367E	26°28.8856′S	137°56.3538′W	4287.6	24.4	24.4	23.15	95	0	3	11		
U1367F	26°28.8960′S	137°56.3538′W	4288.9	55.5	38.5	4.33	11	17	5	63.75		
		Site U1367 totals:		175.6	137.4	101.34	80.6	38.2	20	102.75	4.28	
U1368A	27°55.0017′S	123°09.6562′W	3740	13.6	0	0	0	13.6	0	10.25		Washdown hole - No cores
U1368B	27°55.0024′S	123°09.6679′W	3739.1	16	16	15.84	99	0	3	5		
U1368C	27°54.9916′S	123°09.6681′W	3738.5	16.3	16.3	16.34	100	0	2	2.25		
U1368D	27°54.9920′S	123°09.6561′W	3739.1	15	15	15.04	100	0	2	2.25		
U1368E	27°54.9918′S	123°09.6442′W	3740.9	10.6	10.6	10.58	100	0	2	8.5		
U1368F	27°55.0021′S	123°09.6433′W	3741	115.1	115.1	31.74	28	0	14	112.5		
		Site U1368 totals:		186.6	173	89.54	85.4	13.6	23	140.75	5.86	
U1369A	39°18.6177′S	139°48.0383′W	5279.4	12.2	0	0	0	12.2	0	10.5		Washdown hole - No cores
U1369B	39°18.6178′S	139°48.0522′W	5275.2	15.9	15.9	18.14	114	0	3	9		
U1369C	39°18.6070′S	139°48.0519′W	5276.9	14.6	14.6	16.1	110	0	3	5		
U1369D	39°18.6069′S	139°48.0378′W	5276.9	0.1	0.1	0.08	80	0	1	0.75		
U1369E	39°18.6070′S	139°48.0246′W	5277.7	15.5	15.5	15.49	100	0	3	15.25		
		Site U1369 totals:		58.3	46.1	49.81	101	12.2	10	40.5	1.69	
U1370A	41°51.1289′S	153°6.3799′W	5074.6	66.7	0	0	0	66.7	0	14.25		Washdown hole - No cores
U1370B	41°51.1285′S	153°6.3953′W	5074.6	7.8	7.8	7.81	100	0	1	3.75		
U1370C	41°51.1171′S	153°6.3975′W	5074.6	7.8	0	0	0	7.8	0	10		
U1370D	41°51.1156′S	153°6.3812′W	5073.6	68.2	68.2	70.26	103	0	8	16.75		
U1370E	41°51.1158′S	153°6.3668′W	5074.2	65.6	65.6	70.2	107	0	9	20.25		
U1370F	41°51.1267′S	153°6.3674′W	5073.6	64.7	64.7	66.32	103	0	8	21		
		Site U1370 totals:		280.8	206.3	214.59	82.6	74.5	26	86	3.58	
U1371A	45°57.8492′S	163°11.0513′W	5316	123.5	0	0	0	123.5	0	14.75		Washdown hole - No cores
U1371B	45°57.8509′S	163°11.0673′W	5316.35	8.1	8.1	8.15	101	0	1	3.25		
U1371C	45°57.8404′S	163°11.0684′W	5312	9.5	9.5	9.83	103	0	1	1.75		
U1371D	45°57.8394′S	163°11.0512′W	5311.09	126	126	126.87	101	0	14	32.75		
U1371E	45°57.8397′S	163°11.0365′W	5310.24	128.2	128.2	118.16	92	0	14	21.5		
U1371F	45°57.8502′S	163°11.0369′W	5308.32	130.6	130.6	118.44	91	0	14	20		
U1371G	45°57.8637′S	163°11.0360′W	5314.13	1.4	1.4	1.37	98	0	1	2.75		

Table T1 (continued).

Hole	Latitude	Longitude	Water depth (mbsf)	Penetration (m)	Cored (m)	Recovered (m)	Recovery (%)	Drilled (m)	Cores (*N*)	Time on hole (h)	Time on site (days)	Comments
U1371H	45°57.8648′S	163°11.0512′W	5310.31	6.2	6.2	6.19	100	0	1	16.5		
		Site U1371 totals:		533.5	410	389.01	98	123.5	46	113.25	1.83	
Total holes: 42		Expedition 329 totals:		1719.6	1321.8	1168.81	88	397.8	194			